Universidade Federal do Rio Grande do Sul
Centro de Biotecnologia
Programa de Pós-Graduação em Biologia Celular e Molecular

Novos enfoques no estudo dos mecanismos de ação de metaloproteinases e outras proteínas tóxicas envolvidas no envenenamento ofídico e lonômico

Antônio Frederico Michel Pinto

Porto Alegre
Outubro de 2006

Universidade Federal do Rio Grande do Sul
Centro de Biotecnologia
Programa de Pós-Graduação em Biologia Celular e Molecular

Novos enfoques no estudo dos mecanismos de ação de metaloproteinases e outras proteínas tóxicas envolvidas no envenenamento ofídico e lonômico

Antônio Frederico Michel Pinto

Orientador: Prof. Dr. Jorge Almeida Guimarães
Co-Orientador: Prof. Dr. Jay William Fox

Tese submetida ao Programa de Pós-Graduação em Biologia Celular e Molecular (PPGBCM) da UFRGS como parte dos requisitos para a obtenção do grau de Doutor.

Porto Alegre, Outubro de 2006

ANTONIO FREDERICO MICHEL PINTO

NOVOS ENFOQUES NO ESTUDO DOS MECANISMOS DE AÇÃO DE METALOPROTEINASES E OUTRAS PROTEÍNAS TÓXICAS ENVOLVIDAS NO ENVENENAMENTO OFÍDICO E LONÔMICO

Tese submetida ao Programa de Pós-Graduação em Biologia Celular e Molecular (PPGBCM) da UFRGS como parte dos requisitos para a obtenção do grau de Doutor.

Banca Examinadora

Dr. Jorge Almeida Guimarães (UFRGS) – Orientador

Dr. Elói de Souza Garcia (FioCruz – RJ)

Dr. Guido Lenz (UFRGS)

Dr. Russolina Benedeta Zingali (UFRJ)

Dr. Daniel Macedo Lorenzini (UFRGS)

Ao meu avô, Erni Germano Michel

Agradecimentos

Agradeço ao meu orientador, Dr. Jorge Almeida Guimarães, pelo exemplo de cientista e pessoa, pelo apoio e ensinamentos;

Ao meu co-orientador do estágio de doutorado sanduíche, Dr. Jay William Fox, por um ano de trabalho gratificante;

Aos meus co-orientadores não-oficiais, Dra. Célia Carlini, Dr. Carlos Termignoni, por todos os ensinamentos de valor inestimável;

Aos membros da Banca Examinadora Dra. Russolina Zingali, Dr. Elói Garcia, Dr. Guido Lenz e Dr. Daniel Lorenzini;

À Renata Terra pelo amor, suporte e por estar sempre do meu lado nos momentos críticos;

À minha família pelo suporte necessário na realização dos meus sonhos;

Aos amigos Markus Berger, José Reck Jr., Kátia Moura da Silva, Walter Beys e Lucélia Santi pela amizade e companheirismo,

Aos colegas do Laboratório de Bioquímica Farmacológica Ana Veiga, Simone Kobe e Hugo Verli;

Aos demais colegas do Laboratório de Peptídeos e Enzimas Proteolíticas e Laboratório de Proteínas Tóxicas;

Aos professores do Programa de Pós-Graduação em Biologia Celular e Molecular;

Aos demais amigos de Centro de Biotecnologia da UFRGS;

Aos secretários da pós-graduação Luciano Saucedo e Sílvia Centeno.

Índice

Apresentação

Esta tese de doutorado é fruto do trabalho desenvolvido ao longo de quatro anos no Programa de Pós-Graduação em Biologia Celular e Molecular. Esta tese foi realizada sob orientação do Professor Dr. Jorge Almeida Guimarães, do Laboratório de Bioquímica Farmacológica do Centro de Biotecnologia da Universidade Federal do Rio Grande do Sul, e co-orientação do Professor Dr. Jay William Fox, da Biomolecular Research Facility, Department of Microbiology da University of Virginia.

Minha trajetória científica iniciou-se no final de 1997, quando ingressei no Laboratório de Bioquímica Farmacológica, sob orientação do Prof. Dr. Jorge Guimarães. Trabalhei inicialmente na linha pesquisa de anti-trombóticos do carrapato *Boophilus microplus*, sob co-orientação do Prof. Dr. Carlos Termignoni, e iniciei a pesquisa com as proteínas tóxicas de *L. obliqua* em 1999, gerando meu trabalho de conclusão (2000). Durante o mestrado (2001-2002), continuei o estudo com as toxinas da taturana *L. obliqua*. Ao longo do doutorado (2002-2006), foram aprofundados os conhecimentos sobre os princípios ativos das secreções venenosas de *L. obliqua* e seus efeitos no envenenamento, além da realização de importantes projetos paralelos. Durante o estágio de Doutorado-sanduíche (2005-2006), iniciei a pesquisa na área de metaloproteinases de veneno de serpentes, sob a co-orientação do Dr. Jay Fox.

Tendo em vista a abrangência dos temas abordados durante o Doutorado, esta tese está divida em dois grandes capítulos: Metaloproteinases de Venenos de Serpentes e Proteínas Tóxicas da Lagarta *Lonomia obliqua*. Os resultados aqui descritos são apresentados na forma de artigos já publicados ou manuscritos em fase final de

preparação. Por fim, são feitas considerações finais sobre as abordagens utilizadas no estudo dos mecanismos de ação de metaloproteinases e proteínas tóxicas envolvidas nos envenenamentos ofídico e lonômico.

Resumo

Venenos e outras secreções animais vêm sendo explorados como fonte de substâncias ativas na hemostasia em mamíferos. Esses princípios ativos, com funções primárias na alimentação e defesa, afetam elementos chave de quase todas as vias fisiológicas animais, tendo um enorme potencial como base para o desenvolvimento de novas drogas.

No envenenamento ofídico, hemorragias locais e sistêmicas são causadas em grande parte pela ação de metaloproteinases hemorrágicas presentes nos venenos (SVMPs). Os estudos com metaloproteinases até então descritos baseiam-se principalmente em metodologias bioquímicas clássicas.

Neste trabalho, as metaloproteinases e suas interações com outras proteínas são abordadas através de técnicas de dinâmica molecular, ressonância plasmônica de superfície e proteômica quantitativa. O perfil de inibição da atividade proteolítica de SVMPs por inibidores teciduais de metaloproteinases (TIMPs) foi avaliado. Experimentos de modelagem e dinâmica molecular mostraram similaridades nas bases moleculares da interação das TIMPs tanto com SVMPs quanto com metaloproteinases endógenas (MMPs e ADAMs), seus alvos fisiológicos. O domínio rico-em-cisteínas das SVMPs da classe PIII está envolvido na interação com proteínas de matriz extracelular. Os sítios de interação do domínio rico-em-cisteínas de jararragina com fator de von Willebrand (vWF) foram identificados por ressonância plasmônica de superfície. Um modelo de interação entre os domínios das duas proteínas foi proposto. Considerando a presença de domínios A de vWF em diversas proteínas de matriz extracelular, o domínio

de rico-em-cisteínas funcionaria direcionando as metaloproteinases para substratos específicos, promovendo hemorragia. Além disso, através de uma metodologia de proteômica quantitativa, foi verificada pela primeira vez a ação proteolítica de metaloproteinases em proteínas de matriz extracelular íntegra de células em cultura.

Já no envenenamento lonômico, um quadro clínico hemorrágico é observado apesar da ausência de metaloproteinases no veneno. O estudo de proteínas tóxicas da lagarta *Lonomia obliqua* baseia-se no isolamento e caracterização bioquímica dos princípios ativos relacionados com aspectos da patologia do envenenamento. Nos últimos anos, esses estudos se focaram em uma única secreção da lagarta, identificando o seu potencial pró-coagulante, fibrin(ogen)olítico, hemolítico, edematogênico e nociceptivo.

Neste trabalho, foram identificadas diferenças quali-quantitativas em quatro secreções venenosas de *L. obliqua*. A diferente participação de cada uma dessas secreções durante o contato com as lagartas pode levar a grande variabilidade de sintomas e gravidade do acidente. Utilizando a metodologia de microarranjos de DNA, analisamos o efeito do veneno da lagarta no padrão de expressão gênica de células em cultura e identificamos a expressão aumentada de genes possivelmente relacionados ao quadro clínico do envenenamento. Proteínas potencialmente tóxicas de *L. obliqua* descritas em um estudo de transcriptoma, juntamente com os dados de expressão gênica aqui demonstrados possibilitam uma maior compreensão dos efeitos do veneno na hemostasia e sintomas do lonomismo.

Abstract

Animal venoms and other secretions have been explored as source of active substances on the mammal hemostasis. These active principles, which have primary function in feeding and defense, act on key elements of almost all physiologic pathways and have an enormous potential in the development of new therapeutic drugs.

In ophidic envenomations, local and systemic hemorrhages are caused mainly by the action of hemorrhagic metalloproteinases from the venom (SVMPs). Previous studies with metalloproteinases were based mostly in classical biochemical methodologies.

Here, the metalloproteinases and their interactions with other proteins were examined by molecular dynamics, surface plasmon resonance and quantitative proteomics methodologies. The inhibition profile of the SVMPs proteolytic activity by tissue inhibitors of metalloproteinases (TIMPs) was evaluated. Modeling and molecular dynamics procedures showed similarities in the molecular bases of the interaction of TIMPs both with SVMPS and endogenous metalloproteinases (MMPs and ADAMs). PIII SVMP cysteine-rich domain is involved in the interaction with extracellular matrix proteins. Using surface plasmon resonance, we identified the interaction sites between jararhagin cysteine-rich domain and von WIllebrand factor (vWF). An interaction model of these two proteins was proposed. Considering the presence of vWF A domains in several matrix proteins, the cysteine-rich domain probably works targeting the metalloproteinases to specific substrates, leading to hemorrhage. Moreover, using a quantitative proteomic approach, it was shown for the first time the metalloproteinases proteolytic action upon organized extracellular matrix proteins in culture cells.

In lonomic envenomation, a hemorrhagic clinical profile is observed regardless the absence of metalloproteinases. The caterpillar's toxic proteins studies are based on isolation and biochemical characterization of active principles related to the patophisiology of the envenomation. In the last few years, these studies were focused on one caterpillar's secretion, containing pro-coagulant, fibrin(ogen)olytic, hemolytic, edematogenic and nociceptive activities.

In this work, we identified quali-quantitative differences in four *Lonomia obliqua* venomous secretions. The different participation of each of these secretions during the accident could lead to the variability of symptoms and severity of the envenomation. Using a microarray methodology, we analyzed the effects of the caterpillar venom on the cultured cells gene expression profile and identified increased expression of genes possibly involved with the clinical manifestations. Potentially toxic proteins from *L. obliqua* identified in a transcriptome study, together with the gene expression data described here allow a better understanding of the venom effects in hemostasis during lonomism.

1. Introdução

1.1. A Hemostasia

A hemostasia representa um complexo, redundante e eficiente mecanismo fisiológico de defesa contra a perda não controlada de sangue. O estado normal de fluidez do sangue circulante é mantido pelas propriedades não-trombogênicas das paredes intactas das células dos vasos. O dano a esses vasos provoca uma pronta resposta hemostática que previne hemorragia.

O sistema é um conjunto de processos finamente regulados e com máxima eficiência incluindo a parede vascular, estruturas e agentes vasoativos envolvidos na vasoconstrição e vasodilatação, fatores que levam à adesão e agregação das plaquetas circulantes que formam um tampão hemostático e a ativação dos fatores da cascata de coagulação que levam à formação de coágulos de fibrina. Para permitir a regeneração total do tecido danificado, os coágulos são subseqüentemente removidos pelo sistema fibrinolítico. Em situações em que qualquer componente desses mecanismos esteja alterado, a hemostasia é comprometida e o resultado pode ser tanto trombose como hemorragia (Dahlback, 2000).

A lesão tecidual e rompimento dos vasos induzem a agregação plaquetária pela exposição de colágeno até então indisponível para o contato com proteínas plasmáticas e componentes celulares da circulação. Em pequenos vasos, as plaquetas sozinhas são capazes de parar um sangramento. Em sua forma inativa, as plaquetas são discóides, mas

quando ativadas elas tornam-se arredondadas, estendendo numerosos pseudópodos (fenômeno de *shape change*), levando a adesão e agregação. Isso ocorre quando as plaquetas são expostas a ADP, trombina, adrenalina, colágeno e outros agonistas. A primeira reação de plaquetas em um vaso danificado é a sua interação com proteínas adesivas, como fator de von Willebrand (vWF) e o colágeno no subendotélio, através dos receptores glicoprotéicos GPIb-IX-V e GPVI e a integrina α2β1. A ativação das plaquetas leva a liberação de outros agonistas, tais como ADP, tromboxana (TXA_2) e serotonina (5-HT). A secreção provoca o recrutamento e agregação de outras plaquetas à primeira camada, levando à formação de um tampão celular. Juntamente com a mudança de forma e adesão, um rearranjo nas fosfolipoproteínas de membrana forma uma superfície catalítica pró-coagulante (Andrews e Berndt, 2004; Braud et al., 2000; Jenny e Mann, 1998; Marcus e Safier, 1993).

Paralelamente à agregação plaquetária, a reação de coagulação é iniciada culminando na formação de fibrina. Em 2001, um modelo de hemostasia baseada em células foi proposto, enfatizando a interação de fatores da coagulação com superfícies celulares específicas (Hoffman, 2003a; Hoffman, 2003b; Hoffman e Monroe, 2001; Roberts et al., 2006). O modelo de coagulação baseado em células é uma evolução conceitual do processo da cascata da coagulação formulado em 1964 por Davie e Ratnoff e MacFarlane (Davie e Ratnoff, 1964; Macfarlane, 1964). Este modelo baseia-se em uma série de três etapas que ocorrem em superfícies de diferentes tipos celulares. Como mostra a Figura 1, a primeira fase, ou iniciação, ocorre em células extravasculares carreadoras de fator tecidual (*tissue factor*, TF). Na fase de amplificação, plaquetas e co-fatores são ativados em preparação para a geração de trombina em larga escala.

Finalmente, a propagação ocorre na superfície de plaquetas, resultado na ativação de grandes quantidades de trombina e subseqüente formação do coágulo de fibrina.

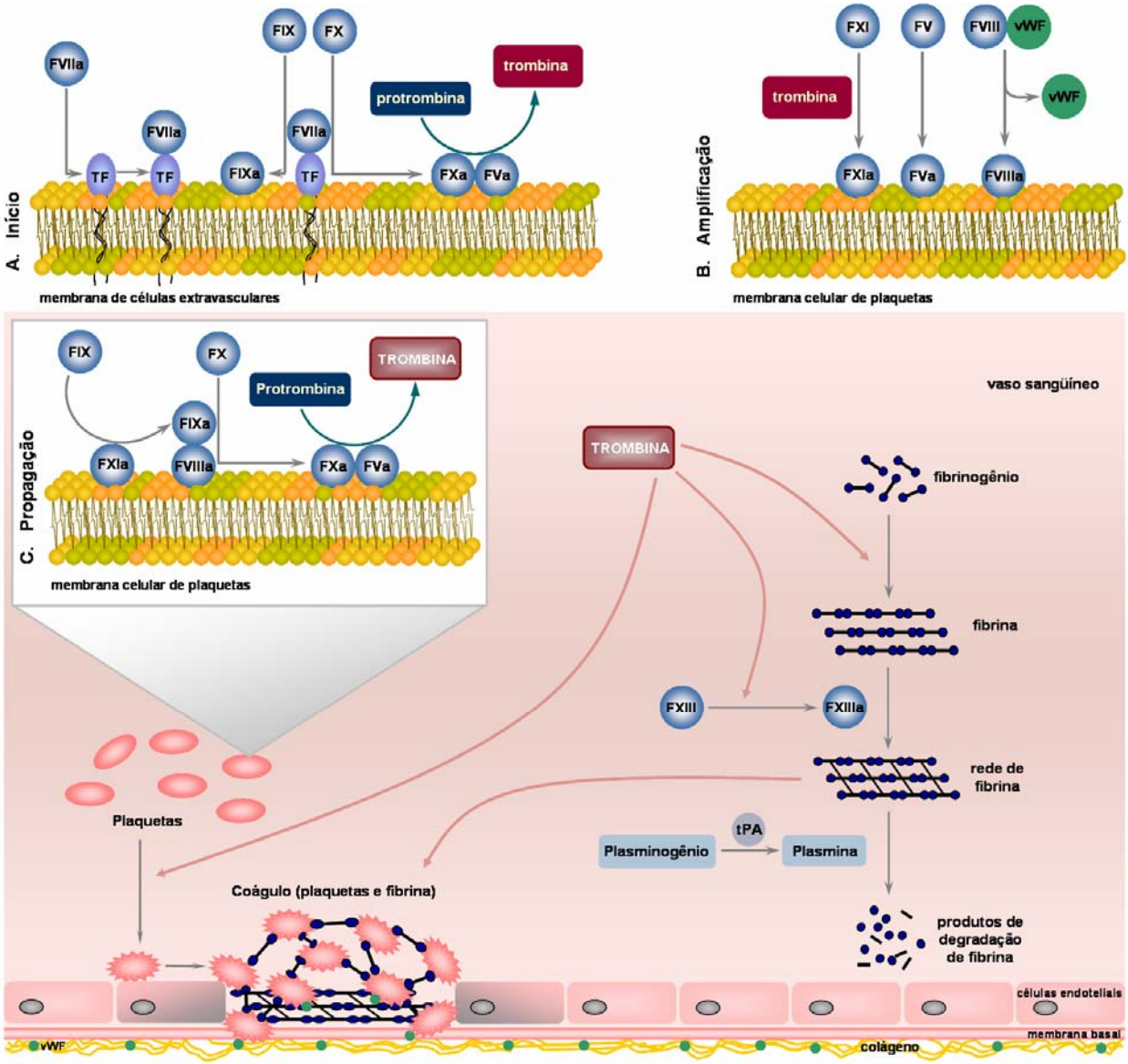

Figura 1. Modelo da cascata de coagulação baseado em células. A. Fase inicial; B. Fase de amplificação; C. Fase de propagação. Fatores da coagulação estão representados em azul. Trombina ativa representada em vermelho. TF, fator tecidual; vWF, fator de von Willebrand; tPA, ativador de plasminogênio tipo tecidual. (Figura cedida por Markus Berger)

O passo de iniciação (Figura 1A) ocorre nas superfícies de células contendo TF (fibroblastos do estroma, células mononucleares, macrófagos e células endoteliais que não expõem TF ao sangue até que ocorra dano vascular ou inflamação) que estão normalmente fora da vasculatura. O complexo fator VIIa/TF ativa pequenas quantidades de fatores IX e X. Esse fator Xa associado ao seu cofator, fator Va, forma o complexo protrombinase na superfície de células carreadores de TF. O fator V pode ser ativado por fator Xa ou por outras proteases não-coagulantes. A presença de inibidores específicos (*tissue factor pathway inhibitor*, TFPI e anti-trombina) localiza o fator Xa somente na superfície em que ele é formado.

Além disso, baixos níveis de atividade da via de TF ocorrem no espaço extravascular todo o tempo. Algumas proteínas da coagulação atravessam a camada endotelial dos vasos, sendo encontradas na linfa em quantidades que variam de acordo com suas massas moleculares (proteínas menores são encontradas em maior quantidade). Assim, fator VII pode ser encontrado ligado a TF mesmo na ausência de lesão vascular e fatores IX e X podem ser ativados quando passam pelos tecidos. Esse fenômeno, chamado coagulação basal, não leva à formação de coágulos em circunstâncias normais devido a ausência de componentes de alta massa molecular do processo de coagulação, como plaquetas e complexo fator VIII/vWF. O processo de coagulação prossegue para a fase de amplificação apenas quando algum dano vascular permite que plaquetas e fator VIII/vWF entrem em contato com tecido extravascular.

A fase de amplificação (Figura 1B) é preparatória para a subseqüente ativação de trombina em grande escala na fase de propagação. A pequena quantidade de trombina gerada nas células carreadoras de TF possui várias funções, entre elas a ativação de

plaquetas, expondo receptores e sítios de ligação para fatores da coagulação ativos e liberando formas de fator V parcialmente ativadas em suas superfícies. A trombina formada na fase inicial também ativa os fatores V e VIII na superfície de plaquetas ativadas. Nesse processo, o complexo fator VIII/vWF se dissocia, permitindo que vWF plasmático atue como mediador adicional na adesão e agregação plaquetária. Também nessa fase, o fator XI na superfície de plaquetas é ativado a fator XIa.

A fase de propagação (Figura 1C) ocorre na superfície das plaquetas ativadas aderidas e agregadas no local da lesão. O fator IXa, tanto o ativado na fase de iniciação quanto o ativado por fator XIa, se liga ao fator VIIIa nas plaquetas. Já que o fator Xa não pode se mover das células carreadores de TF até as plaquetas ativadas, este deve ser suprido diretamente na superfície plaquetária pelo complexo fator IXa/VIIIa (complexo Xase). O fator Xa rapidamente se associa ao fator Va ligado às plaquetas na fase de amplificação. A formação de complexo protrombinase leva a ativação de protrombina em grandes quantidades, levando à clivagem de fibrinogênio e formação de fibrina.

Trombina também ativa fator XIII a fator XIIIa, uma transglutaminase plasmática. Fator XIIIa catalisa a modificação covalente entre monômeros de fibrinas, formando a rede estável de fibrina. A reação envolve a formação de uma ligação amida entre o grupamento carbonil de resíduos de glutamina de uma molécula de fibrina e o animo-grupo da cadeia lateral de resíduos de lisina em outra molécula de fibrina, formando o coágulo de fibrina estável (rede de fibrina) (Hettasch e Greenberg, 1998).

Todo o processo de coagulação é regulado por outros componentes fisiológicos circulantes, tais como o inibidor da via do fator tecidual, fosfolipase A_2, fosfodiesterase, 5'-nucleotidase, antitrombina III e a via anticoagulante da proteína C/trombomodulina,

que inativa os fatores Va e VIIIa. Além disso, a via regulatória composta pelo sistema do plasminogênio também tem um papel importante na degradação da rede de fibrina gerada pela ativação do processo hemostático. O sistema de plasminogênio possui também participação em vários processos celulares. A via é ativada por dois ativadores fisiológicos de plasminogênio (PA): ativador de plasminogênio do tipo tissular (t-PA) e ativador de plasminogênio tipo uroquinase (u-PA). A via de ativação mediada por t-PA está primariamente envolvida na homeostase da fibrina. Por outro lado, a via mediada por u-PA está envolvida em fenômenos como migração celular e remodelagem de tecidos. O plasminogênio ativado gera plamina, que atua na degradação de fibrina e fibrinogênio e na ativação de metaloproteases de matriz (MMPs) responsáveis pela degradação da matriz extracelular. A inibição do sistema de regulação do plasminogênio ocorre na etapa de ativação de plasminogênio, pela ação específica de inibidores de ativadores de plasminogênio (PAI) e diretamente na plasmina ativa, através da serpina α2-antiplasmina (Collen, 1999; Vaughan e Declerck, 1998).

1.2. Toxinas de Origem Animal que afetam a Hemostasia

Venenos e outras secreções animais vêm sendo explorados como fonte de substâncias ativas na hemostasia em mamíferos. Esses princípios ativos possuem funções na alimentação e defesa, afetando elementos chave de quase todas as vias fisiológicas animais.

Venenos de serpentes contêm uma vasta gama de componentes enzimáticos e não-enzimáticos envolvidos no processo de imobilização, morte e digestão das presas, bem como na defesa. Existem mais de 200 espécies conhecidas de serpentes venenosas, classificadas nas famílias Elapidae, Viperidae, Crotalidae, Hydrophidae e Colubridae.

Venenos de serpentes apresentam diversas atividades enzimáticas capazes de bloquear junções neuro-musculares, induzir necrose tecidual e causar desordens hemostáticas sistêmicas (Lu et al., 2005). Entre proteínas e peptídeos biologicamente ativos encontrados em venenos de serpentes estão fosfolipases, fosfodiesterases, L-amino ácido oxidases, acetilcolinesterases, enzimas proteolíticas das classes serino e metalo proteinases, arginina esterases, 5'-nucleotidases, hialuronidases, nucleosidases, neurotoxinas pré- e pós-sinápticas, neurotoxinas ligadoras de canais de potássio, citotoxinas, miotoxinas, cardiotoxinas e inibidores de agregação plaquetária (desintegrinas) (Markland, 1998).

Entre os artrópodes, espécies de diversos grupos produzem agentes que atuam no processo hemostático. Apesar dos muitos obstáculos, o sangue é uma fonte muito rica em nutrientes e a habilidade de utilizá-lo como alimento evoluiu múltiplas vezes. Em pelo menos 20 famílias de artrópodes, distribuídas em duas classes (Arachnida e Insecta) e

numerosas ordens, a hematofagia evoluiu independentemente (Champagne, 2005). Embora apenas poucas das mais de 15000 espécies em mais de 500 gêneros de artrópodes hematófagos tenham sido estudadas, uma enorme diversidade de compostos anti-hemostáticos já foram descritos. Como regra, a saliva desses animais possui pelo menos um componente anti-coagulante, um anti-plaquetário e uma substância vasodilatadora (Ribeiro e Francischetti, 2003).

Além dos artrópodes hematófagos, alguns insetos da Ordem Lepidoptera também possuem importância médica. Na fase larval ou de lagarta, algumas espécies produzem venenos com papel fundamental na defesa contra predadores que entrem em contrato com os pêlos urticantes ou espículas que revestem os corpos desses animais. Muitas espécies de lepidópteros podem causar envenenamentos em humanos, nos quais os sintomas mais comuns são reações cutâneas, urticária, dor e sensação de queimação no local do contato. Em alguns casos específicos, o contato com essas lagartas pode causar distúrbios na coagulação, hemorragias e insuficiência renal aguda pela ação de princípios ativos com ação hidrolítica encontrado em alguns venenos (Arocha-Pinango e Guerrero, 2001; Arocha-Pinango et al., 2000; Diaz, 2005).

2. Capítulo I

Metaloproteinases de Venenos de Serpentes

O capítulo a seguir apresenta as etapas do trabalho envolvendo estudos com metaloproteinases de venenos de serpente. Essa etapa foi iniciada durante o estágio de doutorado realizado na University of Virginia, Estados Unidos, sob a co-orientação do Prof. Dr. Jay William Fox.

Inicialmente, uma breve introdução sobre venenos de serpentes, envenenamentos e estrutura e função de metaloproteinases será apresentada. Os resultados deste capítulo estão na forma de dois artigos completos (o primeiro já publicado, o segundo aceito para publicação) e dados de um manuscrito em fase de preparação. Cada conjunto de dados contém uma introdução detalhada do assunto, metodologia aplicada, descrição dos resultados obtidos, discussão e bibliografia consultada.

2.1. Introdução

2.1.1. Venenos de Serpentes e Envenenamentos

Venenos de serpentes são misturas complexas de proteínas e peptídeos biologicamente ativos que induzem uma ampla variedade de efeitos nas suas presas e em vítimas humanas. Muitos desses componentes são proteínas ativas com função de imobilizar e matar suas presas, bem como auxiliar na digestão. Uma grande variabilidade quali-quantitativa na composição dos venenos de serpentes de diferentes gêneros tem sido descrita (Fox e Serrano, 2005). Não raro também é a observação de que venenos de serpentes apresentam diferenças em sua composição dentro da mesma espécie dependendo de fatores individuais como sexo, idade, origem geográfica, dieta e variações sazonais (Francischetti et al., 1998; Furtado et al., 1991; Hite et al., 1994). Por exemplo, estudos prévios com venenos de mais de 100 espécimes de *Calloslasma rhodostoma* usando focalização isoelétrica revelou variação geográfica que foi correlacionada com variação na atividade biológica dos venenos (Daltry et al., 1996). Além disso, estudos com serpentes criadas em cativeiro mostraram que a variação intra-específica nos venenos é um fator genético (Monteiro et al., 1998). Essa variação deve ser considerada tanto para a pesquisa básica com venenos de serpentes quanto no tratamento de envenenamento por serpentes. Na pesquisa básica, a variação na composição dos venenos pode afetar os grupos de serpentes doadoras a serem usadas para a produção de veneno

para estudo. No tratamento de envenenamentos, essa variação deve ser considerada na escolha das serpentes doadoras para a produção de anti-sôro (Serrano et al., 2005b).

Tradicionalmente, venenos animais têm sido estudados com o objetivo de compreender aspectos estrutura/função de proteínas individuais e elucidar os mecanismos de seus efeitos tóxicos. Essa abordagem é tipicamente realizada através do isolamento, caracterização bioquímica e determinação da atividade biológica *in vitro* e *in vivo*. Tal abordagem tem sido bem sucedida, produzindo informações a respeito dos quadros patológicos induzidos por venenos e o tratamento dos mesmos (Braud et al., 2000; Markland, 1998; Marsh, 1994). Dentre os componentes estudados, destacam-se as metaloproteinases de venenos de serpentes, enzimas envolvidas nos dramáticos efeitos hemorrágicos produzidos pelos envenenamentos.

2.1.2. Metaloproteinases de Venenos de Serpentes – Estrutura e Função

Hemorragias locais e sistêmicas resultantes do envenenamento por serpentes são causadas em grande parte pela ação de metaloproteinases hemorrágicas presentes nos venenos (Fox e Serrano, 2005). A hemorragia ocorre em decorrência da degradação proteolítica de proteínas de membrana basal envolvidas na manutenção da estrutura capilar e integridade estrutural (Fox e Serrano, 2005). Metaloproteinases de venenos de serpentes (*snake venom metalloproteinases*, SVMPs) responsáveis por essa degradação compreendem um subgrupo da subfamília das reprolisinas da classe M12 de metaloproteinases (Bjarnason e Fox, 1994). A classificação dessas enzimas é baseada na

massa molecular e presença de diferentes domínios na sua estrutura: SVMPs do tipo PI possuem apenas o domínio metaloproteinase; as PII possuem domínios metaloproteinase e desintegrina; SVMPs da classe PIII são sintetizadas com domínios metaloproteinase, tipo-desintegrina e rico-em-cisteína, e as PIV possuem a estrutura das PIII mais domínios do tipo lectina conectados por pontes dissulfeto (Bjarnason e Fox, 1995) (Figura 2). Embora a atividade hemorrágica seja a mais relacionada com as SVMPs, algumas dessas enzimas não são hemorrágicas. Algumas dessas enzimas possuem ainda outras atividades, entre elas clivagem de vWF, degradação de fibrinogênio, ativação de fatores da coagulação e inibição da agregação plaquetária (Tabela I).

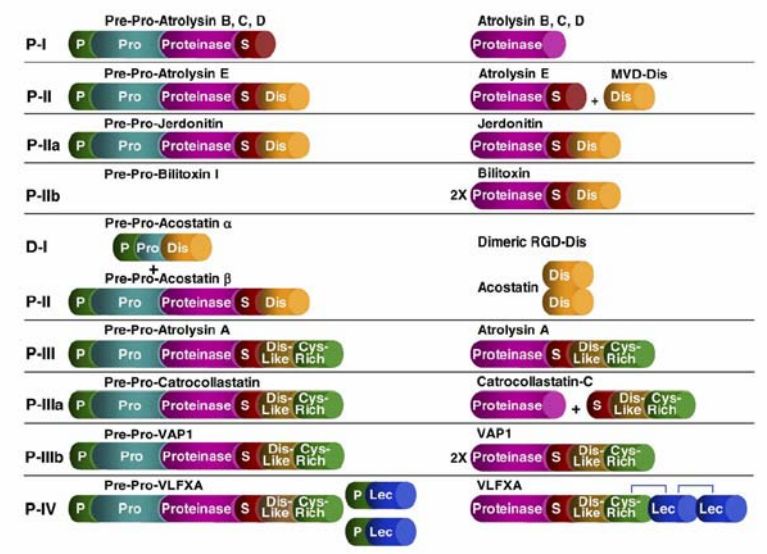

Figura 2. Esquema das classes de metaloproteinases de veneno de serpentes. À esquerda, SVMPs em forma inativa, à direita, SVMPs em sua forma madura. Verde escuro, peptídeo sinal; ciano, pró-segmento; lilás, domínio metaloproteinase; vermelho, espaçador; amarelo, domínio desintegrina; marrom, domínio tipo-desintegrina, verde claro, domínio rico-em-cinteína; azul, domínio tipo lectina (Fox e Serrano, 2005).

Tabela I. Atividades biológicas de algumas metaloproteinases de venenos de serpentes (Modificado de Fox e Serrano, 2005).

SVMP		Serpente	Atividade
Classe	Enzima		
PI	Atrolisina C	*Crotalus atrox*	Hemorrágica
	Acutolisina A	*Agkistrodon acutus*	Hemorrágica
	BaP1	*Bothrops asper*	Hemorrágica; Mionecrótica; Pró-Inflamatória
	Fibrolase	*Agkistrodon contortrix*	Fibrinolítica
	HT-2	*Crotalus ruber*	Hemorrágica
	Atroxase	*Crotalus atrox*	Fibrinolítica
	LHF-II	*Lachesis muta*	Hemorrágica
	H2-proteinase	*Trimeresurus flavoviridis*	Proteolítica; Não-Hemorrágica
	HR2A	*Trimeresurus flavoviridis*	Hemorrágica
	Graminelisina I	*Trimeresurus gramineus*	Apoptótica
PII	Atrolisina	*Crotalus atrox*	Hemorrágica
	MT-d	*Agkistrodon halys*	Proteolítica
	Jerdonitina	*Trimeresurus jerdonii*	Inibidora da Agregação Plaquetária
	Bilitoxina-I	*Agkistrodon bilineatus*	Hemorrágica
PIII	Atrolisina A	*Crotalus atrox*	Hemorrágica; Inibidora da Agregação Plaquetária
	Catrocolastatina	*Crotalus atrox*	Inibidora da Agregação Plaquetária
	Jararragina	*Bothrops jararaca*	Hemorrágica; Inibidora da Agregação Plaquetária
	HF3	*Bothrops jararaca*	Hemorrágica; Ativadora de Fagocitose em Macrófagos
	HR1a	*Trimeresurus flavoviridis*	Hemorrágica
	HR1b	*Trimeresurus flavoviridis*	Hemorrágica
	Caoutiagina	*Naja kaouthia*	Clivagem de vWF; Inibidora da Agregação Plaquetária
	VAP1	*Crotalus atrox*	Apoptótica
	HV1	*Crotalus atrox*	Apoptótica
	Acurragina	*Agkistrodon acutus*	Hemorrágica
	Ecarina	*Echis carinatus*	Ativadora de Protrombina
	Beritractivase	*Bothrops erythromelas*	Ativadora de Protrombina
PIV	RVV-X	*Vipera russelli*	Ativadora de Fator X
	VLFXA	*Vipera lebetina*	Ativadora de Fator X

A classe PIII das SVMPs possui o repertório mais variado de atividades e são consideradas as metaloproteinases de veneno mais pontentes. Elas são estruturalmente relacionadas com a família de proteínas ADAMs ("A Disintegrin And Metalloproteinase") (Takeda et al., 2006), de mamíferos, que contém além dos domínios metaloproteinase, desinterina e rico-em-cisteína um domínio tipo fator de crescimento epitelial, uma região transmembrana e um calda citoplasmática (Blobel, 2005; Porter et al., 2005).

Em 1989, Baramova e colaboradores determinaram que enzimas do tipo PI, PII e PIII são capazes de degradar uma variedade de proteínas de matriz extracelular, como fibronectina, laminina, colágeno tipo IV, nidogênio e gelatinas (Figura 3) (Baramova et al., 1989). Essa degradação apresenta alguns sítios em comum, mas diferentes especificidades. Mais recentemente, um estudo de degradação de matrigel usando duas SVMPs, BaP1 (metaloproteinase da classe PI isolada de *Bothrops asper*) e jararragina (metaloproteinase da classe PIII isolada de *Bothrops jararaca*) foi realizado (Escalante et al., 2006). Matrigel é uma mistura complexa de componentes de membrana basal contendo suas principais proteínas (laminina, colágeno tipo IV, nidogênio/entactina e proteoglicanos), entre outros componentes em menores concentrações. Foi mostrado que as duas metaloproteinases degradam matrigel de forma ligeiramente diferente: BaP1 exerce suas ação proteolítica limitada tanto em laminina quanto em nidogênio, enquanto jararragina degrada predominantemente nidogênio (Figura 4). A degradação de proteínas de matriz extracelular pode levar a perda da integridade dos capilares resultando em hemorragia nesses locais.

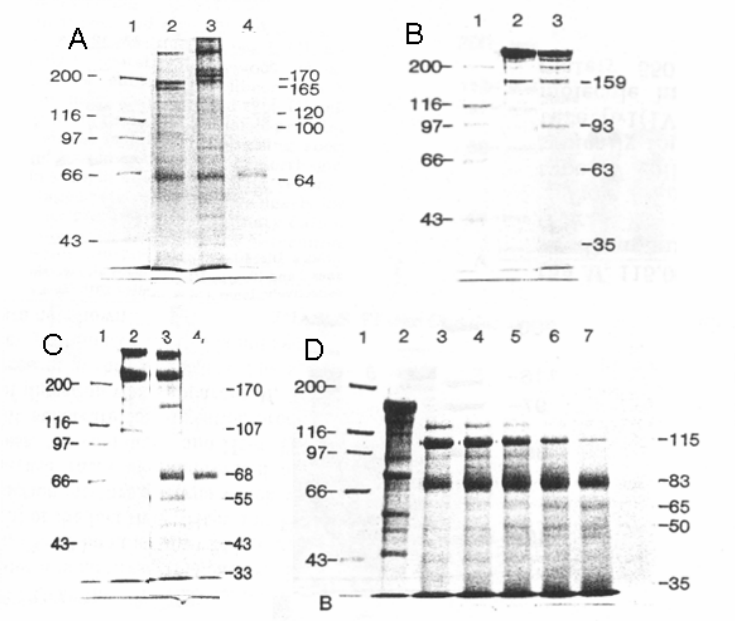

Figura 3. **A**. Digestão de colágeno tipo IV por Atrolisina A. Coluna 1, marcador de massa molecular, coluna 2, colágeno tipo IV, coluna 3, colágeno tipo IV, digestão de 4 horas, coluna 4, atrolisina A, controle. **B**. Digestão de fibronectina por Atrolisina A. Coluna 1, marcador de massa molecular, coluna 2, fibronectina, coluna 3, fibronectina, digestão de 4 horas. **C**. Digestão do complexo laminina/niogênio por Atrolisina A. Coluna 1, marcador de massa molecular, coluna 2, laminina/nidogênio, coluna 3, laminina/nidogênio, digestão de 4 horas, coluna 5, atrolisina A, controle. **D**. digestão de nidogênio (40μg) por Atrolisina A. Coluna 1, marcador de massa molecular, coluna 2, nidogênio, controle, colunas 3-7, nidogênio, digestão de 1, 2, 4, 8 e 24 horas, respectivamente. (Modificado de Baramova et al., 1989)

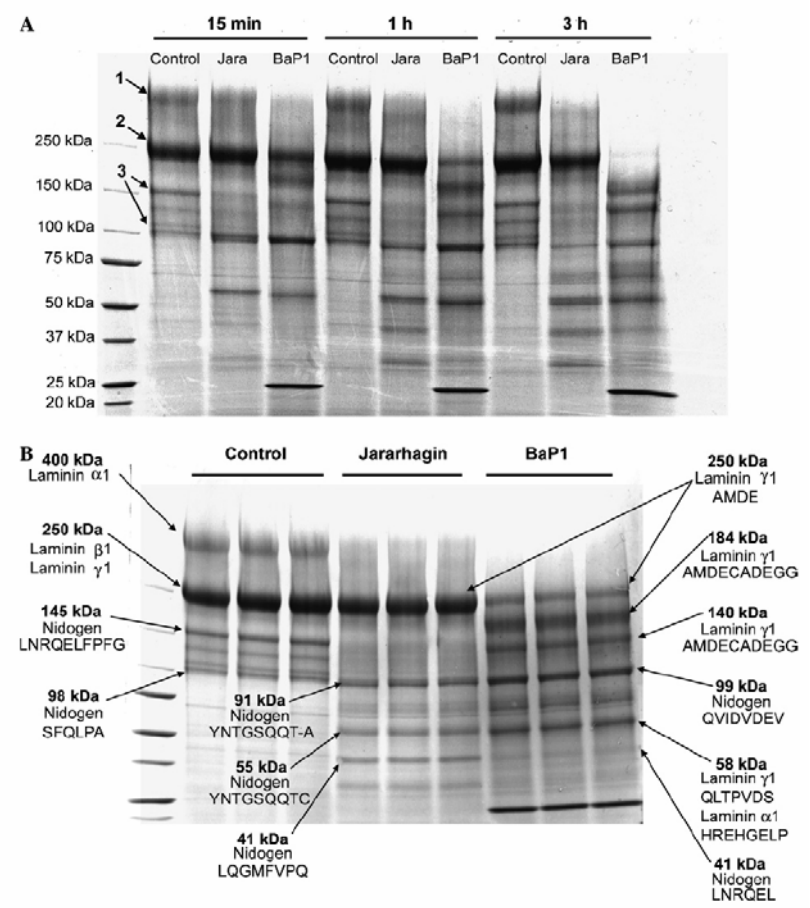

Figura 4. Hidrólise de Matrigel por BaP1 e jararragina. A. Matrigel foi incubado com cada enzima. Controles foram incubados sem enzima pelo mesmo período. No controle, as bandas mais abundantes de matrigel correspondem a (1) laminina, cadeia α-1, (2) laminina, cadeias β e γ e (3) cadeias de nidogênio. Ocorre degradação dos componentes do matrigel nos primeiro 15 minutos de incubação com as enzimas. B. Identificação de sítios de clivagem dos componentes de matrigel (laminina e nidogênio). As massas moleculares dos fragmentos de degradação e seqüências N-terminais estão indicadas. (Modificado de Escalante et al., 2006)

É interessante notar que a atividade hemorrágica, a habilidade de produzir extravasamento vascular no local do envenenamento, é uma propriedade das SVMPs PI, PII e PIII. Assim, a presença de certos domínios não necessariamente denota capacidade hemorrágica. Considerando que as SVMPs PIII apresentam a maior atividade hemorrágica dentre as SVMPs, inúmeros estudos investigando o papel dos domínios tipo-desintegrina/rico-em-cisteína têm sido realizados. Usami e colaboradores demonstraram

que jararragina-C, o produto proteolítico da PIII hemorrágica jararragina contendo os domínios tipo-desintegrina/rico-em-cisteína, isolada do veneno da serpente *Bothrops jararaca*, inibe a agregação plaquetária estimulada por colágeno e ADP (Usami et al., 1994). Essa atividade dos domínios tipo-desintegrina/rico-em-cisteína das SVMPs PIII foi corroborada por Jia e colaboradores, que mostraram que as formas recombinantes desses domínios da proteína atrolisina A, uma PIII de *Crotalus atrox*, era capaz de inibir a agregação plaquetária induzida por colágeno (Jia et al., 1997). Nesse mesmo estudo, foi proposto que a região responsável pela inibição da agregação plaquetária seria a região do domínio tipo-desintegrina posicionalmente análoga à alça RGD das desintegrinas. Para executar sua função biológica, a região em questão do domínio tipo-desintegrina (seqüência RSECD) teria como requisito a restrição conformacional da cisteína por uma ponte dissulfeto (Jia et al., 1997).

A primeira estrutura tridimensional de uma SVMP da classe PIII foi recentemente elucidada (Takeda et al., 2006). A estrutura cristalográfica da VAP1 (vascular apoptosis protein 1), de *Crotalus atrox*, indica claramente que o motivo ECD apresenta-se estericamente indisponível para interação (Figura 5). Assim, o(s) sítio(s) de interação com integrina localiza(m)-se, muito provavelmente, em alguma região do domínio rico-em-cisteínas, na porção carboxi-terminal da estrutura da proteína (Takeda et al., 2006).

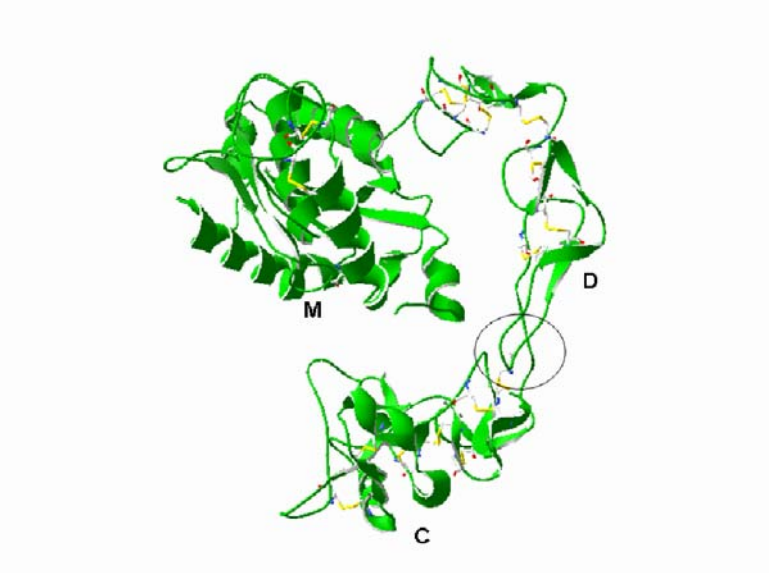

Figura 5. Estrutura tridimensional de uma metaloproteinas de veneno de serpente da classe PIII. M, domínio metaloproteinase; D, domínio tipo-desintegrina; C, domínio rico-em-cisteína. O círculo indica a localização do motivo ECD.

A capacidade do domínio rico-em-cisteínas de executar sozinho a atividade dos domínios tipo-desintegrina/rico-em-cisteína na inibição da agregação plaquetária foi demonstrada por Jia e colaboradores, usando a forma recombinante do domínio rico-em-cisteína de atrolisina A (Jia et al., 2000). Recentemente, outros estudos mostraram que o domínio rico-em-cisteína de SVMPs PIII é responsável pela interação que precede a degradação de vWF (Serrano et al., 2005a). Esses resultados indicam que o papel funcional do domínio rico-em-cisteína das PIII é localizar e ligar-se às proteínas alvo, tais como integrina $\alpha_2\beta_1$ e vWF nos eventos de agregação plaquetária.

2.2. Objetivos

Esta etapa do trabalho teve como objetivos principais: 1. identificar as bases moleculares da interação de inibidores teciduais de metaloproteinases e metaloproteinases de venenos de serpentes; 2. analisar a interação do domínio rico-em-cisteínas de metaloproteinases com o fator de von Willebrand; 3. analisar a atividade proteolítica de metaloproteinases sobre proteínas de matriz extracelular de células em cultivo.

Esses objetivos foram realizados pelas seguintes etapas:

1.1. Avaliação do perfil de inibição dos inibidores teciduais de metaloproteinases (TIMPs) na atividade proteolítica da metaloproteinase PI atrolisina C;

1.2. Análise dos requerimentos estruturais e bases moleculares da interação da atrolisina C com os inibidores TIMP-1, TIMP-2 e N-TIMP-3 usando ferramentas de modelagem molecular;

2.1. Avaliar a interação de peptídeos sintéticos baseados na estrutura do domínio rico-em-cisteínas da jararragina com fator de von Willebrand (vWF) em ressonância plasmônica de superfície;

2.2. Avaliar a ação dos peptídeos capazes de interagir com vWF na agregação plaquetária;

2.3. A partir de um modelo tri-dimesional de jararragina, localizar os peptídeos capazes de interagir com vWF na estrutura do domínio rico-em-cisteína;

2.4. Baseado nos dados experimentais obtidos, propor um modelo de interação do domínio rico-em-cisteínas com o domínio A1 de vWF;

3.1. Estabelecer uma metodologia de proteômica quantitativa para a análise de degradação de proteínas de superfície em matriz extracelular de células em cultura;

3.2. Identificar fragmentos de proteínas de matriz extracelular degradadas pela metaloproteinase PIII atrolisina A através de análise de espectrometria de massas.

2.3. Resultados

2.3.1. Fatores Estruturais da interação da reprolisina atrolisina C e inibidores teciduais de metaloproteinases (TIMPs)

Antônio F.M. Pinto, Renata M.S. Terra, Jorge A. Guimarães, Masahide Kashiwagi, Hideaki Nagase, Solange M.T. Serrano, Jay W. Fox. 2006. Structural features of the reprolysin atrolysin C and tissue inhibitors of metalloproteinases (TIMPs) interaction. Biochemical and Biophysical Research Communications 347:641-648.

Este trabalho apresenta estudos de inibição da metaloproteinase atrolisina C (uma SVMP da classe PI) pela família de inibidores teciduais de metaloproteinases (TIMPs). As TIMPs são uma família de proteínas com grau de identidade de seqüência de 41 a 52% e que compartilham o mesmo arcabouço estrutural. Mesmo assim, os quatro membros dessa família de inibidores (TIMP-1 a -4) apresentam perfis de inibição bastante característicos para diferentes metaloproteinases endógenas (metaloproteinases de matriz, MMPs e *A Disintegrin and Metaloproteinase*, ADAMs).

Considerando a habilidade das TIMPs de interagir e inibir MMPs e ADAMS e a notável similaridade entre SVMPs, MMPs e ADAMs, é concebível que TIMPs sejam capazes de inibir também SVMPs. Esse efeito inibitório atuaria na diminuição da ação proteolítica e hemorrágica das SVMPs durante o envenenamento. Analisamos o perfil de inibição das TIMPs sobre a atividade proteolítica da atrolisina C. Utilizando ferramentas de modelagem e dinâmica molecular, investigamos as bases moleculares da interação entre TIMPs e SVMPs.

Este trabalho foi desenvolvido na Biomolecular Research Facility (University of Virginia) em colaboração com o Laboratório de Bioquímica Farmacológica (UFGRS), Laboratório Especial de Toxinologia Aplicada (Instituto Butantan) e Department of Matrix Biology (Imperial College). Este trabalho foi submetido à revista *Biochemical and Biophysical Research Communications* em Junho de 2006 e aceito para publicação em Julho de 2006.

Available online at www.sciencedirect.com
SCIENCE DIRECT
Biochemical and Biophysical Research Communications 347 (2006) 641–648
37
BBRC
www.elsevier.com/locate/ybbrc

Structural features of the reprolysin atrolysin C and tissue inhibitors of metalloproteinases (TIMPs) interaction

Antônio F.M. Pinto [a,b], Renata M.S. Terra [b], Jorge A. Guimarães [b], Masahide Kashiwagi [c], Hideaki Nagase [c], Solange M.T. Serrano [d], Jay W. Fox [a,*]

[a] *Department of Microbiology, University of Virginia, P.O. Box 800734, Charlottesville, VA 22908-0734, USA*
[b] *Centro de Biotecnologia, Universidade Federal do Rio Grande do Sul, Porto Alegre, Brazil*
[c] *Department of Matrix Biology, The Kennedy Institute of Rheumatology Division, Imperial College London, London W6 8LH, UK*
[d] *Laboratório Especial de Toxinologia Aplicada-CAT-CEPID, Instituto Butantan, 05503-900, São Paulo, Brazil*

Received 14 June 2006
Available online 5 July 2006

Abstract

Atrolysin C is a P-I snake venom metalloproteinase (SVMP) from *Crotalus atrox* venom, which efficiently degrades capillary basement membranes, extracellular matrix, and cell surface proteins to produce hemorrhage. The tissue inhibitors of metalloproteinases (TIMPs) are effective inhibitors of matrix metalloproteinases which share some structural similarity with the SVMPs. In this work, we evaluated the inhibitory profile of TIMP-1, TIMP-2, and the N-terminal domain of TIMP-3 (N-TIMP-3) on the proteolytic activity of atrolysin C and analyzed the structural requirements and molecular basis of inhibitor–enzyme interaction using molecular modeling. While TIMP-1 and TIMP-2 had no inhibitory activity upon atrolysin C, the N-terminal domain of TIMP-3 (N-TIMP-3) was a potent inhibitor with a K_i value of approximately 150 nM. The predicted docking structures of atrolysin C and TIMPs were submitted to molecular dynamics simulations and the complex atrolysin C/N-TIMP-3 was the only one that maintained the inhibitory conformation. This study is the first to shed light on the structural determinants required for the interaction between a SVMP and a TIMP, and suggests a structural basis for TIMP-3 inhibitory action and related proteins such as the ADAMs.

Keywords: TIMP; Atrolysin C; SVMP; Molecular docking; Molecular dynamics simulation; Binding affinity

Extracellular matrix components modulate cellular behavior and interactions with the surrounding environment. One class of endopeptidases involved in extracellular matrix degradation is the zinc metalloproteinases including the matrix metalloproteinases (MMPs), ADAMs (a disintegrin and metalloproteinases), and ADAMTSs (ADAMs with thrombospondin motifs). Many human diseases are related to disregulation of these metalloproteinase activities including arthritis, cancer, and atherosclerosis [1–3].

Snake venom metalloproteinases (SVMPs) are a subgroup of the reprolysins with an active role in the pathogenesis of snake envenomation. SVMPs have been shown to participate in the hemorrhagic process by proteolytically degrading extracellular matrix and capillary basement membranes which in part lead to the disruption of local capillary networks, hemorrhage, and edema [4]. The classification of these enzymes is based on their different domain structures, presented as follows: P-I (SVMPs with only metalloproteinase domain), P-II (SVMPs with metalloproteinase and disintegrin domains), P-III (SVMPs with metalloproteinase, disintegrin-like, and cysteine-rich domains), and P-IV (SVMPs with P-III domain structure plus two lectin-like domains connected by disulfide bonds) [5]. Atrolysin C is a P-I SVMP from *Crotalus atrox* venom which efficiently degrades basement membrane proteins surrounding capillaries, thus permitting the flux of capillary contents into the stroma and producing hemorrhage [6]. The three-dimensional structure of atrolysin C shows

* Corresponding author. Fax: +1 434 982 2514.
E-mail address: jwf8x@virginia.edu (J.W. Fox).

0006-291X/$ - see front matter © 2006 Elsevier Inc. All rights reserved.
doi:10.1016/j.bbrc.2006.06.143

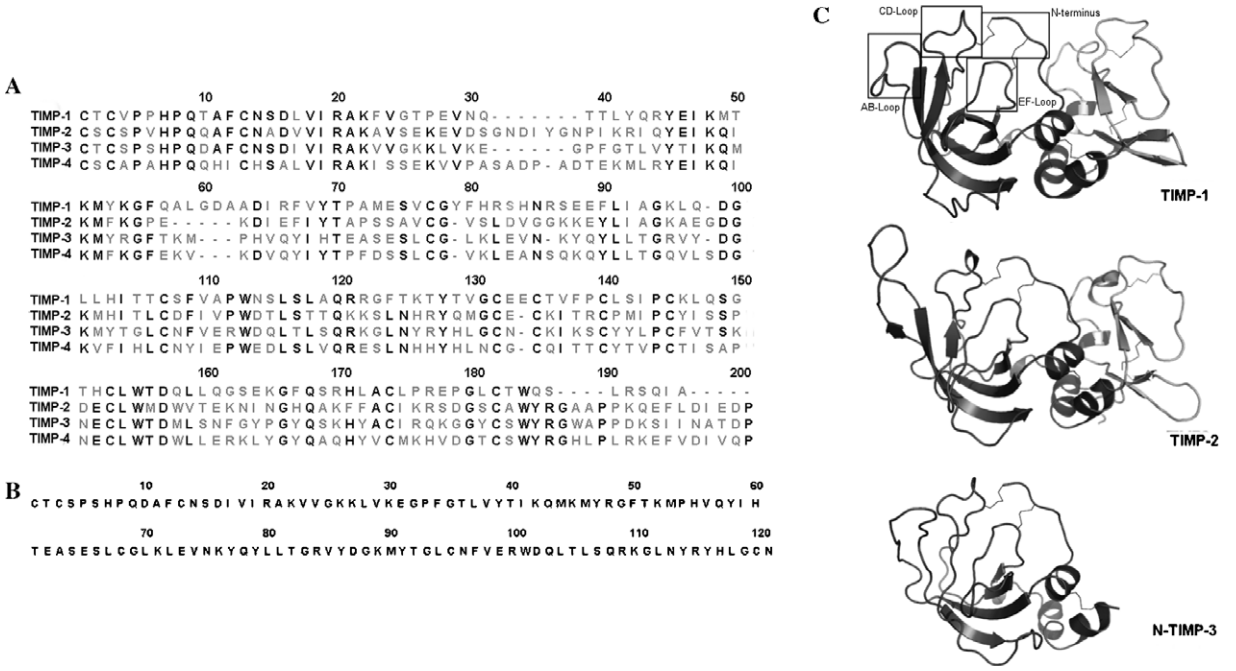

Fig. 1. TIMPs sequences and structures. (A) Sequence alignment of TIMPs showing identical residues in black. (B) Amino acid sequence of N-TIMP-3. (C) Crystallographic TIMP-1 (PDB code 1UEA) and TIMP-2 (PDB code 1BUV) structures were used as templates for modeling the N-TIMP-3 structure. N-terminal domains are shown in light grey and C-terminal in dark grey. Regions of TIMPs important for the interaction with metalloproteinases are boxed in the TIMP-1 structure.

a noticeable similarity with MMPs and human ADAMs [7], and displays the characteristic structural features including (1) an active-site helix with zinc ligands and (2) an extended binding site defined by an antiparallel β-strand [6].

The activity of MMPs on extracellular matrix is regulated by a family of endogenous inhibitory proteins, the tissue inhibitors of metalloproteinases (TIMPs). The TIMP family comprises four members (TIMP-1 to -4) with 184–194 residues (mature protein) which share between 41% and 52% sequence identity including six conserved disulfide bonds (Fig. 1A). All TIMPs have two domains and the larger N-terminal domain is responsible for the metalloproteinase inhibition, while the smaller C-terminal domain mediates the interaction with the hemopexin domains of certain pro-MMPs (Fig. 1C) [8,9].

TIMPs inhibit MMPs with relatively low selectivity and some, but not all, ADAMs can be inhibited by TIMPs with dissociation constants in the subnanomolar range [8–10]. Some members of the ADAM family, for example ADAM10, 12, 17, 19, and ADAMTS-4 and -5, have been shown to be efficiently inhibited by TIMP-3 but significantly less susceptible to the inhibitory effect of TIMP-1 and TIMP-2, except by the inhibition of ADAM10 by TIMP-1 [9]. To date there are four known resolved structures of TIMPs complexed with active MMPs [11–13]. These structures show TIMPs interacting with the catalytic domain of the MMP through six separated chain segments forming a tight non-covalent 1:1 complex. The main contact is made by the first five residues of the inhibitor binding to the active site cleft in a quasi-substrate manner. Based on the similarities between tertiary structures and interactions of MMPs with TIMP-1 and TIMP-2, it is generally believed that TIMP-3 should display a more or less identical configuration.

Given the ability of the TIMPs to interact with and inhibit MMPs it is conceivable that they might also inhibit SVMPs. Here, we examined the inhibitory pattern of TIMPs upon the proteolytic activity of atrolysin C. The differences in the inhibitory capability of TIMPs upon atrolysin C were also studied by molecular modeling and molecular dynamics in order to investigate the molecular basis of TIMPs–atrolysin C interactions.

Materials and methods

Inhibition assays of TIMPs on atrolysin C. Human recombinant TIMP-1 and TIMP-2 were expressed in mammalian cells and purified from conditioned medium as described before [14,15]. N-terminal domain of human TIMP-3 with His-tag at C-terminus was expressed in *Escherichia coli*, folded *in vitro*, and purified as described previously [16]. Atrolysin C solution was prepared to be 20 nM in TNC buffer (50 mM Tris–HCl, pH7.5, 150 mM NaCl, 1 mM $CaCl_2$, and 0.02% Brij-35). The enzyme solution (100 μl) was mixed with equal volume of TIMP solutions prepared at various concentrations in the TNC buffer. The proteinase-inhibitor mixtures (200 μl) were incubated at 37 °C for 1 h prior to addition of substrate. Twenty microliters of Azocoll50 (Calbiochem) solution (8 mg/ml in the TNC buffer) was added to each reaction and incubated for 18 h at 37 °C in bioshaker at 180 rpm. After incubation the reaction mixture was centrifuged at 3000 rpm for 3 min to precipitate the remaining substrates, the supernatant was harvested and its absorbance at 520 nm was measured to estimate the proteinase activity.

Protein structures and modeling. Atomic coordinates of TIMP-1 [11], TIMP-2 [12], and atrolysin C [6] were extracted from RCSB Protein Data Bank (web address http://www.rcsb.org/pdb) [17] with the entry codes 1UEA, 1BUV, and 1ATL, respectively. The theoretical model for N-TIMP-3 was built using the protein-modeling server Swiss-Model version 3.7 (GlaxoSmithKline, Geneva, Switzerland; web address http://www.swissmodel.expasy.org) and the resolved structures of TIMP-1 (PDB code 1UEA) and TIMP-2 (PDB codes 1BR9, 1BUV, 1GXD, and 2TMP) as templates. The modeled structure was refined through energy minimization (see *Simulations parameters and protocols* for details) and checked with the PROCHECK tool at 2.8 Å [18].

Inhibitor/proteinase binding model. Energy minimized TIMP-1, TIMP-2, and N-TIMP-3 as ligands and atrolysin C as receptor were used as inputs to the fully automated ZDOCK server (web address http://zdock.bu.edu/) [19] for protein docking computation. ZDOCK uses a fast Fourier transform-based algorithm [20] to perform a global search in the translational and rotational space. The predictions are ranked in a descending order on the basis of a scoring function for one target, being the biological knowledge essential to choose the best complex. Thus, the inhibitor orientation from the crystal structure of TIMP-1/MMP3 (PDB code 1UEA) and TIMP-2/MT1-MMP (PDB code 1BUV) complexes were used as templates. A manual inspection of output complexes was performed to select complexes in which the N-terminal loop (Cys1-X-Cys3-X) of TIMPs was oriented in the atrolysin C catalytic cleft (Hys142-Glu143) in a substrate-like fashion. Besides the TIMPs N-terminal orientation, specific interactions between the Cys1 from TIMPs and the catalytic Zn^{2+} from atrolysin C were chosen as starting parameters for molecular dynamics simulations. All complexes were analyzed using LigPlot tool [21] and based on these criteria one complex for each TIMP was proposed as the best model.

Molecular dynamics simulations. Energy minimization calculations, MD simulations, and trajectory analysis were performed using the GROMACS simulation suite [22]. Molecular visualization was done in SPDBV environment [23].

Simulations parameters and protocols. The proteins were neutralized with the necessary number of chloride or sodium counter ions and immersed in a rectangular box filled with up to 13,857 single point charge (SPC) water molecules [24]. The calculations were performed using the Gromos96 force-field and periodic boundary conditions with a cut-off radius of 1.6 nm. Electrostatic interactions were calculated with Generalized Reaction-Field method [25]. The LINCS [26] and SETTLE [27] methods were applied to constrain covalent bonds lengths. A time step of 2 fs was chosen for integrating the equations of motion.

An initial relaxation of the systems was performed through 1000 steps of the steepest descent energy minimization algorithm. The systems were heated slowly from 50 to 310 K, in steps of 5 ps, each one increasing the temperature by 50 K. Temperature and pressure were then keep constant. The simulations were carried out for 2 ns.

Simulation analysis. MD analyses were carried out to obtain a characterization of the dynamics properties of the systems. The final structures of the complexes were analyzed with LigPlot tool [21]. Resulting contact maps obtained with g_mdmat from the GROMACS package [22] were visually analyzed.

Results

Inhibition assays of atrolysin C by TIMPs

As depicted in Fig. 2, both TIMP-1 and TIMP-2 were unable to inhibit the proteolytic activity of atrolysin C upon Azocoll as substrate. In contrast, N-TIMP-3 inhibited atrolysin C in a dose-dependent manner producing a maximal inhibitory effect at a concentration of (0.6 μM) (Fig. 2). An apparent K_i value of 150 nM for N-TIMP-3 was estimated for the inhibitory effect.

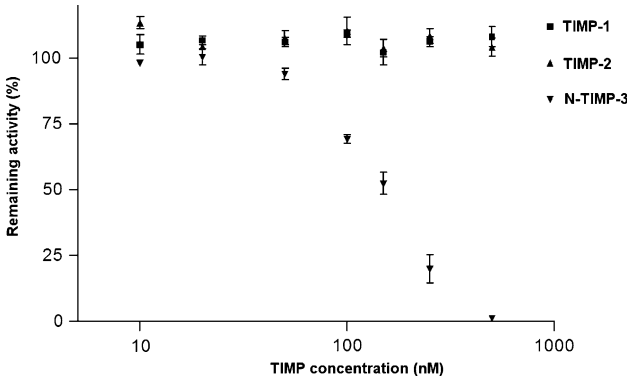

Fig. 2. Inhibition of atrolysin C by TIMPs. The relationship between TIMPs concentration (nM) and the proteolytic activity (%) of atrolysin C is shown. Azocoll was used as substrate. TIMP-1 (■) and TIMP-2 (▲) have no inhibitory activity while N-TIMP-3 (▼) is a potent inhibitor ($K_i \sim 150$ nM).

N-TIMP-3 model construction

In order to gain insight into the interaction between atrolysin C and N-TIMP-3, a model of the three-dimensional structure of the latter (amino acid sequence showed in Fig. 1B) was constructed using TIMP-1 and TIMP-2 crystallographic and NMR structures as templates. The hypothetical model was predicted with the automated server Swiss-Model version 3.7 and manually inspected. The resulting structure (Fig. 1C) was then submitted to docking to atrolysin C in order to obtain the enzyme–inhibitor interaction pattern.

Inhibitor-proteinase binding and molecular dynamics (MD) simulations

To date, four structures of TIMPs complexed with MMPs have been resolved (PDB codes 1BUV, 1BQQ, 1OO9, and 1UEA). Since, mammalian MMPs show a high degree of sequence identity in their active sites (over 75%) and considering that the enzyme's amino acids responsible for the contacts with their inhibitors are well characterized for some proteins of this family, the crystallographic complex MT1-MMP and TIMP-2 (PDB code 1BUV) was chosen to validate the algorithm of ZDOCK used in the studied system. The testing of the algorithm was done by submitting free TIMP-2 and MT1-MMP to the docking server and evaluating the obtained model for its similarity to the known crystallographic structure (data not shown).

Once the template model was correctly reproduced, the crystallographic structure of atrolysin C (PDB code 1ATL) was submitted to docking to the modeled structure of N-TIMP-3 and to the crystallographic structures of TIMP-1 (PDB code 1UEA) and TIMP-2 (PDB code 1BUV). After a detailed analysis (see Materials and methods), one complex for each inhibitor was selected as the best model for interaction. All selected complexes from the docking procedure were submitted to 2 ns unrestrained MD simulations. The behavior of the complexes was monitored visually and

the contacts were evaluated by contact maps using g_mdmat from the Gromacs package. The characterization of MD simulations was done by essential analyses.

The RMSD of the C-α during 2 ns of MD simulation was calculated with respect to the initial docking structure. The simulation of the complex between atrolysin C and N-TIMP-3 showed maintenance of the predicted docking structure. On the other hand, the obtained complexes of TIMP-1 and TIMP-2 with atrolysin C were not stable in MD simulation, suggesting the displacement of these inhibitors from the active site of the proteinase. An increase in the mobility of these two complexes can be easily observed (Fig. 3).

The amino acids responsible for the N-TIMP-3/atrolysin C interactions are summarized in Table 1 and Fig. 1C. The interacting sites of atrolysin C with its inhibitors were separated in four parts as previously described [6]. In our modeled complex we observed the maintenance of the coordination of Zn^{2+} by the Cys1 carbonyl group of N-TIMP-3 and the absence of the water molecule bound to Glu143 and Zn^{2+}. While the N-terminal portion of the inhibitor closely interacts with the active and extended binding sites of atrolysin C, the CD-loop of N-TIMP-3 makes contacts with Glu143, Glu151, and His152 of the catalytic site. The EF-loop was responsible for the interaction of the inhibitor with one of the walls from the extended binding site of the enzyme.

Interestingly, the TIMP-1/atrolysin C complex did not show a docking conformation, and the proteins remain in contact only by non-bonded interactions. The interface between the two proteins was made by TIMP-1 CD-loop and atrolysin C strand 2 of the extended binding site. Important interactions between the inhibitor N-terminal and the coordination of catalytic zinc by TIMP-1 Cys1 residue could not be observed after 2 ns of unrestrained MD simulation. TIMP-2/atrolysin C complex behaves similarly to the TIMP-1/atrolysin C complex, with main contacts made by hydrophobic interactions. The TIMP-2 molecule was displaced from the active binding site of the enzyme and the residual ineffective interactions were associated solely with the inhibitor's C-terminal domain (data not shown).

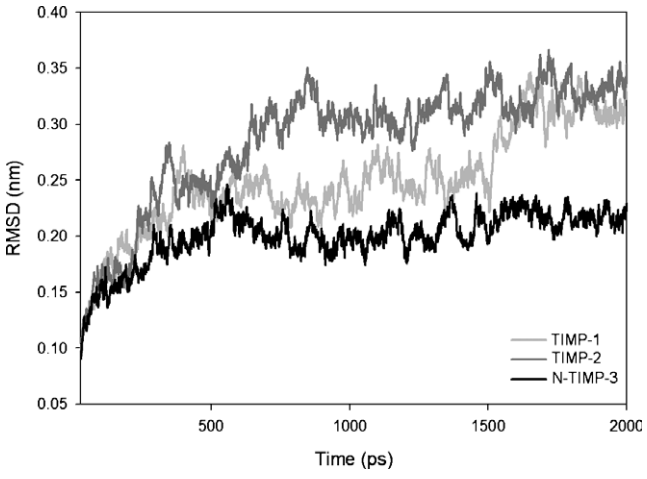

Fig. 3. C-α root mean square deviation (RMSD) of 2 ns molecular dynamics simulations of atrolysin C complexed with TIMP-1 (light grey), TIMP-2 (dark grey), and N-TIMP-3 (black line) with respect to the original docking structures.

Discussion

Although different TIMPs bind to most MMPs, some differences in inhibitory properties among TIMPs have been reported. For example, TIMP-2 and -3 but not TIMP-1 are effective inhibitors of membrane-type MMPs. TIMP-3 but not TIMP-1, -2, and -4 is a good inhibitor of ADAM17/TACE (tumor necrosis factor α-converting enzyme). The difference in the inhibition potential of the members of TIMP family with the reprolysins is not well understood. Lee and co-workers significantly advanced this field by delineating the structural requirements of TIMP-3 with ADAM17/TACE in order to develop a therapeutic agent against TACE-related diseases [28–31]. It is also known that the interaction of TIMP-3 N-terminal with TACE is not disturbed by the presence of the C-terminal portion [28]. Considering these properties of the TIMPs, we investigated the activity of TIMPs utilizing a well-characterized P-I SVMP, atrolysin C. Parallel to what was observed for other MMPs, only one member of the TIMP family demonstrated the ability to inhibit the proteolytic activity of the atrolysin C. TIMP-1 and TIMP-2 were completely inactive as inhibitors of atrolysin C while N-TIMP-3 was a potent inhibitor of this enzyme, with an apparent K_i value of 150 nM.

In order to further explore the inhibitory mechanism of N-TIMP-3 with atrolysin C, we mapped the structural requirements of these interactions using hypothetical atrolysin C/TIMP models. We then performed molecular modeling of the inhibitor, as well as the docking of the three enzyme–inhibitor complexes followed by 2 ns unrestrained MD simulations.

The complexes between metalloproteinases and TIMPs all have the same basic characteristics: six segments of TIMP molecules take part in filling the active-site cleft of MMP structure. There is, however, a great variation in the orientation of TIMPs in the MMP active site, indicating that each TIMP can adapt in a specific way to the surface of individual targets. The first five residues of TIMPs bind to the active-site cleft of the metalloproteinase in a quasi-substrate manner. Ligand Cys1 occupies the P1 site and plays a crucial role in the inhibitory mechanism since it coordinates in a bidentate manner to the enzyme's catalytic Zn^{2+} through both its α-amino and carbonyl groups. The side chains of the amino acids carboxy to Cys1 are inserted in the MMP active-site cleft forming intermolecular main chain hydrogen bonds similar to that of a substrate. The second TIMP residue extends into the S1′ pocket without filling it properly. Residues 3, 4, and 5 side chains touch the corresponding S2′, S3′, and S4′ pockets

Table 1
Amino acid interactions in atrolysin C/N-TIMP-3 complex

	Atrolysin C residue	N-TIMP-3 residue	N-TIMP-3 region	Interaction type
Zn^{2+}				
	Zn^{2+}	Cys1	N-terminus	Metal coordination
Zn^{2+} ligands				
	His142	Cys1	N-terrninus	Hydrophobic contact
		Thr2	N-terminus	Hydrophobic contact
		Cys3	N-terminus	Water-mediated
	His152	Cys1	N-terminus	Hydrogen bond
		Cys1	N-terminus	Hydrophobic contact
		Cys3	N-terminus	Water-mediated
		Glu65	CD-loop	Hydrophobic contact
		Ser66	CD-loop	Hydrogen bond
		Ser66	CD-loop	Hydrophobic contact
Active site helix				
	Thr139	Thr2	N-terminus	Hydrophobic contact
	Glu143	Cys1	N-terminus	Hydrophobic contact
		Thr2	N-terminus	Hydrophobic contact
		Ser66	CD-loop	Hydrophobic contact
Sharp turn				
	Glu151	Glu65	CD-loop	Water-mediated
		Ser66	CD-loop	Hydrophobic contact
Extended binding site				
Strand 1				
	Pro168	Cys3	N-terminus	Hydrogen bond
		Cys3	N-terminus	Hydrophobic contact
		Cys3	N-terminus	Water-mediated
	Gly169	Cys3	N-terminus	Hydrophobic contact
		Pro5	N-terminus	Hydrophobic contact
	Leu170	Cys3	N-terminus	Hydrogen bond
		Cys3	N-terminus	Hydrophobic contact
		Ser4	N-terminus	Hydrophobic contact
		Pro5	N-terminus	Hydrophobic contact
Strand 2				
	Asp104	Asn 14	1st Helix	Water-mediated
		Arg84	EF-loop	Hydrophobic contact
		Arg84	EF-loop	Water-mediated
	Glu105	Arg84	EF-loop	Hydrophobic contact
		Tyr91	EF-loop	Hydrophobic contact
		Thr92	EF-loop	Hydrophobic contact
		Gly93	EF-loop	Hydrophobic contact
		Leu94	EF-loop	Water-mediated
		Cys95	EF-loop	Hydrophobic contact
		Asn96	EF-loop	Hydrophobic contact
	Glu106	Thr2	N-terminus	Hydrophobic contact
		Ser4	N-terminus	Water-mediated
		Ser6	N-terminus	Hydrogen bond
		Ser6	N-terminus	Hydrophobic contact
		Asn14	1st Helix	Hydrogen bond
		Asn14	1st Helix	Hydrophobic contact
		Ser15	1st Helix	Water-mediated
		Thr82	EF-loop	Water-mediated
		Arg84	EF-loop	Hydrophobic contact
		Arg84	EF-loop	Water-mediated
		Cys95	EF-loop	Hydrophobic contact
	Thr107	Thr2	N-terminus	Hydrophobic contact
	Leu108	Thr2	N-terminus	Hydrogen bond
		Thr2	N-terminus	Hydrophobic contact
		Cys3	N-terminus	Hydrophobic contact
		Ser4	N-terminus	Hydrophobic contact
	Gly109	Cys1	N-terminus	Hydrogen bond
		Cys1	N-terminus	Hydrophobic contact
		Thr2	N-terminus	Hydrophobic contact
	Leu110	Cys1	N-terminus	Hydrophobic contact
	Leu113	Ser66	CD-loop	Hydrophobic contact

[10]. For the docking prediction these characteristics were considered and simulated in order to obtain enzyme–inhibitor complexes similar to known resolved complexes. Therefore, our complexes were modeled based on the assumption that the three TIMPs were capable of inhibiting atrolysin C.

In agreement with the *in vitro* enzymatic assays, the MD simulations of the complexes showed a stable N-TIMP-3/atrolysin C complex, while TIMP-1 and TIMP-2 disassembled from the enzyme structure in the first picoseconds. As summarized in Table 1, the main interactions are made by the N-terminal region of N-TIMP-3. Inhibitor Cys1 interacts with the catalytic Zn^{2+} ion and also with two catalytic histidines (His142 and His152) by its carbonyl group. Fig. 4 shows an overview of the complex between N-TIMP-3 and atrolysin C after MD simulation. The interaction site is highlighted in Fig. 4B while Fig. 4C shows the LigPlot analysis of these interactions. In crystallographic structures of MT1-MMP/TIMP-2 and MMP3/TIMP-1 the inhibitor Cys1 interacts with the Zn^{2+} ion through its carbonyl and α-amino groups, forming a bidentate coordination. A coordination of zinc only by Cys1 carbonyl group, as seen in our N-TIMP-3/atrolysin C model, was also observed in a mutational study involving N-TIMP-3. Wei et al. presented an N-TIMP-3 mutation containing an alanine residue N-terminal to the α-amino group of the Cys1 (−1A mutant), leading to a single Zn^{2+} ion coordination. The −1A mutant showed a reduced inhibitory activity on MMPs but was an effective inhibitor to TACE [32].

Other amino acids of the N-terminal loop of the inhibitor are inserted in the active site. N-TIMP-3 Thr2 extends its side chain towards the atrolysin C S1′ pocket. Although not able to completely fulfill the enzyme's pocket, a condition also observed with TIMP/MMP structures [11,12], the presence of threonine in position 2 of N-TIMP-3 seems to be a limiting structural requirement since its β-methyl group is the main factor responsible for the inhibitor's interaction in the enzyme S1′ pocket. This structural requirement is present in TIMP-1 but absent in TIMP-2, whose position 2 is occupied by a serine. At the N-terminal region of N-TIMP-3 two serine residues are also important for the binding with atrolysin C: Ser4 and Ser6 interact with atrolysin C Glu106, Leu108, and Leu170 in the extended binding sites. In TIMP-1, valine replaces serine in position 4 while position 6 is filled by proline and valine in TIMP-1 and TIMP-2, respectively.

In addition to the interaction of N-TIMP-3 N-terminal with atrolysin C, our modeled complex shows two other regions in the inhibitor structure making contacts with the enzyme. Residues Glu65 and Ser66, part of the CD-loop, interact with residues of atrolysin C active site in a similar way reported in TIMP-1/MMP3 and TIMP-2/MT1-MMP crystal structures [11,12]. These interactions are arranged in a nearly opposite orientation to the active

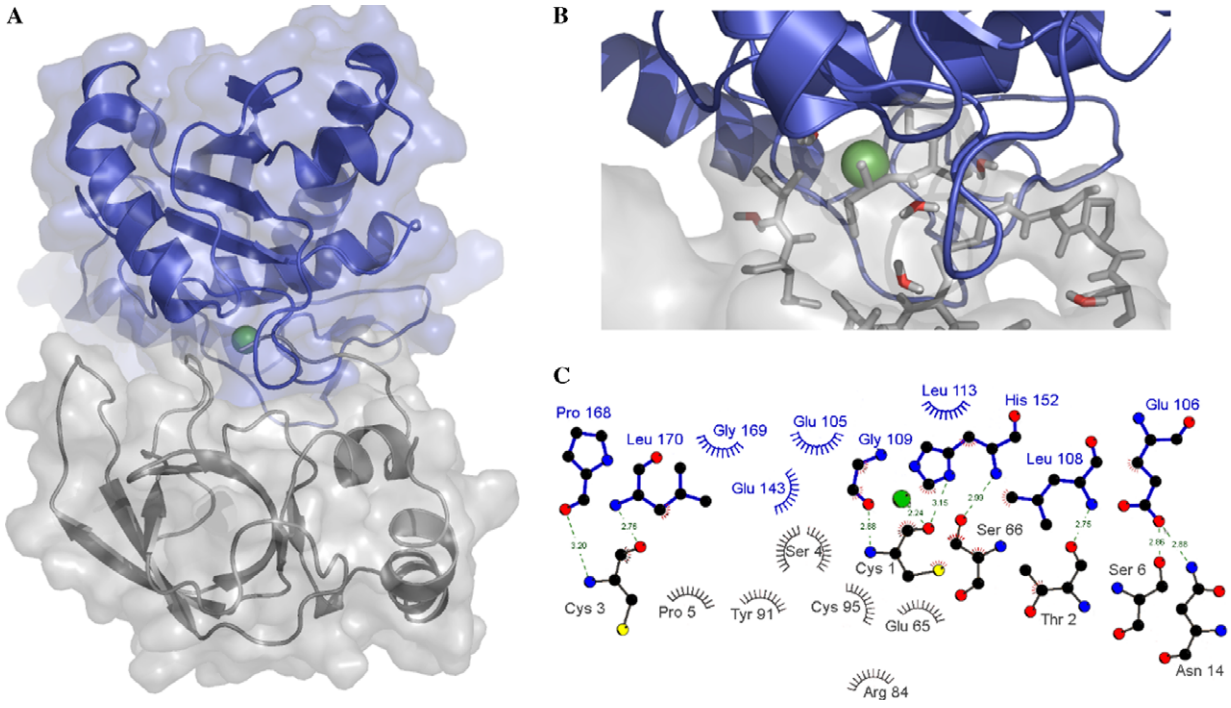

Fig. 4. Atrolysin C/N-TIMP-3 molecular complex structure. (A) Three-dimensional illustration of the interaction between atrolysin C and N-TIMP-3 after 2 ns of unrestrained molecular dynamics simulation. Atrolysin C is shown in blue and N-TIMP-3 is represented in grey. The zinc ion is illustrated as a green sphere. (B) Detailed representation of interface between atrolysin C/N-TIMP-3. N-TIMP-3 interacting amino acids are represented as grey sticks. The zinc ion is shown as a green sphere and water molecules as red and grey sticks. (C) LigPlot analysis [21] of N-TIMP-3/atrolysin C interaction. Atrolysin C amino acids are shown in blue, N-TIMP-3 amino acids are shown in grey, and the Zn^{2+} ion is represented as a light green sphere. Atomic distances are given between green doted lines. Hydrophobic contacts are represented as semi-circles.

site and are predominantly hydrophobic. The third region of contact is located in the EF-loop of N-TIMP-3. Residues of this loop are involved in hydrophobic interactions with Asp104, Glu105, and Glu106 from atrolysin C. By comparison of the sequence alignment of TIMPs (Fig. 1A), these positions in CD and EF-loops in TIMP-1 and TIMP-2 show substitutions in almost all positions. The distinct amino acid composition and the lack of atrolysin C inhibition by TIMP-1 and TIMP-2 suggest important structural determinants in enzyme inhibition. On the other hand, the AB-loop, important for interaction between TIMP-2 and MT1-MMP complex [12], seems to not be important in the formation of N-TIMP-3/atrolysin C modeled complex.

In addition to direct contacts through hydrogen bonds and hydrophobic interactions, our model also shows 11 interactions mediated by solvent molecules. The N-TIMP-3 residues involved in these interactions are located in the same regions described above (N-terminal, CD-loop, and EF-loop).

In conjunction with exploring the role of endogenous inhibitors such as TIMPs in the envenoming process, the knowledge of interaction at the molecular level can give insights into the design of more effective inhibitors for both SVMPs and perhaps, given their structural similarities, the ADAMs. TIMP-3 and N-TIMP-3 interactions have been thoroughly studied due to their broad range as metalloproteinase inhibitors and some of their molecular requirements for inhibition are already known. Similar to what has been found for the ADAMs, N-TIMP-3 was the only TIMP capable of inhibiting the activity of atrolysin C. Using a hypothetical model, our work highlights some of the structural and molecular requirements involved in the interaction between a natural inhibitor and a SVMP. Due to the structural similarity between the SVMPs and the ADAMs, studies with SVMPs can underscore aspects of the function and regulation of the ADAMs and their interactions with inhibitor molecules. Knowledge of the structural requirements for the inhibitory activity of TIMPs upon MMPs, ADAMs, and SVMPs will facilitate the design of selective TIMP variants for investigating the biological roles of specific metalloproteinases and for developing therapeutic agents for diseases associated with the activity of metalloproteinases.

Acknowledgments

We thank the Brazilian agency CAPES, Brasília, Brazil, for the PDEE fellowship to A.F.M. Pinto. This work was supported by NIH Grant AR40994 (H.N.), a Wellcome Trust grant (H.N.), CAPES (A.F.M.P.), the University of Virginia Cancer Center (J.W.F.), and Polifarma Inc. (J.W.F.).

References

[1] M. Egeblad, Z. Werb, New functions for the matrix metalloproteinases I cancer progression, Nat. Rev. Cancer 2 (2002) 161–174.
[2] C.P. Blobel, ADAMs: key components in EGFR signaling and development, Nat. Rev. Mol. Cell Biol. 6 (2005) 32–43.
[3] S. Porter, I.M. Clark, L. Kevorkian, D.R. Edwards, The ADAMTS metalloproteinases, Biochem. J. 286 (2005) 15–27.
[4] P. Gallagher, Y. Bao, S.M.T. Serrano, G.D. Laing, R.D.G. Theakston, J.M. Gutiérrez, T. Escalante, P. Zigrino, A.M. Moura-da-Silva, R. Nischt, C. Mauch, C. Moskaluk, J.W. Fox, Role of the snake venom toxin jararhagin in proinflammatory pathogenesis: *in vitro* and *in vivo* gene expression analysis of the effects of the toxin, Arch. Biochem. Biophys. 441 (2005) 1–15.
[5] J.W. Fox, S.M.T. Serrano, Structural considerations of the snake venom metalloproteinases, key members of the M12 reprolysin family of metalloproteinases, Toxicon 45 (2005) 969–985.
[6] D. Zhang, I. Botos, F.X. Gomis-Rüth, R. Doll, C. Blood, F.G. Njoroge, J.W. Fox, W. Bode, E.F. Meyer, Structural interactions of natural and synthetic inhibitors with the venom metalloproteinase, atrolysin C (form d), PNAS 91 (1994) 8447–8451.
[7] F.X. Gomis-Rüth, Structural aspects of the metzincin clan of metalloendopeptidases, Mol. Biotechnol. 24 (2003) 157–202.
[8] K. Brew, D. Dinakarpandian, H. Nagase, Tissue inhibitors of metalloproteinases: evolution, structure and function, Biochim. Biophys. Acta 1477 (2000) 267–283.
[9] A.H. Baker, D.R. Edwards, G. Murphy, Metalloproteinase inhibitors: biological actions and therapeutic opportunities, J. Cell Sci. 115 (2002) 3719–3727.
[10] K. Maskos, Crystal structure of MMPs in complex with physiological and pharmacological inhibitors, Biochimie 86 (2005) 249–263.
[11] F.X. Gomis-Rüth, K. Maskos, M. Betz, A. Bergner, R. Huber, K. Suzuki, N. Yoshida, H. Nagase, K. Brew, G.P. Bourenkov, H. Bartunik, W. Bode, Mechanism of inhibition of the human metalloproteinase stromelysin-1 by TIMP-1, Nature 389 (1997) 77–81.
[12] C. Fernadez-Catalan, W. Bode, R. Huber, D. Turk, J.J. Calvete, A. Lichte, H. Tschesche, K. Maskos, Crystal structure of the complex formed by the membrane type 1-matrix metallproteinase with the tissue inhibitor of metalloproteinase-2, the soluble progelatinae A receptor, EMBO J. 17 (1998) 5238–5248.
[13] S. Arumugam, S.R. Van Doren, Global orientation of bound MMP-3 and N-TIMP-1 in solution via residual dipolar couplings, Biochemistry 42 (2003) 7950–7958.
[14] W. Huang, K. Suzuki, H. Nagase, S. Arumugan, S.R. Van Doren, K. Brew, Folding and characterization of the amino-terminal domain of human tissue inhibitor of metalloproteinase-1 (TIMP-1) expressed at high yield in *E. coli*, FEBS Lett. 384 (1996) 155–161.
[15] L. Troeberg, M. Tanaka, R. Wait, Y.E. Shi, K. Brew, H. Nagase, *E. coli* expression of TIMP-4 and comparative kinetic studies with TIMP-1 and TIMP-2: insights into the interactions of TIMPs and matrix metalloproteinase 2 (gelatinase A), Biochemistry 41 (2002) 15025–15035.
[16] M. Kashiwagi, M. Tortorella, H. Nagase, K. Brew, TIMP-3 is a potent inhibitor of aggrecanase 1 (ADAM-TS4) and aggrecanase 2 (ADAM-TS5), J. Biol. Chem. 276 (2001) 12501–12504.
[17] H.M. Berman, J. Westbrook, Z. Feng, G. Gilliland, T.N. Bhat, H. Weissig, I.N. Shindyalov, P.E. Bourne, The protein data bank, Nucleic Acids Res. 28 (2000) 235–242.
[18] R.A. Laskowski, M.W. MacArthur, D.S. Moss, J.M. Thornton, PROCHECK: a program to check the stereochemical quality of protein structures, J. Appl. Cryst. 26 (1993) 283–291.
[19] R. Chen, Z. Weng, A novel shape complementarity scoring function for protein–protein docking, Proteins 51 (2003) 397–408.
[20] R. Chen, Z. Weng, Docking unbound proteins using shape complementarity, desolvation and electrostatics, Proteins 47 (2002) 281–294.
[21] A.C. Wallace, R.A. Laskowski, J.M. Thornton, LIGPLOT: a program to generate schematic diagrams of protein-ligand interactions, Protein Eng. 8 (1995) 127–134.
[22] E. Lindahl, B. Hess, D. van der Spoel, Gromacs 3.0: a package for molecular simulation and trajectory analysis, J. Mol. Model. 7 (2001) 306–317.

[23] N. Guex, M.C. Peitsch, Swiss Model and the Swiss-PdbViewer: an environment for comparative protein modeling, Electrophoresis 18 (1997) 2714–2723.
[24] H.J.C. Berendsen, J.R. Grigera, T.P. Straatsma, The missing term in effective pair potentials, J. Phys. Chem. 91 (1987) 6269–6271.
[25] I.G. Tironi, R. Sperb, P.E. Smith, W.F.A. van Gunsteren, A generalized reaction-field method for molecular dynamics simulations, J. Chem. Phys. 102 (1995) 5451–5459.
[26] B. Hess, H. Bekker, H.J.C. Berendsen, J.G.E.M. Fraaije, LINCS: a linear constraint solver for molecular simulations, J. Comput. Chem. 18 (1997) 1463–1472.
[27] S. Miyamoto, P.A. Kollman, SETTLE: an analytical version of the SHAKE and RATTLE algorithm for rigid water models, J. Comput. Chem. 13 (1992) 952–962.
[28] M.H. Lee, V. Knäuper, J.D. Becherer, G. Murphy, Full-length and N-TIMP-3 display equal inhibitory activities toward TNF-α convertase, Biochem. Biophys. Res. Commun. 280 (2001) 945–950.
[29] M.H. Lee, K. Maskos, V. Knäuper, P. Dodds, G. Murphy, Mapping and characterization of the functional epitopes of tissue inhibitor of metalloproteinases (TIMP)-3 using TIMP-1 as the scaffold: a new frontier in TIMP engineering, Protein Sci. 11 (2002) 2493–2503.
[30] M.H. Lee, M. Rapti, G. Murphy, Delineating the molecular basis of the inactivity of tissue inhibitor of metalloproteinase-2 against tumor necrosis factor-α-converting enzyme, J. Biol. Chem. 279 (2004) 45121–45129.
[31] M.H. Lee, M. Rapti, G. Murphy, Total conversion of tissue inhibitor of metalloproteinase (TIMP) for specific metalloproteinase targeting: fine-tuning TIMP-4 for optimal inhibition of tumor necrosis factor-α-converting enzyme, J. Biol. Chem. 280 (2005) 15967–15975.
[32] S. Wei, M. Kashiwagi, S. Kota, Z. Xie, H. Nagase, K. Brew, Reactive site mutations in tissue inhibitor of metalloproteinase-3 disrupt inhibition of matrix metalloproteinases but not tumor necrosis factor-α-converting enzyme, J. Biol. Chem. 280 (2005) 32877–32882.

2.3.2. Mapeamento de sítios de ligação de domínio A de fator de von Willebrand no domínio rico-em-cisteínas de metaloproteinases de venenos de serpentes

Antonio F. M. Pinto, Renata M. S. Terra, Jorge A. Guimarães, Jay W. Fox. 2006. Mapping von Willebrand Factor A Domain Binding Sites on a Snake Venom Metalloproteinase Cysteine-Rich Domain. Archives of Biochemistry and Biophysics.

Apenas recentemente a primeira estrutura tridimensional de uma metaloproteinase de veneno de serpente da classe PIII foi resolvida. Além das dificuldades normais de cristalização, as SVMPs ainda se apresentam em diferentes isoformas, devido muito provavelmente ao número ímpar de resíduos de cisteína em sua estrutura. Quando resolvida, a estrutura cristalográfica do domínio rico-em-cisteínas mostrou um dobramento inédito. Esse domínio tem sido implicado em muitas das atividades das SVMPs, tais como inibição de agregação plaquetária e interações proteína-proteína.

Nesse trabalho, identificamos uma região específica do domínio rico-em-cisteínas da SVMPs da classe PIII jararragina capaz de interagir com o domínio A de fator de von Willebrand (vWA). Com o uso de ferramentas de bioinformática, construímos um modelo tridimensional de jararragina, identificando a região de interação com vWF no domínio rico-em-cisteínas.

Considerando que numerosas proteínas de matriz possuem domínios A de fator de von Willebrand, isso leva a especulação de que a interação do domínio rico-em-cisteínas

das SVMPs com vWA seja uma característica chave no direcionamento da toxina para substratos relevantes que, quando clivados, levam à hemorragia.

Este trabalho, desenvolvido na Biomolecular Research Facility (University of Virginia) em colaboração com o Laboratório de Bioquímica Farmacológica (UFGRS), foi submetido em setembro de 2006 à revista *Archives of Biochemistry and Biophysics*. Em 12 de outubro de 2006, recebemos a carta de aceite do trabalho.

Available online at www.sciencedirect.com
ScienceDirect
Archives of Biochemistry and Biophysics 457 (2007) 41–46
47
ABB
www.elsevier.com/locate/yabbi

Mapping von Willebrand factor A domain binding sites on a snake venom metalloproteinase cysteine-rich domain

Antonio F.M. Pinto [a,b], Renata M.S. Terra [b], Jorge A. Guimaraes [b], Jay W. Fox [a,*]

[a] *Department of Microbiology, University of Virginia, P.O. Box 800734, Charlottesville, VA 22908-0734, USA*
[b] *Centro de Biotecnologia, Universidade Federal do Rio Grande do Sul, P.O. Box 15005, Porto Alegre, RS, Brazil*

Received 18 September 2006, and in revised form 7 October 2006
Available online 10 November 2006

Abstract

The PIII class of the snake venom metalloproteinases (SVMPS) are acknowledged to be one of the major hemorrhage producing toxins in crotalid venoms. This class of SVMPS are structurally distinguished by the presence of disintegrin-like and cysteine-rich domains carboxy to the metalloproteinase domain and thus share structural homology with many of the ADAMs proteins. It has been suggested that the presence of the carboxy domain are the key structural determinants for potent hemorrhagic activity in that they may serve to target the proteinases to specific key extracellular matrix and cell surface substrates for proteolysis leading to hemorrhage production at the capillaries. Following from previous studies in our laboratory in this investigation we scanned the cysteine-rich domain of the PIII hemorrhagic SVMP jararhagin using synthetic peptides in an attempt to identify regions which could bind to von Willebrand factor (vWF), a known binding partner for jararhagin. From these studies we identified two such peptide, Jar6 and Jar7 that could support binding to vWF as well as block the recombinant cysteine-rich domain of jararhagin binding to vWF. Using the coordinates for the recently solved crystal structure of the PIII SVMP VAP1, we modeled the structure of jararhagin and attempted to dock the modeled cysteine-rich structure of that protein to the A1 domain of vWF. These studies indicated that effective protein–protein interaction between the two ligands was possible and supported the data indicating that the Jar6 peptide was involved, whereas the Jar7 peptide was observed to be sterically blocked from interaction. In summary, our studies have identified a region on the cysteine-rich domain of a PIII SVMP that interacts with vWF and based on molecular modeling could be involving in the interaction of the cysteine-rich domain of the SVMP with the A1 domain of vWF thus serving to target the toxin to the protein for subsequent proteolytic degradation.

Keywords: Snake venom metalloproteinases; von Willebrand factor; Cysteine-rich domain; SVMP; vWF A domains

The local and systemic hemorrhage resulting from envenomation by crotalid snakes is in large part due to the hemorrhagic metalloproteinases present in these venoms [1]. In general it is considered that hemorrhage occurs following proteolytic degradation of extracellular matrix proteins and endothelial cell surface proteins involved in the maintenance of capillary structural and functional integrity [1]. The snake venom metalloproteinases (SVMPs)[1] responsible for this degradation comprise a subgroup of the reprolysin subfamily of the M12 class of metalloproteinases [2]. The classification of these enzymes is based on size and different domain structures: PI SVMPs have only a metalloproteinase domain; PII have metalloproteinase and disintegrin domain; PIII SVMPs are synthesized with metalloproteinase, disintegrin-like and cysteine-rich domain and PIV have the PIII domain structure plus lectin-like domains connected by disulfide bonds [1]. The PIII class, the most potent SVMP class, is related to the ADAM (A Disintegrin And Metalloproteinase) protein family, which contains besides the metalloproteinase, disintegrin-like and cysteine-rich domains an epidermal growth factor-like region, a transmembrane region and a cytoplasmic tail [3].

* Corresponding author. Fax. +1 434 982 2514.
E-mail address: jwf8x@virginia.edu (J.W. Fox).

[1] *Abbreviations used:* SVMP, snake venom metalloproteinase; ADAM, a disintegrin and metalloproteinase; RP-HPLC, reversed phase-high performance liquid chromatography.

0003-9861/$ - see front matter © 2006 Elsevier Inc. All rights reserved.
doi:10.1016/j.abb.2006.10.010

Closely related to the ADAMs are the multidomain, extracellular ADAMTS proteins. ADAMTS proteins are distinguished from the ADAMs proper primarily by the fact that they lack the transmembrane and cytoplasmic domains of the ADAMs and have one or more thrombospondin motif domains [4]. One member of the ADAMTS family, ADAMTS-13, has been observed to play a critical role in human hemostasis by binding to and proteolytically degrading multimeric vWF to small complexes which are less able to spontaneously give rise to thrombi [5,6]. Genetic lesions in ADAMTS-13 which abolish or decrease its ability to degrade large multimeric vWF leads to the disease thrombotic thrombocytopenic purpura distinguished by microvascular vWF and platelet rich thrombi leading to anaemia, renal failure and neurological dysfunction [7,8]. Several studies have shown that ADAMTS-13 interaction with vWF is via its disintegrin-like/cysteine-rich domain and this interaction is necessary for effective degradation of vWF [9]. Similar studies have shown that the PIII SVMPs are also capable of binding to and proteolytically cleaving vWF [10,11].

In light of the fact that the PIII class display the greatest hemorrhagic potency of the SVMPs there have been several studies investigating the role of the disintegrin-like/cysteine-rich domains, the distinguishing features of this class. Usamai and colleagues demonstrated that jararhagin-C, the disintegrin-like/cysteine-rich domains proteolytic product from the PIII hemorrhagic SVMP jararhagin, isolated from the venom of *Bothrops jararaca* inhibited collagen and ADP-stimulated platelet aggregation [12]. This activity for the disintegrin-like/cysteine-rich domains of PIII SVMPs was corroborated by Jia and colleagues who showed that a recombinant disintegrin-like/cysteine-rich domain containing protein based on atrolysin A, a PIII hemorrhagic SVMP from *Crotalus atrox*, was capable of inhibiting collagen-stimulated platelet aggregation [13]. The capability of the cysteine-rich domain alone to recapitulate the activity of the disintegrin-like/cysteine-rich domains for inhibiting platelet aggregation was demonstrated by Jia and colleagues using a recombinant cysteine-rich domain from atrolysin A [14]. Recently, these studies were extended to shown that the cysteine-rich domain of PIII SVMPs was responsible for the interaction to, and presumably the degradation of von Willebrand factor (vWF) [15]. These data indicated a functional role of the cysteine-rich domain of the PIII SVMPs in targeting them to proteins involved in platelet aggregation such as the $\alpha 2\beta 1$ integrin and vWF. Recent studies from our laboratory have shown that the cysteine-rich domain of the jararhagin is capable of targeting other proteins which contain vWF A domains, such as collagen XII and XIV and matrilins, for proteolytic degradation (under review for publication). Finally, the crystal structure of a PIII SVMP, vascular apoptosis protein 1, from *Crotalus atrox*, was recently reported [16]. From the crystal structure of VAP1 it was clearly observed that the ECD sequence motif, which has been suggested to be involved in integrin binding by this domain, was sterically unavailable for interaction. Thus the site(s) of interaction with integrins likely reside elsewhere with the protruding cysteine-rich domain at the carboxy region of the structure an obvious candidate [16].

In this study, we describe the use of synthetic peptides spanning the cysteine-rich domain of the hemorrhagic PIII SVMP jararhagin to localize the site of interaction on this domain with vWF. Using this approach we identified two peptides capable of binding to vWF and blocking the binding of recombinant jararhagin cysteine-rich domain to vWF. Mapping of these peptides on the structure of the cysteine-rich domain of VAP1 suggest that only the region in the domain represented by the peptide Jar6 is sterically available for protein–protein interaction. In addition, we show via molecular modeling that the cysteine-rich domain of jararhagin could potentially interact with the A1 domain of vWF supported in part by the interaction deliminated by the Jar6 peptide.

Materials and methods

Peptide synthesis

Peptides were designed based on the sequence of the cysteine-rich domain of jararhagin, a PIII SVMP from *Bothrops jararaca* venom. All peptides were synthesized on a Symphony multiple peptide synthesizer (Rainin) using Fmoc (*N*-(9-fluorenyl) methoxycarbonyl) chemistry according to the manufacture's recommendation. Peptides were purified to homogeneity by RP-HPLC (reversed phase-high performance liquid chromatography) and desalted by gel filtration chromatography. Following purification the peptides, all of which had cysteinyl residues near the N- and C-terminal were cyclized by air oxidation as previously described [13].The peptides were then analyzed by MALDI-TOF mass spectrometry to confirm the correct mass and cyclization of the peptide. Lyophilized peptides were dissolved in HBS-EP buffer [10 mM Hepes, pH 7.4, 150 mM NaCl, 3.4 mM EDTA and 0.005% (v/v) surfactant P20; BIAcore™] to final concentration of 1 μg/μl immediately prior to use. One cyclized peptide, Jar6, was also reduced and carboxyamidomethylated [15].

Expression of recombinant atrolysin a cysteine-rich domain

The expression vector for the cysteine-rich domain of atrolysin A (A/C) was constructed as described elsewhere [15]. Briefly, cDNA fragment of atrolysin A (301–413) was amplified by PCR from the plasmid pMbacA/C and subcloned into the pET102/D-TOPO bacterial expression vector (Invitrogen). BL21 Star (DE3) *Escherichia coli* cells (Invitrogen) were transformed by heat shock with the plasmid pET102/D-A/C, according to the manufacturer's instructions and grown overnight at 37 °C. Bacterial cells were inoculated in LB and expression of recombinant proteins was induced by 1 mM IPTG (isopropyl *b*-D-thiogalactoside) for 3 h at 37 °C. Cell pellet was lysed by French press in lysis buffer [50 mM potassium phosphate, pH 7.8, 400 mM NaCl, 100 mM KCl, 10% (v/v) glycerol, 0.5% (v/v) Triton X-100, 0.1 mg/ml lysozyme, 10 mM imidazole and 1 mM PMSF], and resulting suspension centrifuged at 10000*g* for 30 min at 4 °C. Soluble fraction was applied onto a Talon metal affinity column (Clontech). The column was washed with binding buffer and bound proteins were eluted with binding buffer containing 0.15 M imidazole. Protein homogeneity was determined by SDS–PAGE and MALDI-TOF mass spectrometry.

Surface plasmon resonance assays

Protein–peptide and protein–protein interactions were studied by surface plasmon resonance using the BIAcore™ 3000 system, at 25 °C. vWF

(MP Biomedicals, USA) was covalently immobilized on a BIAcore™ CM-5 sensorchip (carboxylated dextranmatrix) according to the manufacturer's instructions. The CM-5 chip was activated with a 1:1 mixture of 75 mg/ml EDC [1-ethyl-3-(3-dimethylaminopropyl)carbodi-imide] and 11.5 mg/ml NHS (*N*-hydroxysuccinimide) for 7 min. vWF (10 μg/ml in 10 mM sodium citrate, pH 4.5) was injected over the CM-5 chip for 7 min at a flow rate of 5 μl/min, at 4 °C. Remaining active groups on the matrix were blocked with 1 Methanolamine/HCl, pH 8.5. Immobilization of vWF on a CM-5 sensorchip resulted in a surface concentration of 12.5 ng/mm^2. Recombinant A/C and peptides solutions were prepared in HBS-EP buffer [10 mM Hepes, pH 7.4, 150 mM NaCl, 3.4 mM EDTA and 0.005% (v/v) surfactant P20; BIAcoreTM] and were injected at a flow rate of 50 μl/min. The non-linear fitting of association and dissociation curves according to a 1:1 model was used for the calculation of kinetic constants (BIAevaluation software, version 3.1).

Platelet aggregation assay

Venous blood from healthy donors was mixed with 3.8% trisodium citrate (9:1 v/v) and centrifuged at room temperature at 350*g*, twice for 3 min and once for 5 min, to obtain platelet-rich plasma (PRP). Platelets in PRP were diluted to the final concentration of 2.5×10^8 cells/ml. Platelet aggregation in the presence of jararhagin cys-rich domain peptides (up to concentrations of 1 mM) was assayed by adding collagen in a final concentration of 5 μg/ml. All aggregation patterns were recorded at 37 °C over 6 min, under constant stirring in an aggregometer at 1000 rpm.

Protein structures and modeling

Atomic coordinates of the vascular apoptosis-inducing protein-1 (VAP-1) from *Crotalus atrox* venom [16] were extracted from RCSB Protein Data Bank (web address http://www.rcsb.org/pdb) [17] with the entry code 2ERO. The PDB entry code for von Willebrand A1 domain structure was 1AUQ [18]. The theoretical model for jararhagin was built with the protein-modeling server Swiss-Model version 3.7 (GlaxoSmithKline, Geneva, Switzerland; web address http://www.swissmodel.expasy.org), using the resolved structures of VAP-1 as template. The modeled structure was refined through energy minimization using Gromos96 implemented in Swiss PDB viewer. The modeled structure was then checked with the PROCHECK tool at 2.5 [19].

To determine the binding potential of the modeled structure of jararhagin cys-rich domain to vWF A1 domain we tested molecular docking using Hex 4.5 software [20] (web address http://www.csd.abdn.ac.uk/hex/). The protein docking structures were evaluated based on the experimental data. The best model was then submitted to an 800 ps molecular dynamics simulation.

Molecular dynamics (MD) simulation and trajectory analysis were performed using the GROMACS simulation suite [21]. Molecular visualization was done in SPDBV environment [22]. The proteins were neutralized with the necessary number of chloride counter ions and immersed in a rectangular box filled with single point charge (SPC) water molecules [23]. The calculations were performed using the Gromos96 force-field and periodic boundary conditions with a cut-off radius of 1.6 nm. Electrostatic interactions were calculated with Particle-mesh Ewald (PME) [24]. The LINCS [25] and SETTLE [26] methods were applied to constrain covalent bonds lengths. A time step of 1 fs was chosen for integrating the equations of motion. An initial relaxation of the system was performed through 1000 steps of the steepest descent energy minimization algorithm. The system was heated slowly from 50 to 310 K, in steps of 5 ps, each one increasing the temperature by 50 K. Temperature and pressure were then keep constant. MD analyses were carried out to obtain a characterization of the dynamics properties of the systems. The final structures of the complexes were analyzed with LigPlot tool [27].

Results

Identification of peptides from jararhagin cysteine-rich domain that interact with vWF

Eleven cyclized peptides designed based on the jararhagin cysteine-rich domain sequence (Table 1) were assayed for binding to a sensor chip with immobilized vWF by surface plasmon resonance. Kinetic evaluation of the interaction of recombinant A/C domain with vWF according to a 1:1 model was used as control, which showed a high-affinity binding, as indicated by the high association rates and the low dissociation rates. These rates gave an equilibrium dissociation constant (K_D) of 74.4 nM for the recombinant domain. Only two of the peptides assayed, Jar6 (^{365}PCAPEDVKCG^{374}) and Jar7 (^{372}KCGRLYCK^{379}) showed significant binding capability with equilibrium dissociation constants of 3.5 and 5.8 μM, respectively (Fig. 1 and Table 1). Reduction and alkylation of Jar6 gave rise to a complete loss of binding activity to vWF (data not shown) suggesting that the cyclized structure of the peptide maybe critical for the presentation of residues in the loop to the binding site on vWF.

Specificity of interaction of cysteine-rich peptides and vWF

The specificity of the interaction of Jar6 and Jar7 with vWF was tested in a competition assay using surface plasmon resonance. The binding of A/C domain was partially

Table 1
Surface plasmon resonance kinetic evaluation of the interaction of cysteine-rich domain and jararhagin peptides (Jar1–11) with vWF immobilized on CM-5 sensor chip in the BIAcore 3000 system

Peptide		k_a(1/Ms)	K_d(1/s)	K_D(M)
A/C		0.25×10^6	18.7×10^{-3}	0.074×10^{-6}
Jar1	^{315}YCYNGNCP^{322}		No binding	
Jar2	^{320}NCPIMYHQCY^{329}		No binding	
Jar3	^{327}QCYALFGADVYEAEDSCF^{344}		No binding	
Jar4	^{342}SCFKDNQKGNYYGYCR^{357}		No binding	
Jar5	^{355}YCRKENGKKIPCA^{357}		No binding	
Jar6	^{365}PCAPEDVKCG^{374}	0.96×10^3	3.38×10^{-3}	3.50×10^{-6}
Jar7	^{372}KCGRLYCK^{379}	0.58×10^3	2.40×10^{-3}	5.85×10^{-6}
Jar8	^{377}YCKDNSPGQNNPCK^{390}		No binding	
Jar9	^{388}PCKMFYSNDDEHKGMVLPGTKCA^{410}		No binding	
Jar10	^{408}KCADGKVCS^{416}		No binding	
Jar11	^{414}VCSNGHCV^{421}		No binding	

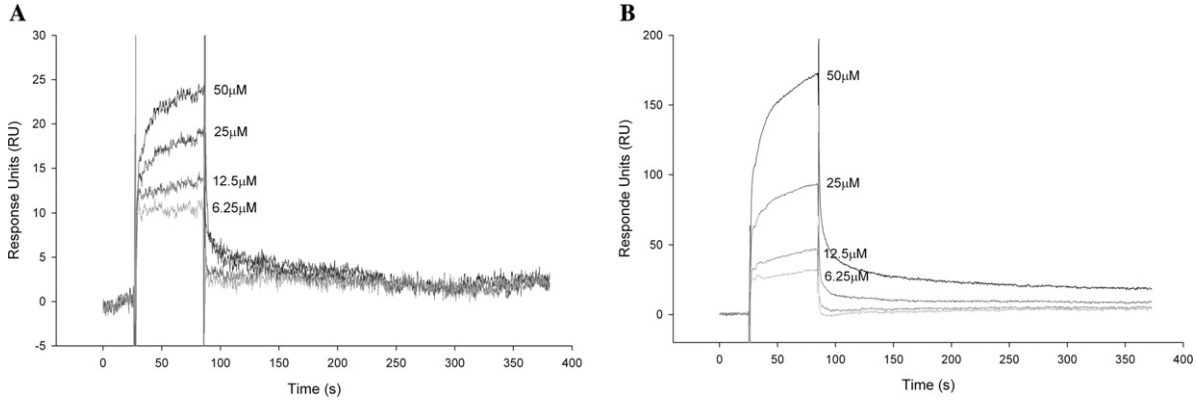

Fig. 1. Interaction of jararhagin peptides with von Willebrand factor (vWF). Jar6 (A) and Jar7 (B) at different concentrations were injected over immobilized vWF at a flow rate of 50 μl/min.

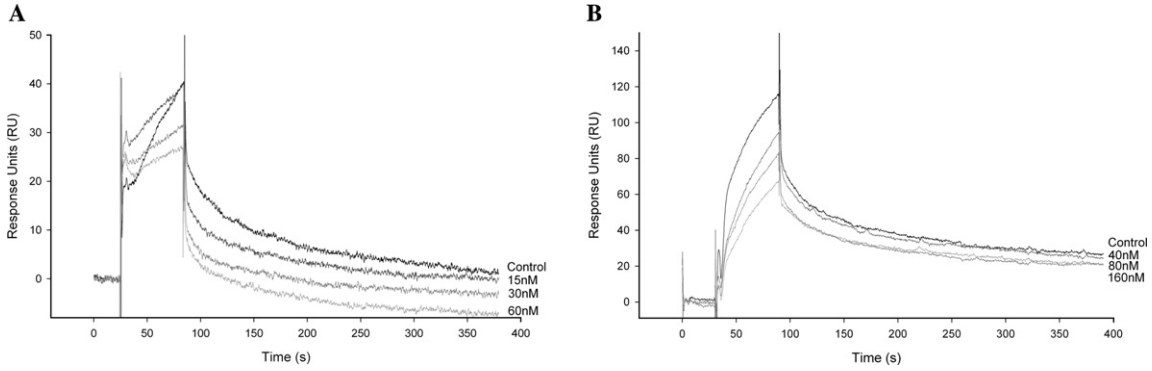

Fig. 2. Inhibition of binding of cysteine-rich domain binding to vWF by jararhagin peptides. Jar6 (A) and Jar7 (B) at different concentrations were injected over immobilized vWF in the presence of 16.7 nM cysteine-rich domain. Concentrations of peptides are indicated.

inhibited in the presence of the peptides. As seen in Fig. 2A, Jar6 inhibits A/C at low peptide concentration (15–60 nM). Fig. 2B shows only a low inhibition of A/C domain binding to vWF by the peptide Jar7 at higher concentrations (40–160 nM). This difference in effective competition concentration correlates with the observed differences of the K_D value of Jar6 and Jar7 (3.5 and 5.8 μM, respectively) binding to vWF. Thus, the results indicate that the peptides and full-length domain are competing for the same binding site in the vWF structure.

Effect of cysteine-rich peptides on platelet aggregation

Collagen-stimulated platelet aggregation using PRP or isolated platelets was measured in the presence of either Jar6 or Jar7 to assess the activity of the peptides to block platelet aggregation. No inhibition of isolated platelets or PRP aggregation using either peptide at concentrations up to 1 mM was observed (data not shown).

Mapping Jar6 and Jar7 peptides on the modeled cys-rich domain of jararhagin

Fig. 3A shows the modeled jararhagin structure based on the VAP1 structure deposited in the RCSB PDB databank [16]. According to the Ramachandran Plot of the structure obtained from PROCHECK, 99.5% of the residues are in allowed conformations. As one would expect the jararhagin modeled structure appears similar to the crystal structure of VAP1.

Figs. 3B and C show the localization of peptides Jar6 and Jar7 in the cysteine-rich domain structure, respectively. The peptide Jar7 is located in a small β-sheet and shows minimal access to the solvent, suggesting that its interaction with vWF is an artifact and likely irrelevant to the biological activity of jararhagin cysteine-rich domain. As shown in Fig. 3B, peptide Jar6 is highly accessible to the solvent and thus could play a role in protein–protein interaction.

Docking of the jarahagin cys-rich domain model to the crystal structure of the vWF A1 domain

Given our results of the jararhagin Jar6 and Jar7 peptide binding to vWF and the possibility that the cysteine-rich domain of jararhagin could be interacting the vWF A domains [15] we assessed whether the model for the jararhagin cysteine-rich domain could productively dock with the A1 domain of vWF. The molecular docking was performed using Hex 4.5 software. Previous studies in our laboratory have shown that recombinant cys-rich domain blocks the binding of ristocetin to vWF (unpublished

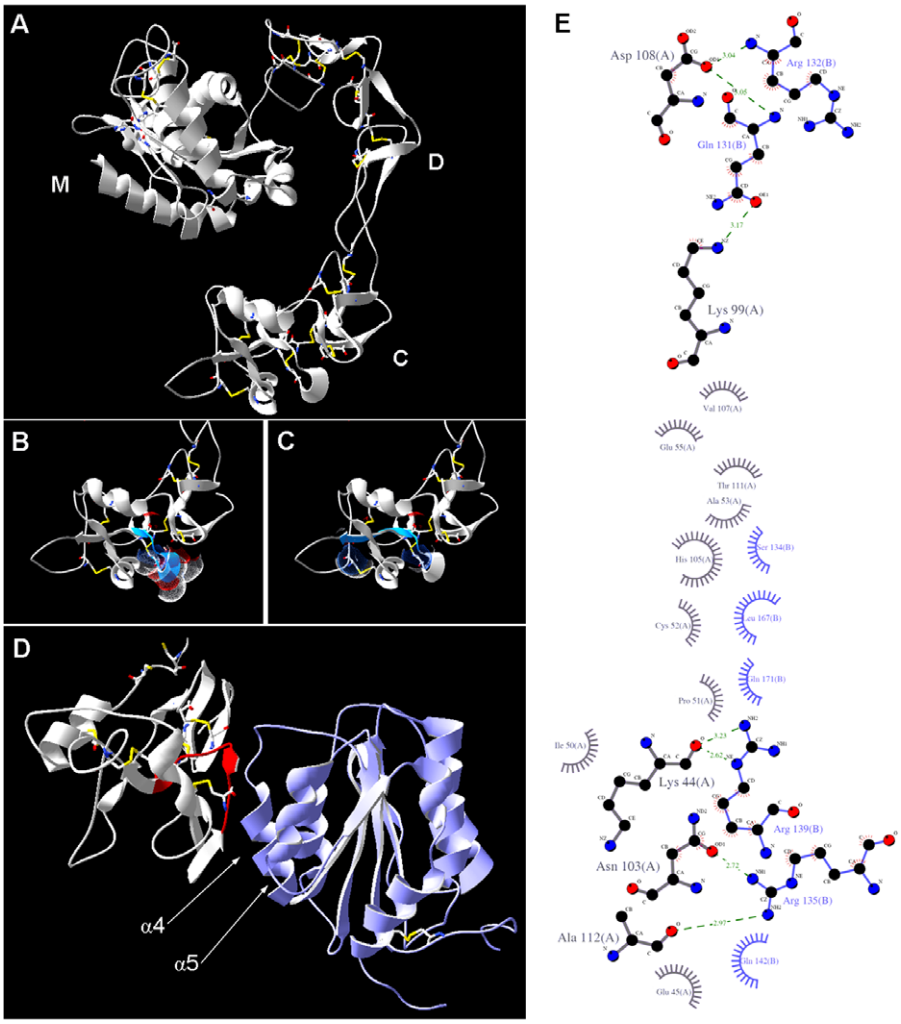

Fig. 3. Structural analysis of the P-III SVMP jararhagin model. (A) Jararhagin view. Metalloproteinase (M), disintegrin (D) and cysteine-rich (C) domains are indicated. Zinc ion is represented as a grey sphere. (B and C) Peptides ^{365}PCAPEDVKCG^{374} (Jar6), ^{372}KCGRLYCK^{379} (Jar7) are represented in blue, respectively. Solvent accessibility of the residues in each peptide is represented in dotted spheres and colored by atoms (carbon in white, oxygen in red and nitrogen in blue). (D) Docked structure of jararhagin cysteine-rich domain (grey) and vWF A1 domain (light blue). The peptide Jar6 region is colored in red. vWF A1 α4 and α5 helices are indicated. Disulfide bonds are represented by yellow sticks. (E) LigPlot [27] analysis of Jararhagin cysteine-rich domain and vWF A1 domain interaction. Jararhagin cysteine-rich domain and vWF A1 domain amino acids are shown in grey and light blue, respectively. Atomic distances are given between green doted lines. Hydrophobic contacts are represented as semi-circles.

data). Ristocetin is a glycopeptide synthesized by actinomycete *Nocardia lurida* which interacts with vWF specifically through the A1 domain. Therefore the A1 domain is a likely candidate for the site of interaction of the cysteine-rich domain [28]. Considering this, the modeled jararhagin cys-rich domain was oriented into the vWA1 domain assuming the region of interaction was similar to the binding site of the C-type lectins botrocetin and bitiscetin [29,30]. The docking structures were evaluated according to the interaction with helices α4 and α5 of vWA1 domain. The best docked structure was selected and submitted to 800 ps molecular dynamics. The resulting structure (Fig. 3D) indicates that jararhgin cys-rich domain could effectively interact with vWA1 domain through the α4 and α5 helices. Fig. 3E shows the LigPlot analysis of these interactions.

Discussion

Due to the potent hemorrhagic activity of the PIII SVMPs it has long been hypothesized that the disintegrin-like and/or cysteine-rich domain of this class of SVMPs must play a critical role in this activity [1]. This is supported by the fact that the PIII SVMPS display a diverse repertoire of protein–protein interactions which likely are critical to their biological/pathological activities. PIII SVMPs have been shown to bind to α2β1 integrins on platelets and cells [13,31,32], collagens [14,15,33] and vWF [11,15,34]. The cysteine-rich domain in these PIIIs has been shown to be involved in these interactions [14,15]. In previous studies two peptides sequences (^{326}HQCYALFGADVYEAEDSC^{343} and ^{371}VKCGRLYCKDNSPGQ^{386}) in the cysteine-rich domain of the PIII metalloproteinases atrolysin

A and jararhagin were identified as capable of blocking platelet aggregation, probably via α2β1 [35]. One of these peptides is located in the hyper-variable region of the cysteine-rich domain described by Takeda and collaborators as a potential protein–protein interaction site [16].

In this investigation, we identified two peptide sequences from the cysteine-rich domain of jararhagin which could bind to vWF and block cysteine-rich domain binding. Localization of the peptide sequences on a modeled cysteine-rich domain of jararhagin based on the VAP1 crystal structure indicated that only one of the peptides, Jar6, could potentially interact with other protein structures. Based on the likelihood that the site of interaction of the cysteine-rich domain of jararhagin and the Jar6 peptide on vWF was the vWF A1 domain we performed molecular docking simulations which showed that the modeled cysteine-rich domain of jararhagin could interact with the vWF A1 domain at the ristocetin binding site and the interaction would involve the Jar6 peptide sequence. Thus, in summary we believe that the interaction of many PIII SVMPs via their cysteine-rich domains can bind to vWF A domains to enhance their biological/pathological activities. This is underscored by previous studies which demonstrated that PIII SVMP binding to vWF and the integrin α2β1, both of which have vWF A1 domains, result in cleavage by the SVMP [11,35]. It is well established that extracellular matrix degradation, particularly in the region of capillaries, as well as the basement membranes surrounding capillaries is critical for the production of hemorrhage, the hallmark pathology associated with PIII SVMP toxins in snake venoms [36,37]. In light of the fact that numerous extracellular matrix proteins contain vWF A domains lead to the speculation that the interaction of the cysteine-rich domains of PIII SVMPs with extracellular matrix proteins with vWF A domains may be a key feature in toxin targeting to relevant substrates that when cleaved serve to promote capillary hemorrhage. Studies are on-going in our laboratory which is focused on these prospects.

Acknowledgments

We thank the Brazilian agency CAPES, Brasília, Brazil for the PDEE fellowship to A.F.M. Pinto. This work was supported by CAPES (A.F.M.P., R.M.S.T., J.A.G.), the University of Virginia Cancer Center (J.W.F.) and Polifarma Inc. (J.W.F.).

References

[1] J.W. Fox, S.M. Serrano, Toxicon 45 (2005) 969–985.
[2] J.B. Bjarnason, J.W. Fox, in: A.J. Barret, N.D. Rawlings, J.F. Woessner (Eds.), Handbook of Proteolytic Enzymes, Academic Press, San Diego, CA, 1998, pp. 1246–1254.
[3] C.P. Blobel, Nat. Rev. Mol. Cell Biol. 6 (2005) 32–43.
[4] S. Porter, I.M. Clark, L. Kevorkian, D.R. Edwards, Biochem. J. 386 (2005) 15–27.
[5] K. Fujikawa, H. Suzuki, B. McMullen, D. Chung, Blood 98 (2001) 1662–1666.
[6] K. Soejima, N. Mimura, M. Hirashima, H. Maeda, T. Hamamoto, T. Nakagaki, C. Nozaki, J. Biochem. (Tokyo) 130 (2001) 475–480.
[7] G.G. Levy, W.C. Nichols, E.C. Lian, T. Foroud, J.N. McClintick, B.M. McGee, A.Y. Yang, D.R. Siemieniak, K.R. Stark, R. Gruppo, R. Sarode, S.B. Shurin, V. Chandrasekaran, S.P. Stabler, H. Sabio, E.E. Bouhassira, J.D. Upshaw Jr., D. Ginsburg, H.M. Tsai, Nature 413 (2001) 488–494.
[8] K. Kokame, M. Matsumoto, K. Soejima, H. Yagi, H. Ishizashi, M. Funato, H. Tamai, M. Konno, K. Kamide, Y. Kawano, T. Miyata, Y. Fujimura, Proc. Natl. Acad. Sci. USA 99 (2002) 11902–11907.
[9] X. Zheng, K. Nishio, E.M. Majerus, J.E. Sadler, J. Biol. Chem. 278 (2003) 30136–30141.
[10] A.S. Kamiguti, C.R. Hay, R.D. Theakston, M. Zuzel, Toxicon 34 (1996) 627–642.
[11] J. Hamako, T. Matsui, S. Nishida, S. Nomura, Y. Fujimura, M. Ito, Y. Ozeki, K. Titani, Thromb. Haemost. 80 (1998) 499–505.
[12] Y. Usami, Y. Fujimura, S. Miura, H. Shima, E. Yoshida, A. Yoshioka, K. Hirano, M. Suzuki, K. Titani, Biochem. Biophys. Res. Commun. 201 (1994) 331–339.
[13] L.G. Jia, X.M. Wang, J.D. Shannon, J.B. Bjarnason, J.W. Fox, J. Biol. Chem. 272 (1997) 13094–13102.
[14] L.G. Jia, X.M. Wang, J.D. Shannon, J.B. Bjarnason, J.W. Fox, Arch. Biochem. Biophys. 373 (2000) 281–286.
[15] S.M. Serrano, L.G. Jia, D. Wang, J.D. Shannon, J.W. Fox, Biochem. J. 391 (2005) 69–76.
[16] S. Takeda, T. Igarashi, H. Mori, S. Araki, Embo. J. 25 (2006) 2388–2396.
[17] H.M. Berman, J. Westbrook, Z. Feng, G. Gilliland, T.N. Bhat, H. Weissig, I.N. Shindyalov, P.E. Bourne, Nucleic Acids Res. 28 (2000) 235–242.
[18] J. Emsley, M. Cruz, R. Handin, R. Liddington, J. Biol. Chem. 273 (1998) 10396–10401.
[19] R.A. Laskowski, M.W. Macarthur, D.S. Moss, J.M. Thornton, J. Appl. Crystallogr. 26 (1993) 283–291.
[20] D.W. Ritchie, G.J. Kemp, Proteins 39 (2000) 178–194.
[21] E. Lindahl, B. Hess, D. van der Spoel, J. Mol. Model. 7 (2001) 306–317.
[22] N. Guex, M.C. Peitsch, Electrophoresis 18 (1997) 2714–2723.
[23] H.J.C. Berendsen, J.R. Grigera, T.P. Straatsma, J. Phys. Chem. 91 (1987) 6269–6271.
[24] T. Darden, D. York, L. Pedersen, J. Chem. Phys. 98 (1993) 10089–10092.
[25] B. Hess, H. Bekker, H.J.C. Berendsen, J.G.E.M. Fraaije, J. Comput. Chem. 18 (1997) 1463–1472.
[26] S. Miyamoto, P.A. Kollman, J. Comput. Chem. 13 (1992) 952–962.
[27] A.C. Wallace, R.A. Laskowski, J.M. Thornton, Protein Engin. 8 (1995) 127–134.
[28] T. Matsui, J. Hamako, Toxicon 45 (2005) 1075–1087.
[29] K. Fukuda, T.A. Doggett, L.A. Bankston, M.A. Cruz, T.G. Diacovo, R.C. Liddington, Structure 10 (2002) 943–950.
[30] N. Maita, K. Nishio, E. Nishimoto, T. Matsui, Y. Shikamoto, T. Morita, J.E. Sadler, H. Mizuno, J. Biol. Chem. 278 (2003) 37777–37781.
[31] A.S. Kamiguti, C.R. Hay, M. Zuzel, Biochem. J. 320 (Pt. 2) (1996) 635–641.
[32] P. Zigrino, A.S. Kamiguti, J. Eble, C. Drescher, R. Nischt, J.W. Fox, C. Mauch, J. Biol. Chem. 277 (2002) 40528–40535.
[33] Q. Zhou, J.B. Smith, M.H. Grossman, Biochem. J. 307 (Pt. 2) (1995) 411–417.
[34] A.S. Kamiguti, J.L. Cardoso, R.D. Theakston, I.S. Sano-Martins, R.A. Hutton, F.P. Rugman, D.A. Warrell, C.R. Hay, Toxicon 29 (1991) 961–972.
[35] A.S. Kamiguti, P. Gallagher, C. Marcinkiewicz, R.D. Theakston, M. Zuzel, J.W. Fox, FEBS Lett. 549 (2003) 129–134.
[36] J.B. Bjarnason, J.W. Fox, Pharmacol. Ther. 62 (1994) 325–372.
[37] E.N. Baramova, J.D. Shannon, J.B. Bjarnason, J.W. Fox, Arch. Biochem. Biophys. 275 (1989) 63–71.

2.3.3. Degradação de matriz extracelular por metaloproteinases de venenos de serpentes: um enfoque proteômico quantitativo

Sabemos que várias proteínas de matriz isoladas são substratos de SVMPs em ensaios *in vitro*. Ainda, sabemos que as SVMPs são capazes de degradar proteínas específicas em misturas complexas de componentes de membrana basal (matrigel). Os avanços tecnológicos na área de proteômica permitiram o uso de uma abordagem proteômica quantitativa até então inédita no estudo de degradação de proteínas de matriz extracelular por metaloproteinases de veneno de serpentes.

Utilizando uma marcação de amino ácidos com isótopos estáveis em cultura de células, fomos capazes de identificar degradação de componentes de matriz extracelular de fibroblasto em cultura.

Este trabalho foi desenvolvido na Biomolecular Research Facility (University of Virginia) juntamente com a divisão de espectrometria de massas desse mesmo laboratório. Os dados aqui apresentados são parte de um manuscrito em fase de preparação.

Degradação de Matriz Extracelular por metaloproteinases de veneno de serpentes: uma abordagem proteômica quantitativa

Introdução

A hemorragia é uma das conseqüências mais marcantes do envenenamento crotálico (Fox e Serrano, 2005). Ela é causada por metaloproteinases de veneno de serpentes (*snake venom metalloproteinases*, SVMPs), membros da subfamília das reprolisinas da família M12 das metaloproteinases (Bjarnason e Fox, 1995). A hemorragia produzida pelas SVMPs é causada principalmente pela degradação da membrana basal de capilares e proteínas de superfícies de células endoteliais provocando extravasamento do conteúdo do capilar para o estroma ao redor (Baramova et al., 1989; Shannon et al., 1989). As SVMPs da classe PIII, que possuem além do domínio metaloproteinase os domínios tipo-desintegrina e rico-em-cisteínas, possuem a maior atividade hemorrágica comparada com as classes PI e PII, sugerindo um papel desse dois domínios na patofisiologia da hemorragia (Fox e Serrano, 2005). Os domínios tipo-desintegrina/rico-em-cisteinas de algumas SVMPs hemorrágicas já foram caracterizados como potentes inibidores da agregação plaquetária induzida por colágeno, provavelmente pela interação do domínio rico-em-cisteinas com a integrina α2β1 de plaquetas (Jia et al., 1997; Jia et al., 2000).

A habilidade do domínio rico-em-cisteínas de interagir com fator de von Willebrand (vWF) também já foi demonstrada (Serrano et al., 2005). Recentemente, outros estudos mostraram que o domínio rico-em-cisteínas de jararragina, uma SVMP da classe PIII isolada do veneno de *Bothrops jararaca*, é capaz de interagir com outras proteínas que

contenham domínios A de vWF (vWA), tais como colágenos XII e XIV e matrilinas. Essa interação direciona o domínio metaloproteinase para esses substratos, levando-os a degradação (dados em revisão para publicação). Assim, os domínios não-proteásicos, particularmente domínio rico-em-cisteínas, aparentemente funcionam direcionando as SVMPs para substratos relevantes que levam a hemorragia (Zigrino et al., 2002).

Em mamíferos, metaloproteinases endógenas estão envolvidas em diversos processos, incluindo ligação e fusão de espermatozóide e óvulo, fusão de mioblastos, processamento de citocinas, receptores de citocinas e proteínas adesivas (Schlondorff e Blobel, 1999). A clivagem e liberação de domínios extracelulares de proteínas de membrana celular é um processo chamado "*shedding*". Citocinas, fatores de crescimento e outros mediadores são clivados de seus precursores de membrana através do *shedding*, permitindo sinalização parácrina. Este processo também está envolvido na clivagem de receptores, ativando-os ou inibindo-os, bem como outras proteínas de superfície (Blobel, 2005; Huovila et al., 2005). A família de proteínas ADAMs (A Disintegrin and Metalloproteinase) são responsáveis pela maioria das clivagens de proteínas de matriz extracelular por *shedding* conhecidas (Huovila et al., 2005). As ADAMs são estruturalmente relacionadas as SVMPs da classe PIII. Além dos domínios metaloproteinase, tipo-desintegrina e rico-em-cisteínas (encontrados nas PIII), as ADAMs possuem uma região tipo-fator de crescimento epidérmico, uma região transmembrana e uma cauda citoplasmática (Blobel, 2005). SVMPs da classe PIII também são conhecidas por sua habilidade de degradar proteínas de matriz extracelular *in vitro* (Baramova et al., 1989; Bjarnason et al., 1988; Escalante et al., 2006; Shannon et al., 1989).

O objetivo desse estudo é estabelecer uma metodologia de proteômica quantitativa para a identificação domínios extracelulares de proteínas de matriz clivados por uma SVMP da classe PIII. Nesse estudo, mostramos pela primeira vez a ação de uma metaloproteinase de veneno de serpente sobre proteínas de matriz extracelular de células em cultura.

Material e Métodos

Células, proteínas de venenos e reagentes

Fibroblastos humanos primários (HS68, ATCC CRL-1635), derivados de prepúcio de neonatos, foram adquiridos no American Type Culture Collection. Atrolisina A foi isolada a partir do veneno de *Crotalus atrox* como descrito previamente (Bjarnason e Tu, 1978). Reagentes de cultura de células e SILAC (amino ácidos marcados com isótopo estável) foram adquiridos da Invitrogen (Carlsbad, CA).

Cultura de Células

Nos experimentos de SILAC (Ong et al., 2002), fibroblastos foram mantidos em meio de cultura SILAC: D-MEM contendo 10% de soro fetal bovino dialisado e suplementado com L-glutamina (4 mM), piruvato de sódio (1,5g/L), glicose (4,5 g/L) e L-arginina (0,1g/L). Lisina marcada ([U-$^{13}C_6$]-L-lisina, pesada) ou não-marcada ([$^{12}C_6$]-L-lisina, leve) foi adicionada ao meio na concentração final de 0,1 g/L. Populações de células marcadas e não-marcadas foram crescidas por oito dias em meio SILAC a 37^{o}C com 5% de CO_2 para alcançar mais de 95% de incorporação do amino ácido marcado.

Tratamento das células e preparação das amostras

Fibroblastos crescidos em meio de cultura SILAC marcado ou não-marcado com lisina pesada foram inicialmente lavados com meio de cultura sem soro fetal bovino. O meio foi aspirado e as células foram incubadas em meio de cultura sem soro fetal bovino na presença (células marcadas com lisina pesada) ou ausência (células controle) de 100 nM de atrolisina A por 30 minutos a 37^{o}C/5% de CO_2. Após incubação, o meio de cultura foi coletado e mantido a -20^{o}C. Alíquotas dos meios das células marcadas com lisina pesada e tratadas com atrolisina A (meio tratado) e células não-marcadas (meio controle) foram precipitadas com 20% de TCA por 2 horas a 4^{o}C e centrifugados (14000 rpm/30 min/4^{o}C). Os sobrenadantes foram descartados e os precipitados foram lavados com acetona por 2 horas a -20^{o}C e centrifugados (14000 rpm/30 min/4^{o}C). Os precipitados dos meios tratado e controle foram solubilizados em uréia 8 M contendo SDS 4% e β-mercaptoetanol 4%, combinados e aplicados em SDS-PAGE.

Eletroforese e preparação das amostras para análise

Eletroforese unidimensional em gel de poliacrilamida (SDS-PAGE) foi realizada segundo o método de Laemmli (Laemmli, 1970), utilizando gel de empacotamento a 4% e gel de corrida a 12%. Padrão de massa molecular (Broad Range, Bio Rad) foi utilizado.

Géis unidimensionais foram corados com Coomassie Blue G-250 e descorados com metanol 50%/ácido acético 10%. Os géis foram cortados em nove fatias de maneira a isolar uma banda majoritária em cada fatia de gel. As fatias foram submetidas à análise por espectrometria de massa.

Digestão tríptica *in gel*

Fatias de géis foram descoradas e desidratadas em methanol 50% por duas horas. As proteínas nas fatias foram reduzidas (DTT 10 mM) à temperatura ambiente por 30min e então alquiladas (iodoacetamida 50 mM) no escuro à temperatura ambiente por 30 min. Os géis foram lavados com bicarbonato de amônio 100 mM seguido por acetonitrila e secos à vácuo. Os géis foram então reidratados em solução de tripsina (20 ng/mL) em bicarbonato de amônio por 30 min em gel. O excesso de tripsina foi removido e a digestão foi realizada por 18 horas a 37^{o}C. Os peptídeos trípticos de cada fatia de gel foram extraídos duas vezes com 30 μL de acetonitrila 50% contendo ácido fórmico 5%. As duas extrações foram liofilizadas e ressuspendidas em 20 μL para análise em espectrometria de massas.

Análise em espectrometria de massa dos peptídeos trípicos

A identificação dos peptídeos foi realizado em espectrômetro de massas LCQ DecaXP acoplado a um HPLC Surveyor (Thermo Electron). Peptídeos trípticos foram separados em coluna de fase reversa C18 (75 μm x 8 cm) com fluxo de 300 nL/min em gradiente de acetronitrila/ácido acético 0,1 M (2-80% de acetonitrila em 30 min). O instrumento foi programado para ciclos de um espectro de massas seguido por espectros de fragmentação (MS/MS) dos quatro íons mais abundantes.

Análise dos dados e identificação dos peptídeos

Os espectros de massas foram extraídos e analisados usando os softwares Proteofarm (desenvolvido no laboratório) e Bioworks Sequest 3.11 (Thermo Electron).

Resultados

Fibroblastos marcados com lisina pesada tratados com atrolisina A não mostraram nenhuma diferença morfológica comparados com as células controle. No tempo testado, as propriedades adesivas das células tratadas com a enzima não foram alteradas. Nenhuma evidência visual de células apoptóticas ou necróticas foi verificada.

Após tratamentos, os meios de cultura foram coletados, submetidos ao procedimento de precipitação, misturados e aplicados em gel unidimensional. Como mostra a Figura 1, o perfil eletroforético dos meios apresenta-se difuso, provavelmente pela alta concentração de sais ainda presente depois da precipitação. O gel foi cortado em nove fatias, seguindo esquema mostrado na Figura 1, isolando uma banda majoritária em cada fatia. As fatias foram então submetidas à digestão in gel e análise em espectrômetro de massas.

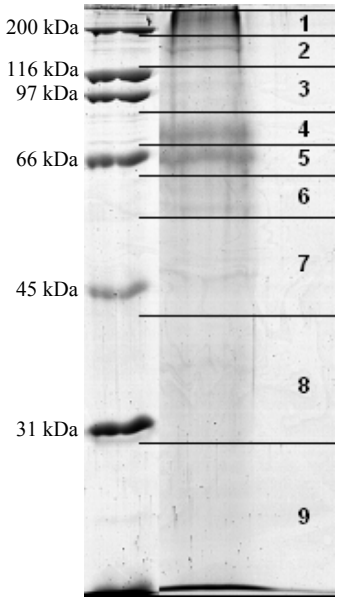

Figura 1. SDS-PAGE da mistura dos meios de cultura de fibroblastos tratados com atrolisina A e fibroblastos controle. A posição e número das fatias dos géis estão indicados. As massas moleculares dos padrões estão indicadas à esquerda: 200 kDa, miosina; 116 kDa, β-galactosidase; 97 kDa, fosforilase B; 66kDa, albumina; 45 kDa, ovalbumina; 31 kDa, anidrase carbônica.

Os peptídeos isolados de cada fatia foram identificados por MS/MS. As massas moleculares foram analisadas e peptídeos contendo lisina leve ([$^{12}C_6$]-L-lisina, 146,1055 Da) ou lisina pesada ([U-$^{13}C_6$]-L-lisina, 152,1259 Da) foram identificados.

Peptídeos com a mesma taxa de lisina pesada e lisina leve foram encontrados nas fatias 6 (piruvato quinase, taxa de 1:1,1) e 8 (gliceraldeído-3-fosfato desidrogenase, taxa de 0,9:1). Foram identificados também peptídeos de proteínas tipo metaloproteinase/desintegrina contendo somente lisinas não-marcadas, provenientes da metaloproteinase utilizada no tratamento das células (dados não mostrados). Peptídeos contendo apenas lisinas pesadas provenientes de proteínas de matriz extracelular foram identificados em sete fatias do gel. A identificação das proteínas e seqüência dos peptídeos contendo lisina pesada é mostrada na Tabela I.

Tabela I. Seqüências de peptídeos marcados com lisina pesada.

Fatia	Massa Molecular Estimada	Proteína Identificada	Seqüência
#1	>180kDa	Colágeno VI, cadeia α3 [P12111] - 340 kDa	VAVIQFSDDPK
			IAVAQYSDDVK
			VEFSLTDYGSK
		Fibronectina [1202277A] - 250 kDa	EINLAPDSSSVVVSGLM*VATK
			SYTITGLQPGTDYK
			YEVSVYALK
		Fibronectina 1, isoforma 6 [NP_997639] - 250 kDa	PRPGVTEATITGLEPGTEYTIYVIALK
			NTFAEVTGLSPGVTYYFK
			ITYGETGGNSPVQEFTVPGSK
			ITYGETGGNSPVQEFTVPGSK
			NLQPASEYTVSLVAIK
			QYNVGPSVSK
#2	120-180 kDa	Colágeno VI, cadeia α1 [CAA67576.1] - 110 kDa	ENYAELLEDAFLK
			LLLFSDGNSQGATPAAIEK
			DTTPLNVLCSPGIQVVSVGIK
		Colágeno VI, cadeia α2 [S09646] - 110 kDa	NLEWIAGGTWTPSALK
		Colágeno VI, cadeia α3 [P12111] - 340 kDa	VGVVQFSNDVFPEFYLK
		Fibronectina [1202277A] - 250 kDa	SYTITGLQPGTDYK
		Fibronectina 1, isoforma 6 [NP_997639] - 250 kDa	NTFAEVTGLSPGVTYYFK
			PRPGVTEATITGLEPGTEYTIYVIALK
			ITYGETGGNSPVQEFTVPGSK
			NLQPASEYTVSLVAIK
			ITYGETGGNSPVQEFTVPGSK
			NLQPASEYTVSLVAIK
			NTFAEVTGLSPGVTYYFK
			QYNVGPSVSK
#3	90-120 kDa	Fibronectina 1, isoforma 6 [NP_997639] - 250 kDa	PRPGVTEATITGLEPGTEYTIYVIALK
			NTFAEVTGLSPGVTYYFK
			ITYGETGGNSPVQEFTVPGSK
			NLQPASEYTVSLVAIK
			QYNVGPSVSK
			TEIDKPSQMQVTDVQDNSISVK
#5	60-70 kDa	Fibulina-2, isoforma A [NP_001004019.1] - 130kDa	IGPAPAFTGDTIALNIIK
			LNAYTGVVYLQR
			DFALDVEM*K
#6	50-60 kDa	Fibronectina [1304205A] - 250 kDa	PRPGVTEATITGLEPGTEYTIYVIALK
#8	25-40 kDa	Anexina V [1HVD] - 36 kDa	DLLDDLKSELTGK
			NFATSLYSM*IK
		Fibronectina [1202277A] - 250 kDa	DLQFVEVTDVK
		Fibronectina [1304205A] - 250 kDa	PRPGVTEATITGLEPGTEYTIYVIALK
			SYTITGLQPGTDYK
#9	<25 kDa	Colágeno VI, cadeia α3 [P12111] - 340 kDa	EVQVFEITENSAK
		Fibronectina [Q91740] - 250 kDa	IGDTWSK
		Fibronectina [1304205A] - 250 kDa	PRPGVTEATITGLEPGTEYTIYVIALK
		Fibronectina 1 [AAA41166.1] - 250 kDa	TYHVGEQWQK

Peptídeos da proteína fibronectina foram os mais identificados no meio de cultura de fibroblastos tratados com atrolisina A, com 31 seqüências com lisina pesada. Os fragmentos de fibrinectina se distribuíram em seis fatias de gel, indicando uma variedade de fragmentos gerados pela ação proteolítica da metaloproteinase. As três cadeias de colágeno tipo VI (α1, α2 e α3) foram identificadas por três, um e cinco peptídeos, respectivamente. A distribuição dos peptídeos das cadeias α1 e α2 de colágeno VI (massa molecular 110 kDa) na fatia 2 do gel (massa molecular estimada em 120-180 kDa) indica baixos níveis de fragmentação. A cadeia α3 de colágeno VI (340 kDa) foi identificada em três fatias (1, 2 e 9), sugerindo certo grau de fragmentação. O fragmento isolado na fatia 9 (EVQVFEITENSAK) pertence ao domínio fibronectina tipo-III da porção C-terminal da molécula de colágeno VI. Fibulina-2 e anexina V foram identificadas nas fatias 5 e 8, respectivamente. Os peptídeos de fibulina, identificados na faixa de 60-70 kDa, correspondem à porção C-terminal da molécula, que íntegra possui 130 kDa. A massa molecular da anexina V madura é de 36 kDa. As duas seqüências de anexina V identificadas na fatia 8 (faixa de 25-40 kDa) estão localizadas tanto na porção N- quanto C-terminal da molécula, sugerindo clivagem da membrana e baixa fragmentação posterior.

Discussão

Atrolisina A é uma das metalloproteinases envolvidas no quadro clínico hemorrágico do envenenamento por *Crotalus atrox*. No processo hemorrágico, a hidrólise de componentes da membrana basal é um evento chave no rompimento de capilares. A degradação *in vitro* de diversos componentes da membrana basal por SVMPs já foi

descrita (Baramova et al., 1989; Bjarnason et al., 1988; Shannon et al., 1989). Estudos do nosso grupo mostraram que SVMPs são capazes de degradar proteínas de matriz específicas mesmo em misturas complexas de membrana basal (matrigel) (Baramova et al., 1991; Escalante et al., 2006). A presença de domínios tipo-desintegrina e rico-em-cisteínas nas SVMPs da classe PIII podem contribuir na direcionamento dessa enzimas para seus substratos específicos, aumentando sua eficiência (Fox e Serrano, 2005).

Uma metodologia de proteômica quantitativa usando SILAC seguida de análise em espectrometria de massa foi usada para testar a habilidade de metaloproteinases de venenos de serpentes de degradar proteínas de matriz extracelular de fibroblastos humanos. A identificação dos peptídeos nesse experimento mostrou a presença de proteínas no meio de cultura com aproximadamente a mesma taxa de lisinas pesadas e leves (piruvato quinase, 1:1,1; liceraldeído-3-fosfato desidrogenase, 0,9:1). Por outro lado, vários peptídeos de proteínas de matriz extracelular contendo apenas lisinas pesadas foram identificados no meio de cultura de fibroblastos tratados com atrolisina A (Tabela I) indicando degradação direta dessas proteínas de matriz por *shedding* de seus ectodomínios.

A proteína marcada com maior número de peptídeos identificados no meio de cultura de células tratadas com atrolina A foi a fibronectina, uma glicoproteína de matriz multifuncional envolvida em eventos celulares como migração, adesão e uma gama de processos fisiológicos como embriogênese, cicatrização, hemostasia e trombose. Como parte da matriz extracelular, a fibronectina interage com receptores de superfície e outros componentes de matriz como colágenos, matrilinas e fibulinas, auxiliando na migração celular e integridade tecidual (Pickford e Campbell, 2004). Experimentos de digestão por

atrolisina A de fibronectina isolada mostram a degradação *in vitro* de fibronectina intacta (~250 kDa) e geração de produtos principais com 159, 93, 63 e 35 kDa além de fragmentos menores (Baramova et al., 1989). Os dados aqui apresentados mostram identificação de fragmentos de fibronectina nas fatias 1 (mais de 180 kDa), 2 (120-180 kDa), 3 (90-120 kDa), 6 (50-60 kDa), 8 (25-40 kDa) e 9 (menos de 25 kDa). As faixas de massa molecular dos fragmentos de fibronectina de matriz extracelular são similares às massas dos fragmentos obtidos com fibronectina isolada, sugerindo um padrão de degradação semelhante tanto na fibronectina isolada quanto na ligada à matriz.

A degradação de tipos diferentes de colágeno por SVMPs já foi descrita. Aqui mostramos que, em condições de degradação em cultura de células, colágeno tipo VI é clivado em membranas de fibroblastos por atrolisina A. Colágeno VI é uma proteína ligadora de vWF localizada diretamente abaixo da camada de células endoteliais. Sua estrutura apresenta tanto domínios fibrilares quanto globulares. Cadeias α1 e α2 de colágeno VI possuem três domínios A de vWF (vWA) cada, enquanto α3 possui 12 desses domínios além de um domínio de inibidor tipo Kunitz e um domínio de fibronectina tipo III. *In vivo*, colágeno VI está em posição fisiológica para interação com plaquetas após lesão vascular. Sua função está associada à adesão e agregação plaquetária em condições de baixo fluxo, como em circulação venosa. Nessas condições, colágeno VI possui maior afinidade por plaquetas que colágeno I. A adesão de plaquetas a colágeno VI se dá via receptores GPIb e αIIbβ3 e é mediado por vWF (Ross et al., 1995; Zangari et al., 1995). A interação do domínio rico-em-cisteínas de SVMPs com proteínas de matriz contendo vWAs promovendo sua degradação foi recentemente demonstrada

(Serrano et al., 2005; dados em revisão para publicação). A degradação de colágeno tipo VI suporta essa hipótese.

Outras proteínas de matriz extracelular foram identificadas no meio de cultura tratado com atrolisina A: fibulina-2 e anexina V. Fibulinas são glicoproteínas secretadas definidas pela presença de dois domínios estruturais: repetições de domínios tipo-fator de crescimento epidérmico com seqüências ligadoras de cálcio consenso e domínios C-terminais tipo-fibulina (Gallagher et al., 2005b). Fibulina-2 possui um domínio N-terminal adicional chamado domínio N, que se divido em um segmento rico em cisteínas (12 cisteínas em 150 animo ácidos) conhecido como Na e uma segmento sem cisteínas chamado Nb. Além dos sítios ligadores de cálcio, fibulinas possuem sítios de ligação a proteínas de membrana basal, fibrilinas, fibronectina e proteoglicanos, participando em estruturas supramoleculares de matriz extracelular (Timpl et al., 2003).

Anexina V é um membro da família de proteínas ligadores de fosfolipídeos. A estrutura primária das anexinas é caracterizada pela presença de domínios homólogos repetidos chamados alças de endonexinas, capazes de ligar fosfolipídeos de maneira cálcio-dependente (Reutelingsperger e van Heerde, 1997). Anexina V está envolvida com interação com colágenos tipo I, II, V, IX e XI, com diferentes afinidades. Essas interações regulam a capacidade ligadora de cálcio da anexina V e aparentemente estão envolvidas em calcificação de tecidos, especialmente cartilagens (von der Mark e Mollenhauer, 1997). A alta afinidade por fosfatidilserina em membranas torna a anexina V um eficiente inibidor do complexo protrombinase da cascata da coagulação. Essa afinidade por fosfatidilserina, bem como controle da coagulação, faz parte de um mecanismo para evitar o potencial pró-coagulante e pró-inflamatório de células

apoptóticas *in vivo*. Em estudos usando avaliação de expressão gênica, baixas concentrações de uma SVMP da classe PIII foram capazes de estimular vias de apoptose em células de cultura (Gallagher et al., 2005a). A degradação proteolítica em anexina V pode provocar interferência na contribuição pró-coaguante e pró-inflamatória das células apoptóticas.

Metaloproteinases de veneno de serpentes provocam hemorragia e sangramento local causados por lesões nas paredes de pequenos vasos. Isso é causado por proteólise dos componentes principais da membrana basal da microvasculatura. Utilizando uma abordagem de proteômica quantitativa, demonstramos pela primeira vez que a atividade proteolíticas das SVMPs não se limita a proteínas de membrana basal, mas se estende às proteínas de matriz extracelular de células de estroma, como fibroblastos.

Referências Bibliográficas

Baramova, E.N., Shannon, J.D., Bjarnason, J.B. e Fox, J.W. (1989) Degradation of extracellular matrix proteins by hemorrhagic metalloproteinases. *Arch Biochem Biophys*, **275**, 63-71.

Baramova, E.N., Shannon, J.D., Fox, J.W. e Bjarnason, J.B. (1991) Proteolytic digestion of non-collagenous basement membrane proteins by the hemorrhagic metalloproteinase Ht-e from Crotalus atrox venom. *Biomed Biochim Acta*, **50**, 763-768.

Bjarnason, J.B. e Fox, J.W. (1995) Snake venom metalloendopeptidases: reprolysins. *Methods Enzymol*, **248**, 345-368.

Bjarnason, J.B., Hamilton, D. e Fox, J.W. (1988) Studies on the mechanism of hemorrhage production by five proteolytic hemorrhagic toxins from Crotalus atrox venom. *Biol Chem Hoppe Seyler*, **369 Suppl**, 121-129.

Bjarnason, J.B. e Tu, A.T. (1978) Hemorrhagic toxins from Western diamondback rattlesnake (Crotalus atrox) venom: isolation and characterization of five toxins and the role of zinc in hemorrhagic toxin e. *Biochemistry*, **17**, 3395-3404.

Blobel, C.P. (2005) ADAMs: key components in EGFR signalling and development. *Nat Rev Mol Cell Biol*, **6**, 32-43.

Escalante, T., Shannon, J.D., Moura-da-Silva, A.M., Gutiérrez, J.M. e Fox, J.W. (2006) Novel insights into capillary vessel basement membrane damage by snake venom hemorrhagic metalloproteinases: A biochemical and immunohistochemical study. *Arch Biochem Biophys*, **in press**.

Fox, J.W. e Serrano, S.M. (2005) Structural considerations of the snake venom metalloproteinases, key members of the M12 reprolysin family of metalloproteinases. *Toxicon*, **45**, 969-985.

Gallagher, P., Bao, Y., Serrano, S.M., Laing, G.D., Theakston, R.D., Gutierrez, J.M., Escalante, T., Zigrino, P., Moura-da-Silva, A.M., Nischt, R., Mauch, C., Moskaluk, C. e Fox, J.W. (2005a) Role of the snake venom toxin jararhagin in proinflammatory pathogenesis: in vitro and in vivo gene expression analysis of the effects of the toxin. *Arch Biochem Biophys*, **441**, 1-15.

Gallagher, W.M., Currid, C.A. e Whelan, L.C. (2005b) Fibulins and cancer: friend or foe? *Trends Mol Med*, **11**, 336-340.

Huovila, A.P., Turner, A.J., Pelto-Huikko, M., Karkkainen, I. e Ortiz, R.M. (2005) Shedding light on ADAM metalloproteinases. *Trends Biochem Sci*, **30**, 413-422.

Jia, L.G., Wang, X.M., Shannon, J.D., Bjarnason, J.B. e Fox, J.W. (1997) Function of disintegrin-like/cysteine-rich domains of atrolysin A. Inhibition of platelet aggregation by recombinant protein and peptide antagonists. *J Biol Chem*, **272**, 13094-13102.

Jia, L.G., Wang, X.M., Shannon, J.D., Bjarnason, J.B. e Fox, J.W. (2000) Inhibition of platelet aggregation by the recombinant cysteine-rich domain of the hemorrhagic snake venom metalloproteinase, atrolysin A. *Arch Biochem Biophys*, **373**, 281-286.

Laemmli, U.K. (1970) Cleavage of structural proteins during the assembly of the head of bacteriophage T4. *Nature*, **227**, 680-685.

Ong, S.E., Blagoev, B., Kratchmarova, I., Kristensen, D.B., Steen, H., Pandey, A. e Mann, M. (2002) Stable isotope labeling by amino acids in cell culture, SILAC, as a simple and accurate approach to expression proteomics. *Mol Cell Proteomics*, **1**, 376-386.

Pickford, A.R. e Campbell, I.D. (2004) NMR studies of modular protein structures and their interactions. *Chem Rev*, **104**, 3557-3566.

Reutelingsperger, C.P. e van Heerde, W.L. (1997) Annexin V, the regulator of phosphatidylserine-catalyzed inflammation and coagulation during apoptosis. *Cell Mol Life Sci*, **53**, 527-532.

Ross, J.M., McIntire, L.V., Moake, J.L. e Rand, J.H. (1995) Platelet adhesion and aggregation on human type VI collagen surfaces under physiological flow conditions. *Blood*, **85**, 1826-1835.

Schlondorff, J. e Blobel, C.P. (1999) Metalloprotease-disintegrins: modular proteins capable of promoting cell-cell interactions and triggering signals by protein-ectodomain shedding. *J Cell Sci*, **112 (Pt 21)**, 3603-3617.

Serrano, S.M., Jia, L.G., Wang, D., Shannon, J.D. e Fox, J.W. (2005) Function of the cysteine-rich domain of the haemorrhagic metalloproteinase atrolysin A: targeting adhesion proteins collagen I and von Willebrand factor. *Biochem J*, **391**, 69-76.

Shannon, J.D., Baramova, E.N., Bjarnason, J.B. e Fox, J.W. (1989) Amino acid sequence of a Crotalus atrox venom metalloproteinase which cleaves type IV collagen and gelatin. *J Biol Chem*, **264**, 11575-11583.

Timpl, R., Sasaki, T., Kostka, G. e Chu, M.L. (2003) Fibulins: a versatile family of extracellular matrix proteins. *Nat Rev Mol Cell Biol*, **4**, 479-489.

von der Mark, K. e Mollenhauer, J. (1997) Annexin V interactions with collagen. *Cell Mol Life Sci*, **53**, 539-545.

Zangari, M., Kaplan, K.L., Glanville, R.W. e Rand, J.H. (1995) Reduced thrombogenicity of type VI collagen as compared to type I collagen. *Thromb Res*, **79**, 429-436.

Zigrino, P., Kamiguti, A.S., Eble, J., Drescher, C., Nischt, R., Fox, J.W. e Mauch, C. (2002) The reprolysin jararhagin, a snake venom metalloproteinase, functions as a fibrillar collagen agonist involved in fibroblast cell adhesion and signaling. *J Biol Chem*, **277**, 40528-40535.

3. Capítulo II

Proteínas Tóxicas da Lagarta Lonomia obliqua

Este segundo capítulo apresenta as etapas do trabalho envolvendo estudos com proteínas tóxicas da lagarta *Lonomia obliqua*, realizados no Centro de Biotecnologia da Universidade Federal do Rio Grande do Sul sob a orientação do Prof. Dr. Jorge Guimarães. Parte da fase experimental aqui relatada foi realizada na University of Virginia, Estados Unidos, sob a co-orientação do Prof. Dr. Jay William Fox.

Uma breve introdução sobre a lagarta *Lonomia obliqua* e a síndrome hemorrágica causada pelo contato acidental com essas lagartas será aprentada. Os resultados deste capítulo estão na forma de um artigo já publicado e um manuscrito em fase final de preparação. Cada conjunto de dados contém uma introdução detalhada do assunto, metodologia aplicada, descrição dos resultados obtidos, discussão e bibliografia consultada.

3.1. Introdução

3.1.1. A Lagarta *Lonomia obliqua*

Reações cutâneas provocadas pelo contato acidental com larvas de lepidópteros são conhecidas desde o início do século passado (von Ihering, 1914). Alguns lepidópteros envolvidos em tais acidentes são potencialmente perigosos, principalmente das famílias Megalopygidae e Saturniidae, provocando manifestações clínicas de intensidade variada. Na América do Sul, envenenamentos com lagartas do gênero *Lonomia* (Lepdoptera, Saturniidae) são freqüentemente descritos, mostrando um quadro clínico essencialmente hemorrágico. No norte da América do Sul (norte do Brasil, Venezuela e Guiana Francesa), acidentes são descritos com a lagarta *Lonomia achelous* (Arocha-Piñango e Layrisse, 1969; Couppie et al., 1998; Fraiha Neto et al., 1985). Casos graves também ocorrem no sul do Brasil, onde a lagarta *Lonomia obliqua* (Figura 6) é a responsável pelos acidentes.

Figura 6. Larva de sexto instar de *Lonomia obliqua*.

O envenenamento provocado pelo contato acidental com lagartas *Lonomia obliqua*, popularmente conhecida como taturana, vem tomando proporções preocupantes na Região Sul do Brasil, especificamente nos estados de Rio Grande do Sul e Santa Catarina, ocorrendo também no Paraná e em São Paulo (Donato et al., 1998). Ocorrem registros de acidentes com lagartas do gênero *Lonomia* no sul do estado de Santa Catarina desde 1983, com o número de casos aumentando no decorrer dos anos (Luccas, 1991).

No Rio Grande do Sul, as taturanas encontram-se amplamente distribuídas, atingindo a maioria das regiões do Estado. O número de acidentes aumenta drasticamente nos meses mais quentes do ano, de novembro a maio, época em que os indivíduos de *Lonomia obliqua* encontram-se na fase larval do seu desenvolvimento (Abella et al., 1998).

Os estudos sobre a biologia dessas lagartas indicam que *Lonomia obliqua* apresenta quatro fases no seu ciclo de vida (Figura 7A): ovo, com período de incubação de 17 a 30 dias; larva, com duração média de 50 a 85 dias, considerando os seis instares; pupa, com duração variável de acordo com as condições do ambiente; e adulto, com, em média, 15 dias de vida (Lorini, 1997; Lorini, 1999). Na fase larval, *Lonomia obliqua* possui hábitos noturnos, alimentando-se de folhas durante a noite. As lagartas possuem hábitos gregários durante o dia, constituindo colônias de indivíduos com elevado grau de mimetismo com as características do tronco das árvores que habitam, apresentando, nessa condição, maior risco de acidentes (Figura 7B).

Em março de 1989, foram atendidos dois casos de pacientes com diátese hemorrágica e insuficiência renal aguda no Rio Grande do Sul e Santa Catarina, após

contato com lagartas desses lepidópteros (Duarte et al., 1990). Desde então, inúmeros outros acidentes vêm sendo registrados a cada ano. Segundo dados do Centro de Informações Toxicológicas do Rio Grande do Sul (CIT-RS), em 2005 foram registrados, no estado, 130 acidentes causados por lagartas dessa espécie. Os acidentes normalmente ocorrem quando a vítima entra em contato com colônias de lagartas presentes em troncos de árvores.

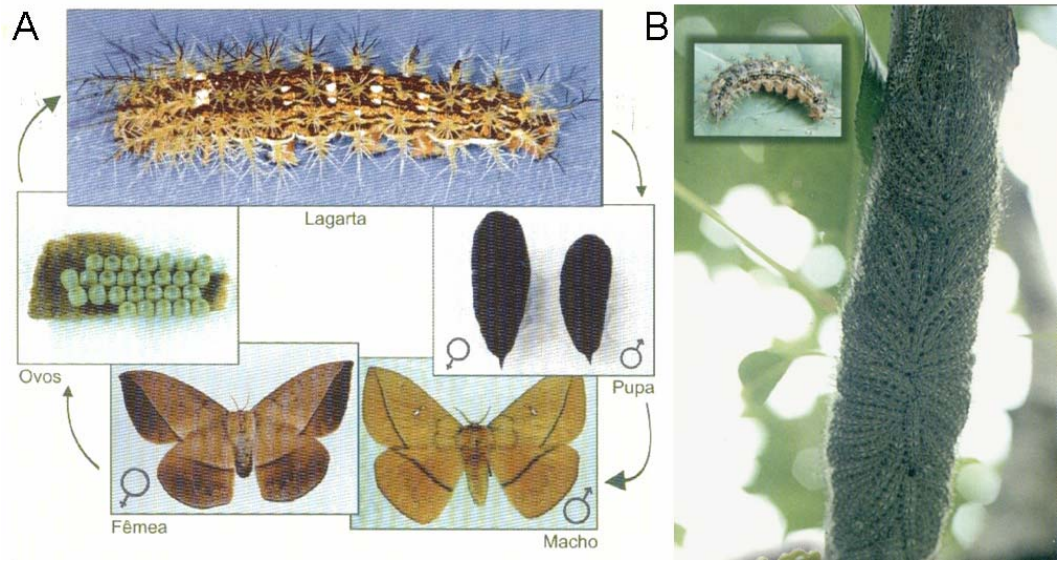

Figura 7. A. Ciclo de vida do lepidóptero *Lonomia obliqua* (Fonte: CIT/RS). B. Colônia de lagartas *Lonomia obliqua* sobre o tronco de uma árvore. No detalhe, uma lagarta isolada (Lorini, 1999).

3.1.2. O Quadro Clínico do Acidente Lonômico

O envenenamento é caracterizado por um quadro clínico hemorrágico agudo que se instala até 72 horas após o contato, apresentando sintomas como equimose intensa, sangramentos e hemorragia interna, salivação sanguinolenta, hematúria intensa e, em

alguns casos, falência renal aguda (Figura 8) (Abella et al., 1998; Costa, 1994; Duarte et al., 1990; Luccas, 1991).

O quadro hemorrágico é compatível com níveis baixos de fibrinogênio, fator V, fator VIII, fator XIII, plasminogênio e α2-antiplasmina, bem como atividade reduzida de proteína C. Além disso, D-dímeros, produtos de degradação de fibrinogênio (FDPs), complexos trombina-antitrombina, fragmentos 1+2 de protrombina foram detectados no sangue de pacientes (Da Silva et al., 1996; Kelen et al., 1996; Zannin et al., 2003).

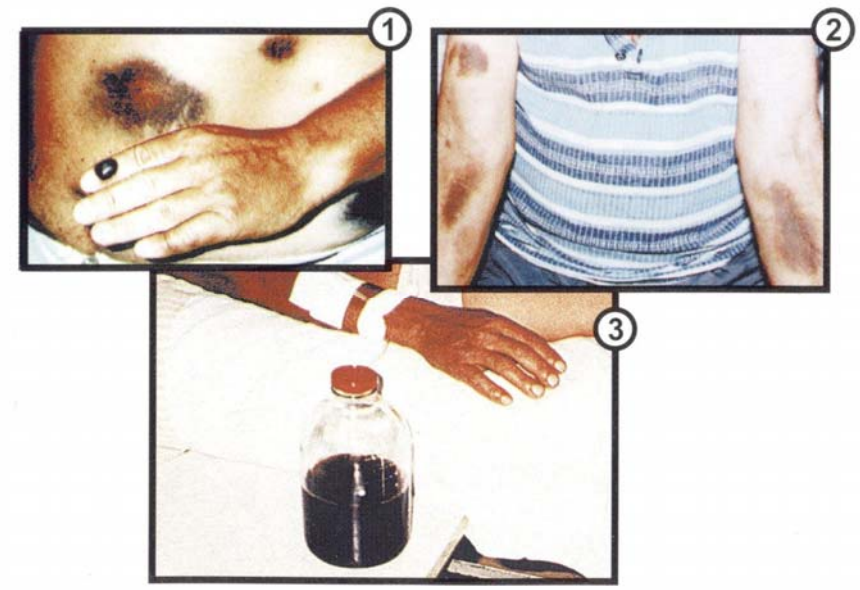

Figura 8. Quadro hemorrágico e sinais clínicos resultantes do envenenamento por acidentes com *Lonomia obliqua*. Em 1, hematomas espalhados pelo corpo e bolha de sangue no dedo do paciente; em 2, hematomas nas partes que entraram em contato com os animais; em 3, urina de paciente com evidente quadro de hematúria (Abella et al., 1998).

Recentemente, Gamborgi e colaboradores relataram que 32% dos pacientes envenenados atendidos no estado de Santa Catarina tiverem de passar por sessões de hemodiálise e 4% vieram a óbito devido à insuficiência renal aguda (Gamborgi et al., 2006). Os sintomas acima são predominantemente hemorrágicos, mas há também manifestações pró-coagulantes descritas (Reis et al., 1999; Zannin et al., 2003),

constituindo uma ação paradoxal do veneno, provavelmente devido aos efeitos de diferentes princípios ativos das secreções venenosas. Efeitos similares foram descritos com acidentes envolvendo a lagarta *L. achelous* (Arocha-Pinango et al., 1992; Guerrero et al., 1999; Guerrero et al., 1997a; Guerrero et al., 1997b).

O diagnóstico do envenanamento é realizado após uma avaliação clínica e descrição, pelo paciente, de contato com o animal. Quando não há identificação do agente causador do acidente, o diagnóstico torna-se difícil e, em muitas vezes, errôneo pela semelhança clínica com acidentes causados por serpentes. O tratamento clínico constitui-se, basicamente, da aplicação do soro anti-lonômico (um concentrado de imunoglobulinas obtidas a partir do soro de cavalos imunizados com extrato de espículas de *Lonomia obliqua*) produzido pelo Instituto Butantan de São Paulo (Da Silva et al., 1996). Em pacientes não diagnosticados e, portanto, não tratados adequadamente com o soro anti-lonômico, o envenenamento pode evoluir para hemorragia cerebral grave, insuficiência renal aguda e conseqüente morte do paciente.

3.1.3. Princípios Ativos de *Lonomia obliqua*

Os estudos de proteínas tóxicas da lagarta *Lonomia obliqua* baseiam-se no isolamento e caracterização bioquímica dos princípios ativos, apresentado sucesso parcial e gerando um conhecimento básico da patologia do envenenamento. Nos últimos anos, esses estudos identificaram componentes do veneno capazes de reproduzir alguns dos aspectos patofisiológicos do envenenamento: um ativador de FX e um ativador de protrombina, envolvidos com o processo de coagulação intravascular (Donato et al.,

1998), enzimas fibrinolíticas identificadas em mais de uma secreção da lagarta e envolvidas com a degradação de fibrinogênio e fibrina (Fritzen et al., 2003; Pinto et al., 2004; Pinto et al., 2006; Veiga et al., 2003), proteínas da lagarta envolvidas com processo de hemólise (Seibert et al., 2004), inflamação (Fritzen et al., 2005), edema e nocicepção (de Castro Bastos et al., 2004) (Tabela II).

Tabela II. Atividades *in vitro* de secreções de *Lonomia obliqua.*

Atividade	Enzima	Referência
Pró-coagulante	Ativador de Protrombina	Donato et al., 1998
	Ativador de Fator X	Donato et al., 1998
Fosfolipásica	Fosfolipase	Seibert et al., 2003
Fibrin(ogen)olítica	Fibrin(ogen)ase	Veiga et al., 2003
	Lonofibrase	Pinto et al., 2004
Hemólise	N/I	Seibert et al., 2003
Nocicepção	N/I	de Castro Bastos et al., 2004
Hialuronidásica	Lonogliase	Gouveia et al., 2005
Inflamação	LOPAP	Fritzen et al., 2005

Um grande avanço nos estudos com *Lonomia obliqua* foi alcançado recentemente através do estudo de transcriptoma de tecidos da lagarta, gerando um catálogo de várias proteínas presentes no veneno da lagarta, incluindo proteínas que não atuam diretamente na coagulação e na fibrinólise tais como proteínas de defesa, lipocalinas, lectinas e serpinas. Essas proteínas são inoculadas na vítima envenenada e, provavelmente constituem princípios ativos envolvidos direta ou indiretamente nas manifestações clínicas. Curiosamente, nenhuma metaloproteinase foi identificada nesse estudo de transcriptoma (Veiga et al., 2005, http://www.ncbi.nlm.nih.gov/ projects/omes/).

3.2. Objetivos

A segunda etapa deste trabalho teve como objetivos: 1. Comparar quatro secreções venenosas de *Lonomia obliqua* a fim de determinar diferenças quali-quantitativas na constituição protéica e atividades biológicas presentes nas secreções; 2. Avaliar o efeito do veneno de *Lonomia obliqua* no padrão de expressão gênica de células em cultura.

Esses objetivos foram realizados pelas seguintes etapas:

1.1. Comparar o perfil eletroforético de diferentes secreções de *Lonomia obliqua* bem como sua imuno-reatividade ao soro anti-lonômico;

1.2. Avaliar a atividade amidolítica das proteases presentes nas secreções de *Lonomia obliqua*, utilizando diversos substratos cromogênicos;

1.3. Estudar o efeito de inibidores sobre essas proteases;

1.4. Caracterizar a atividade pró-coagulante presente nos diferentes extratos da taturana;

1.5. Comparar a atividade fibrin(ogen)olítica da secreções de *L. obliqua*;

2.1. Avaliar os efeitos do extrato de espículas de *Lonomia obliqua* a expressão gênica de fibroblastos utilizando a tecnologia de microarranjo de DNA;

2.2. A partir dos dados de expressão gênica, validar as hipóteses propostas dos efeitos celulares provocados pela ação do veneno da lagarta.

3.3. Resultados

3.3.1. Proteases de secreções venenosas de *Lonomia obliqua*: comparação das atividades pró-coagulantes, fibrin(ogen)olíticas e amidolíticas

Antônio F.M. Pinto, Kátia R.L.M. Silva, Jorge A. Guimarães. 2006. Proteases from *Lonomia obliqua* venomous secretions: Comparison of procoagulant, fibrin(ogen)olytic and amidolytic activities. Toxicon 47:113-121.

Em 2001, um trabalho do nosso grupo descreveu morfologicamente o sistema de produção de veneno na lagarta *Lonomia obliqua* (Veiga et al., 2001). Nenhuma estrutura glandular foi encontrada, as secreções venenosas da lagarta são produzidas por um epitélio secretor especializado presente na base das espículas e ao longo da cutícula do animal.

Essas observações levaram a questão de qual seria a relevância de outras secreções da lagarta, além do extrato de espículas, no envenenamento. Para responder essa pergunta, um estudo comparativo usando quatro secreções venenosas de *Lonomia obliqua* (extrato de espículas, extrato de tegumento, criosecreção e hemolinfa) foi realizado. A atividade amidolítica sobre vários substratos cromogênicos, atividade pró-coagulante e fibrinogenolítica foram testadas.

Este trabalho foi desenvolvido no Laboratório de Bioquímica Farmacológica da UFRGS. O artigo foi submetido em maio de 2005 à revista *Toxicon* e publicado em janeiro de 2006.

ELSEVIER

Toxicon 47 (2006) 113–121

TOXICON

www.elsevier.com/locate/toxicon

Proteases from *Lonomia obliqua* venomous secretions: Comparison of procoagulant, fibrin(ogen)olytic and amidolytic activities

Antônio F.M. Pinto, Kátia R.L.M. Silva, Jorge A. Guimarães *

Universidade Federal do Rio Grande do Sul, Centro de Biotecnologia, Av. Bento Gonçalves 9500, P.O. Box 15005, Porto Alegre 91501-970, Brazil

Received 12 May 2005; revised 18 September 2005; accepted 8 October 2005

Abstract

The hemorrhagic syndrome caused by *Lonomia obliqua* caterpillars is an increasing problem in Southern Brazil. The clinical profile is characterized by both hemorrhagic and pro-coagulant symptoms, constituting a paradoxical action of the venom. The effects upon blood coagulation and fibrin(ogen)olysis have been shown to result from the combined action of several active principles found mostly in the bristle extract. The present study reports quali-quantitative differences among *L. obliqua* secretions: Cryosecretion, hemolymph, bristle extract and tegument extract. Cryosecretion and hemolymph displayed strong amidolytic activity upon several substrates, presented moderated procoagulant activity and high fibrinogen degrading ability. Bristle and tegument extracts presented low amidolytic activity, but bristle extract showed the most potent procoagulant activity and both extracts presented low fibrinogen degrading ability. The differential involvement of these secretions during the accidents with *L. obliqua* can elucidate the different symptoms presented after envenomation.

Keywords: Lonomia obliqua; Coagulation; Fibrinolysis; Hemostasis; Bleeding disorder

1. Introduction

The Lepdoptera order includes moths and butterflies which have medical importance because they cause respiratory and cutaneous reactions following the contact with hairs of the adult and the spicules of the larvae. The potentially dangerous insects belong to Megalopygidae and Saturniidae families. In Brazil, lepdopteran accidents with cutaneous reactions produced in persons envenomed by these caterpillars have been registered since the beginning of the last century (Von Ihering, 1914). The symptoms produced following the envenomation accident depend on the species involved, the type of active principles present in the venom, the deepness of the contact with the insets and the individual reaction of the patient.

Abbreviations E-64, trans-epoxysuccinyl-L-leucylamido(4-guanidino)-butane; EDTA, ethylene diamine tetraacetic acid; EGTA, ethylene glycol-bis((-aminoethyl ether) *N*,*N*,*N*′,*N*′-tetraacetic acid; DL-BAPNA, benzoyl-DL-arginine-pNA; PMSF, phenylmethylsulfonyl fluoride; SDS-PAGE, sodium dodecyl sulfate polyacrylamide gel electrophoresis; S-2222, Bz-Ile-Glu-Gly-Arg-pNA; S-2238, H-D-Phe-Pip-Arg-pNA; S-2251, H-D-Val-Leu-Lys-pNA; S-2302, H-D-Pro-Phe-Arg-pNA; S-2366, pyroGlu-Pro-Arg-pNA; S-2444, pyroGlu-Gly-Arg-pNA; Tris, tris[hydroxymethyl] aminomethane.

* Corresponding author. Tel.: +55 51 3316 6068; fax: +55 51 3316 7309.

E-mail address: guimar@cbiot.ufrgs.br (J.A. Guimarães).

0041-0101/$ - see front matter © 2005 Elsevier Ltd. All rights reserved.
doi:10.1016/j.toxicon.2005.10.004

In South America, accidents with caterpillars of *Lonomia* genus (Lepdoptera, Saturniidae) have been frequently described, showing essentially a hemorrhagic clinical disorder in envenomed children and adult persons. In the north of South America (Northern Brazil, Venezuela and French Guyana), accidents were described with *Lonomia achelous* caterpillars (Arocha-Piñango e Layrisse, 1969; Fraiha Neto et al., 1985; Couppié et al., 1998). However, due to deflorestation and replacement of the native forest by fruit tree plantation the most dangerous accidents are occurring in Southern Brazil. In these cases, *Lonomia obliqua* caterpillars are responsible for the accidents described since 1989 (Duarte et al., 1990). The envenomation produced by these caterpillars are getting dangerous proportions especially in the states of Rio Grande do Sul, Santa Catarina and Paraná (Donato et al., 1998; Abella et al., 1998). Accidents usually occur when the victim gets in contact with a whole caterpillar colony lying on the surface of tree trunks. In this case, not only the bristles but often the whole animal is smashed in the accident thus allowing that body secretions, including the hemolymph, penetrate the human skin and reach the blood stream. While some toxic principles are found in bristle extracts, others are present in the hemolymph and other venomous preparations of *Lonomia* specimens.

The envenomation is characterized by a hemorrhagic clinical profile installed within a 72 h period after the contact, presenting typical symptoms as intense equimosis, external bleeding and internal (including cerebral) hemorrhage, bloody salivation, intense hematuria and, in some cases, acute renal failure (Duarte et al., 1990). The above symptoms are predominantly hemorrhagic, but there are also pro-coagulant manifestations (Reis et al., 1999; Zannin et al., 2003), constituting a paradoxical action of the venom, probably due to the effects of distinct active principles of the venomous secretion. Similar effects have been described for *L. achelous* caterpillars (Arocha-Piñango et al., 1992; Guerrero et al., 1997a,b, 1999).

Most studies with *L. obliqua* were made using the bristle extract where a prothrombin activator (LOPAP), Factor X activator, phospholipase activity (Lonomiatoxin) and fibrinogenolytic activity were already identified (Donato et al., 1998; Reis et al., 1999; Seibert et al., 2003; Veiga et al., 2003). Recently, starting from another secreted material obtained upon a freezing procedure applied to *L. obliqua* caterpillars (cryosecretion), Lonofibrase, the first fibrin(o-gen)olytic enzyme described in *L. obliqua*, was purified and characterized as an α-fibrinogenase (Pinto et al., 2004). The presence of these different proteins has been confirmed by an exhaustive transcriptome study of distinct *L. obliqua* secretions (Veiga et al., 2005 and http://www.ncbi.nlm.nih.gov/projects/omes/).

Histological and ultra-structural studies of *L. obliqua* caterpillars showed the presence of a secretory epithelium responsible for the venom production. This specialized epithelium underlies the entire tegument as well as the spicules, except the distal region. The venom produced is stored in specialized cuticle regions and inside the spicules. Furthermore, no gland or glandular structure connected to spicule base was found (Veiga et al., 2001). To better characterize and comprehend the diversity of active principles with possible involvement in the paradoxical effects (procoagulant and hemorrhagic) presented by *L. obliqua* venom, additional experiments were performed as described here. We present the comparative results for amidolytic, procoagulant and fibirnogenolytic activities obtained with four different venomous extracts and secretions: bristle extract, the cryosecretion, hemolymph and tegument extract.

2. Material and methods

2.1. Caterpillars and venomous extracts and secretions

L. obliqua caterpillars were kindly provided by Centro de Informações Toxicológicas (CIT), Porto Alegre, Rio Grande do Sul and Secretaria Municipal de Saúde, Videira, Santa Catarina, Brazil. The insects were collected by local inhabitants directly from trees.

Four different secretions were used in this work. Bristle extract was obtained as described by daSilva et al. (1996). Briefly, bristles were cut at the caterpillars tegument insertion, homogeneized in buffer (20 mM Tris. HCl, pH 7.5) and centrifuged at 9,600 × *g* for 20 min. The supernatant was stored at −20 °C until use. Hemolymph was obtained by cutting the caterpillars' head and the abdominal and anal prolegs. The fluid expelled was collected and centrifuged (9600 × *g* for 20 min). The supernatant was stored at −20 °C until use. Tegument was collected after total dissection of the insects, cut in pieces, homogenized in the above buffer and centrifuged (9600 × *g* for 20 min). The supernatant, named Tegument extract, was also stored. Cryosecretion was obtained as described in Pinto et al. (2004). Briefly, caterpillars were exposed to −20 °C for 24 h and then washed with buffer (20 mM Tris–HCl, pH 7.4). The secreted protein-rich fluid was collected and saved.

2.2. Reagents

Bovine fibrinogen, molecular markers, Tris buffer and benzoyl-DL-arginine *p*-nitroanilide (DL-BAPNA) were obtained from Sigma (St Louis, MO, USA). Substrates S-2238, S-2222, S-2366, S-2302, S-2444, S-2251 were obtained from Chromogenix (Milano, Italy). Thrombin was purified from human plasma by the method described by Ngai and Chang (1991). Citrated plasma was obtained from Hospital de Clínicas (UFRGS). All other chemicals were of the highest purity commercially available.

2.3. SDS-PAGE

Polyacrilamide gel electrophoresis was performed according to Laemmli (1970), using 4% stacking gel and 10% running gel in a BioRad system. Phosphorylase B (97 kDa), Bovine albumin (66 kDa), ovalbumin (45 kDa), carbonic anhydrase (30 kDa), SBTI (20.1 kDa) and α-lactalbumin (14.2 kDa) were used as molecular markers.

2.4. Western blot

L. obliqua secretions separated by SDS-PAGE were electrotransfered at 50 mA for 1 h onto nitrocellulose membranes, and thereafter membranes were blocked with PBS-casein 5% buffer (BLOTTO 5%) overnight. Membranes were incubated with anti-lonomic serum (1:500) for 24 h at 4 °C. The anti-lonomic anti-serum used is a horse polyclonal antibodies raised against a crude bristle extract used as antigen (daSilva et al., 1996). The same bristle extract was used both in SDS-PAGE and in Western blot for comparison of their protein pattern with that of the other secretions. Membranes were washed three times with BLOTTO 5% and incubated with alkaline phosphatase-labeled anti-horse IgG (1:10,000). The blot was developed according to manufacturer's recommendations (Sigma, USA) using a chromogenic substrate.

2.5. Amidolytic activity

Amidolytic activity of *L. obliqua* secretions upon synthetic chromogenic substrates was assayed as described (Pinto et al., 2004). Briefly, aliquots of the caterpillar's extracts were incubated in 20 mM Tris–HCl buffer, pH 7.4. The reactions were initiated by adding DL-BAPNA or the more specific substrates S-2238 (thrombin); S-2222 (FXa); S-2366 (FXIa); S-2302 (kallikrein); S-2444 (urokinase) and S-2251 (plasmin) at 0.2 mM (final concentration) in a final volume of 100 μL. Assays were monitored at 37 °C in a SpectraMax spectrophotometer (Molecular Devices, USA) equipped with thermostat and shaking systems.

The enzymatic activity was expressed in enzyme units per microgram of protein (U/μg), where one unity is the amount of secretion that produces one pmol of p-nitroaniline in one minute of reaction at 37 °C.

2.6. Effects of divalent cations

L. obliqua secretions were pre-incubated for 10 min at 37 °C with 5 mM salts of divalent cations: Ca^{2+}, Mg^{2+}, Ba^{2+}, Zn^{2+}, Mn^{2+}, Cu^{2+} and Co^{2+}. The enzymatic activity was determined as described above using the chromogenic substrates.

2.7. Effects of inhibitors

L. obliqua cryosecretion, hemolymph and bristle extract were pre-incubated with 5 mM EDTA, 5 mM EGTA, 5 mM Benzamidine, 2.5 mM PMSF, 25 μM Hg^{2+}, 5 mM L-Cysteine, 10 μM E-64 and 10 mM β-Mercaptoethanol at 37 °C for 20 min. The residual activity was determined using DL-BAPNA and S-2251, S-2444 and S-2222 as substrates for cryosecretion and hemolymph.

2.8. Coagulation assay

The effect of *L. obliqua* secretions upon coagulation was accessed using the recalcification time assay (Hougie, 1963) adapted for the SpectraMax Microplate Reader (Ribeiro et al., 1995). In a final volume of 150, 50 μL of citrated bovine or human plasma was incubated with different amounts of *L. obliqua* samples in 20 mM Tris–HCl buffer, pH 7.4. After 5 min at 37 °C, 10 μL of 150 mM $CaCl_2$ was added and the reaction followed during 20 min at 37 °C and monitored at 650 nm. Since a potent procoagulant effect was seen in some secretions, a procoagulant index (PI_{50}) was used. PI_{50} was defined as the amount of secretion (μg of protein) capable to accelerate coagulation to half the clotting time of control samples.

2.9. Fibrinogen coagulation and fibrinogen degradation assays

Fibrinogen degradation produced by *L. obliqua* secretions was determined using two different methods: (a) fibrinogen coagulation assay in the SpectraMax Microplate Reader, as described above, in which plasma was replaced by fibrinogen and (b) fibrinogen degradation pattern as analyzed by SDS-PAGE. In both cases, the extracts were incubated for 15 min at 37 °C with 0.2 mg of fibrinogen in a final assay volume of 90 μL (20 mM Tris–HCl, pH 7.4). The fibrinogen coagulation assay was initiated by adding 10 μL (0.2 μg) of thrombin solution and the reaction was followed at 37 °C and monitored at 650 nm. For SDS-PAGE analysis of fibrinogen degradation, the reactions were stopped adding the 90 μL of denaturing solution, containing 8 M urea, 4% SDS and 4% β-mercaptoethanol (Datta et al., 1995).

3. Results

3.1. Electrophoretic pattern of L. obliqua secretions

L. obliqua secretions, when analyzed in SDS-PAGE, presented distinct electrophoretic patterns (Fig. 1). Hemolymph and bristle extract showed greater variety of proteins in their electrophoretic patterns. On the other hand, cryosecretion and tegument extracts presented diffused protein patterns. However, in all extracts most proteins

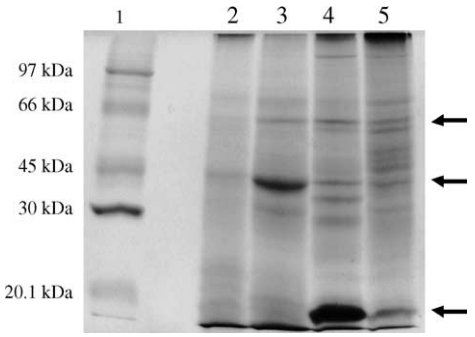

Fig. 1. Polyacrilamide gel electrophoresis. The four *L. obliqua* Secretions (20 μg) were subjected to electrophoresis in 10% running gel. (1) Molecular Markers, (2) Cryosecretion, (3) Hemolymph, (4) Bristle extract, (5) Tegument extract. Arrows indicated bands of 65, 40 and 15 kDa, shared in all extracts.

were found below the range of 80 kDa. Besides a specific pattern presented by each extract, some protein bands (ca proteins corresponding to 65, 40 and 15 kDa.) shared the same pattern mobility in all extracts.

3.2. Immunostaining of L. obliqua secretions

As expected from the similarities among the extracts shown in SDS-PAGE, anti-lonomic antibodies were capable to recognize proteins in all extracts (Fig. 2). Cryosecretion was the less stained extract while hemolymph presented more proteins stained when compared to other samples. Bristle and tegument extracts presented a high degree of similarity in the Western blot. In all samples there was extensive protein recognition in the Mr range between 66

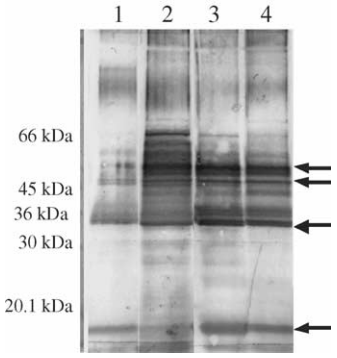

Fig. 2. Immunostaining of *L. obliqua* secretions. The four *L. obliqua* secretions (20 μg) were subjected to electrophoresis in 10% running gel, transferred to a nitrocellulose membrane and immunostained with antilonomic antibodies. Proteins were immunostained with alkaline phosphatase-labeled secondary antibody. (1) Cryosecretion, (2) Hemolymph, (3) Bristle extract, (4) Tegument extract. Extract. Arrows indicated bands of 52, 46, 32 and 15 kDa, shared in all extracts.

and 30 kDa. In this range, three proteins (approximately 52, 46 and 35 kDa) were recognized in all extracts. A protein band localized at a low molecular mass region (approximately 15 kDa) was also stained in all extracts.

3.3. Amidolytic activity

DL-BAPNA and tri-peptide chromogenic substractes designed for proteases acting on the hemostasis cascade were tested as substrates. As shown in Table 1, the extracts presented two distinct behaviors: cryosecretion and hemolymph showed high amidolytic activity upon all substrates whereas bristle and tegument extracts showed much lower amidolytic activity for the chromogenic substrates tested. With all extracts DL-BAPNA was the poorest substrate. Except for DL-BAPNA, S-2238 and S-2251, the cryosecretion and hemolymph showed similar level of activities as expressed in U/μg of protein. Among the subtrates, S-2444 (Urokinase substrate) was the better hydrolyzed by both samples. On the other hand, bristle and tegument extracts showed higher activity upon S-2222 (FXa substrate), but even so in a much lower level than that expressed by the two other extracts.

Table 1 summarizes the results of amidolytic activity of *L. obliqua* extracts upon synthetic chromogenic substrates.

3.4. Inhibitory studies

As shown in Table 2, benzamidine was the most effective inhibitor among all compounds tested. Upon cryosecretion and hemolymph, benzamidine (5 mM) produced an inhibitory effect ranging from 74 to 99% of the amidolytic activity of the tested substrates. With the bristle extract benzamidine produced a partial inhibition (44.8%) upon its best substrate (S-2222). PMSF (2.5 mM) produced only partial inhibitory effect of the amidolytic activity upon specific substrates of cryosecretion and hemolymph extracts (70–80% inhibition in cryosecretion, 63–81% inhibition in hemolymph and 58% in the bristle extract).

Both cryosecretion and hemolymph assayed with DL-BAPNA were greatly susceptible to Hg^{2+} at low concentrations (25 μM). Contrarily, Hg^{2+} produced only a partial inhibition in the amidolytic activity upon specific substrates. E-64 produced poor or no inhibitory effect for all extracts. EDTA and EGTA produced either a slight activation or no inhibition of the amidolytic activity of cryosecretion and hemolymph. This activation was more pronounced with DL-BAPNA as substrate. On the other and, when tested with bristle extract, both EDTA and EGTA inhibited 95 and 73%, respectively, of the activities upon S-2222.

3.5. Effect of divalent cations

As seen with the inhibitory effect of different compounds, both cryosecretion and hemolymph showed

Table 1
Amidolytic activity of *Lonomia obliqua* secretions upon synthetic chromogenic substrates

Substrate	Enzyme	Amidolytic activity			
		Cryosecretion	Hemolymph	Bristle	Tegument
DL-BAPNA	Serine proteases	3.34	13.43	0.16	0
S-2238	Thrombin	12.930	43.24	2.47	1.43
S-2222	FXa	25.88	22.68	7.68	2.82
S-2366	FXIa	15.82	21.90	1.54	0.89
S-2302	Kallikrein	31.89	22.81	2.12	1.53
S-2444	Urokinase	79.23	67.27	1.88	1.63
S-2251	Plasmin	48.53	25.44	1.14	1.21

L. obliqua secretions (10 μg) were preincubated in 20 mM Tris–HCI buffer, pH 7.4, for 20 min. After incubation, reactions were initiated adding 0.2 mM of the indicated chromogenic substrate (Section 2). Amidolytic activity is expressed in units per microgram (U/μg), where one unit is the amount of protein that produced 1 pmol of *p*-anitroamilin in 1 min of reaction at 37 °C.

Table 2
Effect of inhibitors on the amidolytic activity *of Lonomia obliqua* secretions

Inhibitor	Concentration	Relitive activity upon indicated sub strates (%)								
		Cryosecretion				Hemolymph				Bristle
		DL-BAPNA	S-2251	S-2444	S-2222	DL-BAPNA	S-2251	S-2444	S-2222	S-2222
NONE	–	100.0	100.0	100.0	100.0	100.0	100.0	100.0	100.0	100.0
EDTA	5 mM	187.0	111.4	102.7	108.6	135.9	105.9	96.7	96.7	5.1
EGTA	5 mM	136.2	107.6	115.4	114.1	117.2	106.8	113.9	106.5	27.1
Benxamidin	5 mM	3.4	7.2	11.7	25.8	1.4	7.1	10.7	12.8	44.8
PMSF	2.5 mM	27.4	80.6	75.4	70.1	38.8	81.1	69.2	63.4	41.5
Hg^{2+}	25 μM	5.5	65.1	66.0	52.6	1.3	35.9	40.8	57.0	65.0
E-64	10 μM	66.6	92.0	100.0	87.0	55.8	70.9	84.1	65.1	102.2
L-Cystein	5 mM	95.3	NT[a]	NT	NT	102.0	NT	NT	NT	NT
β-Mercaptoethanol	10 mM	89.6	108.3	98.1	92.3	94.4	113.2	98.5	97.6	75.6

L. obliqua secretions (10 μg) were preincubated in 20 mM Tris–HCI buffer, pH 7.4, for 20 min with protease inhibitors, Reaction were initiated adding 0.2 nM of the indicated chromogenic substrate. Amidolytic activity was determined as described in Section 2. Values represent mean of three experiments.

[a] NT, not tested.

similar sensibility to the effect of divalent cations in their amidolytic activity when tested upon BAPNA (Table 3). Compared to control (dialyzed samples), Ca^{2+}, Mg^{2+}, Ba^{2+} and Mn^{2+} increased the activity, while Co^{2+} showed an intermediate activation. Zn^{2+} produced no effect whereas Cu^{2+} inhibited the enzymatic activity of both extracts. On the other hand, the bristle extract presented a different pattern concerning the influence of divalent cations. Contrarily to the other secretions, Mg^{2+}, Ba^{2+} and Mn^{2+} showed no effect (concentration of 5 mM) upon the bristle extract which showed inhibition by Co^{2+}, Zn^{2+}, Cu^{2+} (relative activity of 0.58, 0.23 and 0.15, respectively) and a slight activation of 1.27 fold by Ca^{2+} (Table 3).

3.6. Procoagulant activity

As depicted in Table 4 all *L. obliqua* secretions displayed a dose-dependent procoagulant activity, though presenting different potency levels. Bristle extract showed the strongest procoagulant activity, with a PI_{50} value of 0.6 μg. Hemolymph and the cryosecretion presented intermediate values of PI_{50} (34 and 50 μg, respectively), while the tegument extract showed the lowest PI_{50}, 81 μg.

3.7. Fibrinogenolytic activity

When pre-incubated with *L. obliqua* secretions fibrinogen was no longer clotted by thrombin thus indicating that all extracts displayed fibrinogenolytic activity (Fig. 3). The cryosecretion as well as hemolymph showed high fibrinogenolytic activity being both capable to produce almost complete blockage of fibrinogen clotting (10 and 20 μg, respectively) upon further incubation with thrombin. These results were confirmed using electrophoretic analysis (SDS-PAGE) of the incubations (Fig. 3A and B, inserts). It shows that the fibrinogen chains disappeared completely upon

Table 3
Effect of divalent cations on amidolytic activity of *Lonomia obliqua* secretions

Divalent cation	Concentration (nM)	Relative activity		
		Cryose-cretion	Hemo-lymph	Bristle
None	5	1	1	1
Ca^{+2}	5	4.62	2.13	1.27
Mg^{+2}	5	4.73	1.99	0.98
Ba^{+2}	5	3.75	2.00	0.97
Zn^{+2}	5	0.99	1.09	0.23
Mn^{+2}	5	5.07	2.31	0.97
Cu^{+2}	5	0.25	0.01	0.15
Co^{+2}	5	2.79	1.69	0.58

L. obliqua secretions (10 μg) were preincubated in 20 mM Tris–HCI buffer, pH 7.4, for 20 min with divalent cations. BAPNA (crysecretion and hemolymph) or S-2222 (bristle extract). Amidolytic activity was determined as described in Section 2. Values represent mean of three experiments.

incubation with 0.25 μg of cryosecretion for 15 min. Similarly, 1 μg hemolymph was capable to degrade all fibrinogen chains after 15 min of incubation. In both cases several fibrinogen fragments of low molecular mass were produced (Fig. 3C and D, inserts). On the other hand, the bristle and the tegument extracts presented much lower activity in both the fibrinogen clotting assay and SDS-PAGE analysis.

4. Discussion

L. obliqua's venom was previously reported as possessing mainly procoagulant activity which could be due to the presence of two procoagulant enzymes identified in the bristle extract of the caterpillar: a Factor X activator and a calcium-dependent prothrombin activator (Donato et al., 1998; Reis et al., 2001). However, further studies showed that the presence of calcium ion does not significantly increase the procoagulant activity of bristle extract (Veiga et al., 2003). More recently, it was reported for the first time, the presence of an anticoagulant activity caused by lonofibrase, a fibrin(ogen)olytic enzyme found in another caterpillar's secretion. Lonofibrase degrades preferentially fibrinogen Aα chain, with smaller efficiency in Bβ chain hydrolysis (Pinto et al., 2004). In the present study, we demonstrated the presence of several other potentially important active principles in *L. obliqua* secretions.

Table 4
Procoagulant activity of *Lonomia obliqua* secretions

Lonomia oblique sample	PI_{50}[a]
Cryosecretion	50
Hemolymph	34
Bristle	0.6
Tegument	81

[a] *L. obliqua* secretions were incubated with citrated plasma in 20 mM Tris–HCI buffer, PH 7.4, for 5 min. After incubation, reactions were initiated adding 10 μL of 150 mM $Cacl_2$ and monitored at 650 nm. PI_{50} is expressed as the amount of extract in micrograms capable to reduce in one half the plasm co agulation time.

The electrophoretic pattern of the four extracts showed several similarities among protein bands with some unique and distinct characteristics for each material (Fig. 1). Similarly, most proteins bands in all samples were recognized in the immunoblotting, especially those in the Mr range of 66–30 kDa. Concerning to the 15 kDa band found in all caterpillars secretions, it is suggested that it may correspond to lipocalin, a small extracellular protein able to bind plant pigments and other hydrophobic molecules and to intermediate cell-surface and protein-protein interactions, being thus involved in the mechanism of the well known mimetic behavior presented by these animals (Veiga et al., 2005). The primary antibody used for immunostaining, raised against the bristle extract (daSilva et al., 1996), was able to cross-react with distinct proteins in all extract samples. Since a crude bristle extract was used for raising the anti-lonomic serum, the recognition of several bands in all extracts strongly suggests that the hemorrhagic profile resulting from this envenomation may result from the participation of active principles from several secretions. In fact, we have previously studied the structures involved in the production, secretion and injection of the venom (Veiga et al., 2001). Microscopic and histochemical studies of *L. obliqua*'s secretory system demonstrated the absence of a typical glandular tissue. Instead, a very complex tegument with several cuticular specializations was found. This specialized epithelium is present throughout the caterpillar's tegument, being responsible for the venom production. Then, the caterpillar venom components produced by epithelial cells circulate in hemolimph and are stored in the external tegument and spines, being possibly the basis for the greater protein pattern similarity shown by the extracts. Furthermore, the presence of channel networks in the cuticle and breakaway bristles was also found (Veiga et al., 2001), indicating that this structure could offer an adequate system to make the venom easily available to be injected in the victims during the accident. When caterpillars are exposed to freezing conditions, a procedure we used to obtain cryosecretion, the stored proteins were released constituting this specific material, which also shows the mentioned protein similarity.

Differential enzymatic activity upon different chromogenic substrates specific for identification of blood coagulation-related proteases suggests the presence of distinct enzymes displaying amidolytic activities in *L. obliqua* secretions. This was confirmed by inhibition of the enzymes by protease inhibitors of different classes.

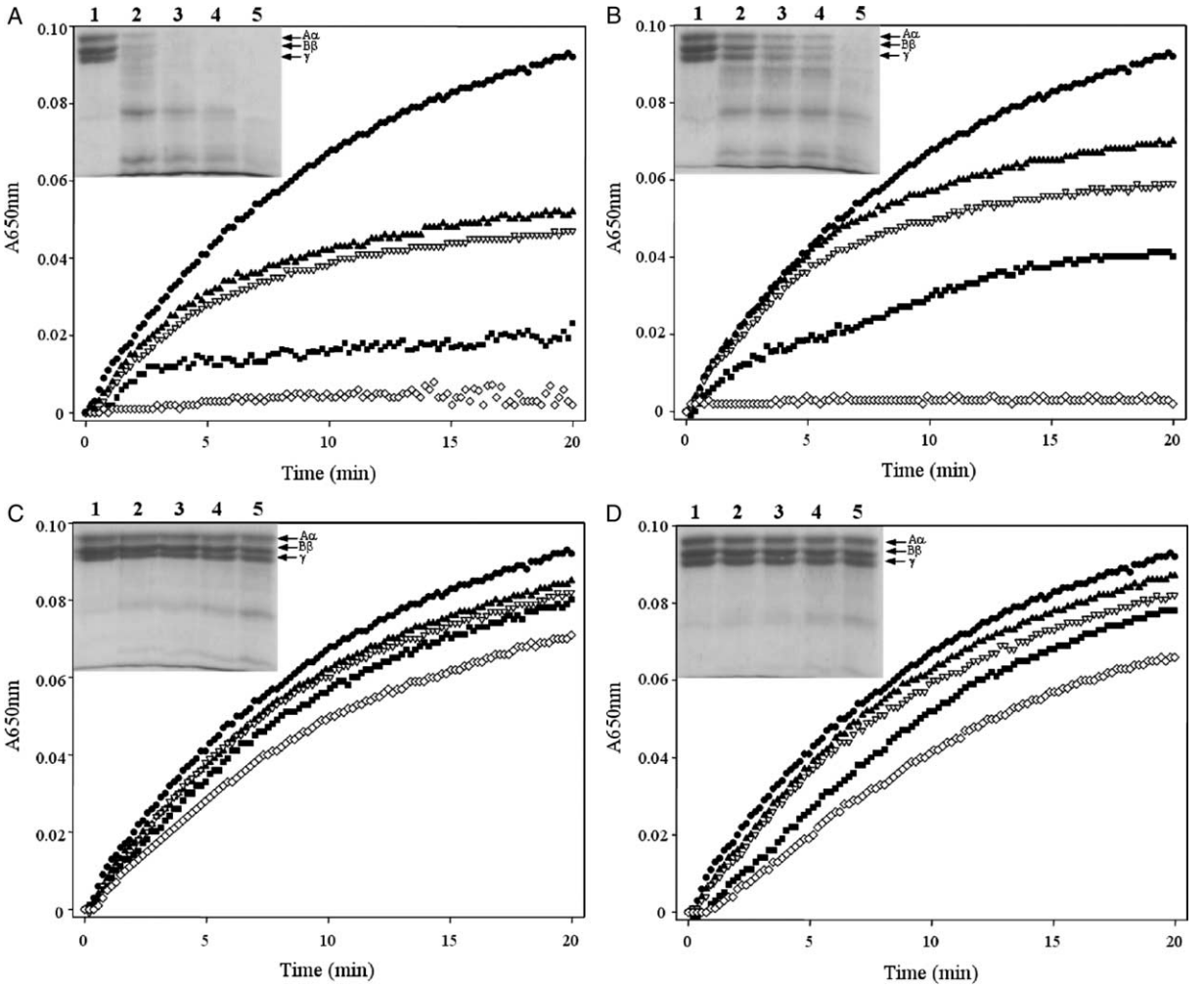

Fig. 3. Fibrin(ogen)olytic Activity. Fibrinogen (FBG) (0.2 mg) was incubated different amounts of *L. obliqua* secretions. After 15 min of incubation, 0.2 μg thrombin was added and the reaction followed at 650 nm. Control (●), 2.5 mg (▲), 5 mg (▽), 10 mg (■) and 20 mg (◇). Insert: reactions in the same conditions were analyzed in SDS-PAGE. (1) 20 μg FBG; (2–5) 20 μg FBG with 0.125, 0.25, 0.5 and 1 μg of extracts, respectively. (A) Cryosecretion; (B) Hemolymph; (C) Bristle extract and (D) Tegument extract. Aα, Bβ and γ FBG chains are indicated.

Concerning the enzyme diversity, the data indicate the presence of a high amidolytic activity on both cryosecretion and hemolymph, acting upon the specific substrates of thrombin, FXa, FXIa, kallikrein, urokinase and plasmin. These data suggest the presence of proteases with different secondary specificity or even wide specificity upon these substrates (Pinto et al., 2000). Inhibitory studies indicate the existence of two main groups of proteases in cryosecretion and hemolimph secretions: (a) serine proteases, strongly inhibited by benzamidine and (b) cystein proteases, susceptible to both E-64 and Hg^{+2}. The presence of a protease from these two groups in *L. obliqua* secretions was confirmed by high-throughput sequencing studies, in which sequences matching with serine protease-like and cathepsin-like enzymes were identified (Veiga et al., 2005). The bristle extract may contain a third group of metal-dependent protease susceptible to EDTA and EGTA. However, surprisingly no metalloprotease sequence was identified in the *L. obliqua* libraries (Veiga et al., 2005).

Despite of the presence of two previously reported enzymes in the bristle extract (Donato et al., 1998; Reis et al., 2001), it presents very low amidolytic activity upon the chromogenic substrates tested, except for S-2222, a FXa specific substrate, for which a moderate activity was found. This activity is probably due mainly to the calcium-dependent prothrombin activator present in this secretion (Reis et al., 1999). Nevertheless, the amidolytic activity was just slightly activated in the presence of 5 mM Ca^{2+} (Table 3), in accordance with previously reported data that showed the calcium independence of prothrombin activation

(Veiga et al., 2003). However, as expected for the prothrombin activator, the amidolytic activity was completely inhibited by EDTA and partially inhibited by benzamidine (Reis et al., 2001). The tegument extract shows similar behavior, presenting minimal amidolytic activity.

As shown in Table 4, all *L. obliqua* secretions presented procoagulant activity as depicted in the reduced clotting time. The strongest activity presented by the bristle extract is mainly due to the presence of two enzymes previously described: a prothrombin activator (LOPAP) and a Factor X (FX) activator (Donato et al., 1998). It seems then that the dissimilar procoagulant potency of the extracts tested is due, probably, to differential quantitative distribution of the proteases in the caterpillar's secretions. The absence of a prothrombin activator LOPAP in cryosecretion was confirmed in previous studies (data not shown). Thus, the procoagulant activity presented by this secretion seems to be due to FX activation. A similar behavior in hemolymph can be explained in the same way. The lower activity in tegument extract is probably due to low concentration of these enzymes in the high protein content of this material.

As previously reported, *L. obliqua* presents lonofibrase, a strong fibrin(ogen)olytic activity described in the cryosecretion (Pinto et al., 2004). However, it was now found that other caterpillar's secretions also display similar activity. As expected, cryosecretion showed higher fibrin(ogen)olytic activity, followed by hemolymph. Fibrinogen chains were fully degraded by the extracts, forming low molecular-weight unclottable fibrinogen fragments (Fig. 3A and B, Inserts). Despite having higher amidolytic activity, the fibrin(ogen)olytic activity of hemolymph was weaker than that of the cryosecretion. Due to its similar origin, probably lonofibrase is involved in the fibri(ogen)olytic activity of hemolymph and other secretions. Concerning the bristle extract, a weak fibrin(ogen)olytic activity was found. However, fibrinogen fragments could be identified in tested conditions by using incubation time of 1 and 24 h, where fibrinogen degradation is clearly visible (Veiga et al., 2003). Furthermore, this activity is more visible using a high proportion of venom:fibrinogen (Fritzen et al., 2003). Possibly, the amount of the enzyme responsible for this activity in the whole extract is very low or it has a slow fibrinogen degrading kinetic.

The present study reports quali-quatitative differences among four *L. obliqua* secretions. These differences are mainly in the protease content. Cryosecretion and hemolymph display strong amidolytic activity upon several substrates tested, presented moderated procoagulant activity and high fibrinogen degrading ability. Bristle and tegument extracts presented low amidolytic activity, but bristle extract showed the most potent procoagulant activity and both extracts presented low fibrinogen degrading ability. It is concluded that the differential involvement of each one of these secretions during the contact with one caterpillar or the whole colony can differentiate the outcome and wide variety of the clinical syndrome caused by *L. obliqua* envenomation.

Acknowledgements

We would like to thank the Centro de Informações Toxicológica (CIT-RS) for donation of caterpillars and support of information concerning envenomation. This work was supported by the Conselho Nacional de Desenvolvimento Científico e Tecnológico (CNPq) and Fundação de Amparo à Pesquisa do Estado do Rio Grande do Sul (FAPERGS).

References

Abella, H.B., Torres, J.B., Marques, M.G.B., Duarte, A.C., Barros, E., 1998. Manual de Diagnóstico e Tratamento de Acidentes por *Lonomia*. CIT (Centro de Informação Toxicológica), Porto Alegre.

Arocha-Piñango, C.L., Layrisse, M., 1969. Fibrinolysis produced by contact with a caterpillar. The Lancet 1, 810–812.

Arocha-Piñango, C.L., De Bosch, N.B., Torres, A., Goldstein, C., Nouel, A., Argüello, A., Carvajal, Z., Guerrero, B., Ojeda, A., Rodriguez, A., Rodriguez, S., 1992. Six new cases of a caterpillar-induced bleeding syndrome. Thrombosis and Haemostasis 67, 402–407.

Couppié, P., Marty, C., Sainte-Marie, D., Pradinaud, R., 1998. Chenilles venimeuses de Guyane Française: 5 observations. Annales de Dermatologie et de Vénéréologie 125, 489–491.

daSilva, W.D., Campos, A.C.M.R., Gonçalves, L.R.C., Souza-e-Silva, M.C.C., Higashi, H.G., Yamagushi, I.K., Kelen, E.M.A., 1996. Development of an antivenom against toxins of *Lonomia obliqua* caterpillars. Toxicon 34, 1045–1049.

Datta, G., Dong, A., Witt, J., Tu, A.T., 1995. Biochemical characterization of Basilase, a fibrinolytic enzyme from *Crotalus basiliscus basiliscus*. Archives of Biochemistry and Biophysics 317, 365–373.

Donato, J.L., Moreno, R.A., Hyslop, S., Duarte, A., Antunes, E., Le Bonniec, B.F., Rendu, F., De Nucci, G., 1998. *Lonomia obliqua* caterpillar spicules trigger human blood coagulation via activation of factor X and prothrombin. Thrombosis and Haemostasis 79, 539–542.

Duarte, A.C., Caovilla, J., Lorini, I., Lorini, D., Mantovani, G., Sumida, J., Manfre, P.C., Silveira, R.C., Dr Moura, S.P., 1990. Insuficiência renal aguda por acidentes com lagartas. Jornal Brasileiro de Nefrologia 12 (4), 184–186.

Fraiha Neto, H., Amaral, I.M., Ballarini, A.J., 1985. *Lonomia achelous* (Cramer) (Lepidoptera, Saturniidae), o 'tapuru da seringueira', agente do acidente hemorrágico por contato com larvas de mariposa no território Federal do Amapá. Resumo do XX Congresso da Sociedade Brasileira de Medicina Tropical, São Paulo, p. 24.

Fritzen, M., Schattner, M., Ribeiro, A.L.Q., Batista, I.F.C., Ventura, J., Prezoto, B.C., Chudzinski-Tavassi, A.M., 2003. *Lonomia obliqua* venom action on fibrinolytic system. Thrombosis Research 112, 105–110.

Guerrero, B.A.G., Arocha-Piñango, C.L., Gil, A., 1997a. *Lonomia achelous* caterpillar venom (LACV) selectively inactivates blood clotting factor XIII. Thrombosis Research 87, 83–93.

Guerrero, B.A.G., Arocha-Piñango, C.L., Gil, A., 1997b. Degradation of human factor XIII by Lonomin V, a purified fraction of *Lonomia achelous* caterpillar venom. Thrombosis Research 87, 171–181.

Guerrero, B.A.G., Perales, J., Gil, A., Arocha-Piñango, C.L., 1999. Effect on platelet FXIII and partial characterization of Lonomin V, a proteolytic enzyme from *Lonomia achelous* caterpillars. Thrombosis Research 93, 243–252.

Hougie, C., 1963. Fundamentals of Blood Coagulation and Clinical Medicine. McGraw-Hill, New York, pp. 25–48.

Laemmli, U.K., 1970. Cleavage of structural proteins during the assembly of the head of bacteriophage T4. Nature 227, 680–685.

Ngai, P.K., Chang, J.Y., 1991. A novel one-step purification of human α-thrombin after direct activation of crude prothrombin enriched from plasma. Biochemical Journal 280, 805–808.

Pinto, A.F.M., Veiga, A.B.G., Blochtein, B., Guimarães, J.A., 2000. Proteases from different secretions are involved on the paradoxial (pro-coagulant and hemorrhagic) envenomation caused by *Lonomia obliqua* caterpillars. In: Ménez, A. et al. (Org.), Toxins from Animals, Plants and Microbes. Program and Abstracts Book—XIIIth World Congress of the International Society on Toxinology-IST, Paris, p. 178.

Pinto, A.F.M., Dobrovolski, R., Veiga, A.B.G., Guimarães, J.A., 2004. Lonofibrae, a novel α-fibrinogenase from *Lonomia obliqua* caterpillars. Thrombosis Research 113, 147–154.

Reis, C.V., Kelen, E.M.A., Farsky, S.H.P., Portaro, F.C.V., Sampaio, C.A.M., Fernandes, B.L., Camargo, A.C.M., Chudzinski-Tavassi, A.M., 1999. A Ca^{++} activated serine protease (LOPAP) could be responsible for the haemorrhagic syndrome caused by the caterpillar *Lonomia obliqua*. The Lancet 353, 1942.

Reis, C.V., Portaro, F.C.V., Andrade, S.A., Fritzen, M., Fernandes, B.L., Sampaio, C.A.M., Camargo, A.C.M., Chudzinski-Tavassi, A.M., 2001. A prothrombin activator serine protease from the *Lonomia obliqua* caterpillar venom (Lopap) biochemical characterization. Thrombosis Research 102, 427–436.

Ribeiro, J.M., Schneider, M., Guimarães, J.A., 1995. Purification and characterization of Prolixin S (Nitrofhorin 2), the salivary anticoagulant of the blood-sucking bug *Rhodnius prolixus*. Biochemical Journal 308, 243–249.

Seibert, C.S., Shinohara, E.M.G., Sano-Martins, I.S., 2003. In vitro hemolytic activity of *Lonomia obliqua* caterpillar bristle extract on human and Wistar rat erythrocytes. Toxicon 41, 831–839.

Veiga, A.B.G., Blochtein, B., Guimarães, J.A., 2001. Structures involved in production, secretion and injection of the venom produced by the caterpillar *Lonomia obliqua* (Lepidoptera, Saturniidae). Toxicon 39, 1343–1351.

Veiga, A.B.G., Pinto, A.F.M., Guimarães, J.A., 2003. Fibrinogenolytic and procoagulant activities in the hemorrhagic syndrome caused by *Lonomia obliqua* caterpillars. Thrombosis Research 111, 95–101.

Veiga, A.B.G., Ribeiro, J.M., Guimarães, J.A., Francischeti, I.M.B., 2005. A catalog for the transcripts from the venomous structure of the caterpillar *Lonomia obliqua*: identification of the proteins potentially involved in the coagulation disorder and hemorrhagic syndrome. Gene 355, 11–27.

Von Ihering, R., 1914. Estudo biologico das lagartas urticantes ou tatoranas. Annaes Paulistas de Medicina e Cirurgia 3, 129–139.

Zannin, M., Lourenço, D.M., Motta, G., Costa, L.R.D., Grando, M., Gamborgi, G.P., Noguti, M.A., Chudzinski-Tavassi, A.M., 2003. Blood coagulation and fibrinolytic factors in 105 patients with hemorrhagic syndrome caused by accidental contact with *Lonomia obliqua* caterpillar in Santa Catarina, Southern Brazil. Thrombosis and Haemostatis 89, 355–364.

3.3.2. Novas perspectivas na patogênese do envenenamento pela lagarta *Lonomia obliqua* baseadas na avaliação da resposta celular por análise da expressão gênica

Antônio F. M. Pinto, Bojan Dragulev, Jorge A. Guimarães, Jay W. Fox. 2006. Novel Perspectives on the Pathogenesis of *Lonomia obliqua* Capterpillar Envenomation Based on Assessment of Host Response by Gene Expression Analysis.

O envenenamento por *Lonomia obliqua* provoca um grave quadro hemorágico. Nos últimos anos, várias enzimas do veneno foram isoladas, caracterizadas e relacionadas com os sintomas do lonomismo. Entretanto, não se possui uma noção exata de quanto de veneno de *Lonomia obliqua* é necessário para o desenvolvimento dos quadros clínicos mais graves. Sabemos que aproximadamente 1 mg de proteína pode ser extraído das espículas de uma única lagarta. O método de extração utilizado faz uso de todas as espículas do animal e ocorre o esgotamento do conteúdo de veneno das espículas.

Essas condições obviamente não ocorrem durante o contato com as lagartas e o envenenamento ocorre da mesma forma. Assim, foi proposto que além dos efeitos diretos do veneno no sistema hemostático, o veneno provocaria uma reação celular capaz de amplificar o quadro clínico do lonomismo.

Utilizando técnicas de microarranjos de DNA, esse trabalho avaliou o efeito do extrato de espículas de *Lonomia obliqua* no perfil de expressão gênica de fibroblastos humanos em cultura.

Este trabalho foi desenvolvido na Biomolecular Research Facility (University of Virginia) e no Laboratório de Bioquímica Farmacológica (UFGRS). Os dados aqui apresentados são parte de um manuscrito em fase final de preparação.

Novel Perspectives on the Pathogenesis of *Lonomia obliqua* Capterpillar Envenomation Based on Assessment of Host Response by Gene Expression Analysis

Antônio F. M. Pinto[1,2], Bojan Dragulev[1], Jorge A. Guimarães[2], Jay W. Fox[1]*

1 *Department of Microbiology, University of Virginia, P.O. Box 800734, Charlottesville, VA 22908-0734, USA*

2 *Centro de Biotecnologia, Universidade Federal do Rio Grande do Sul, Av. Bento Gonçalves 9500, 43431, C.P. 15005, Porto Alegre, Brazil*

* Corresponding Author. Tel.: +1 434 924 0050; Fax: +1 434 982 2514

e-mail address: jwf8x@virginia.edu (J.W. Fox)

Introduction

Venomous animals contain a vast array of enzymatic and non-enzymatic components capable of promoting drastic changes in hemostasis. Some lepidopteran larvae, in particular those from the Saturniidae family, have venoms that produce hemostatic effects (Scoble, 1992). These venoms are their main defense against predators and thus are somewhat differently from snake and spider venoms which primarily function to immobilize and digest the prey.

The envenomations caused by caterpillars from *Lonomia* genus have been reported since late 1960's in Venezuela (Arocha-Pinango and Layrisse, 1969). Among other blood coagulation disturbances, intense fibrinolytic activity was found in envenomed patient's plasma. Plasmin and urokinase-like activities were characterized and fibrinolytic activity on human blood clots were also found in the caterpillar venom (Arocha-Pinango and Pepper, 1981; Coll-Sangrona and Arocha-Pinango, 1998). In Brazil, envenomation with the caterpillar *Lonomia obliqua*, known as lonomism, was first reported in 1989 (Duarte et al., 1996). This envenomation is characterized by ecchymosis, hematuria, bleeding from scars and mucous membranes, intracerebral bleeding and acute renal failure (Arocha-Pinango and Guerrero, 2001; Zannin et al., 2003).

The pathological effects of certain isolated toxins from the whole caterpillar venom have been investigated. These studies identified venom components capable of reproducing some of the pathophysiological aspects of the clinical envenomation profile, such as intravascular coagulation (Donato et al., 1998), fibrinogen and fibrin degradation (Pinto et al., 2004; Pinto et al., 2006; Veiga et al., 2003), inflammation (Fritzen et al., 2005), hemolysis (Seibert et al., 2003), edema and local pain sensation (de Castro Bastos et al., 2004).

The isolation and biochemical characterization approach has been moderately successful with protein toxins from this caterpillar, providing a basic understanding of the venom-induced pathology. Recently, a significant advance was achieved through a transcriptome study, which generated a catalog of putative toxic proteins of the caterpillar venom, and thereby giving rise to hypotheses on the molecular basis of pathogenesis envenomation which could be experimentally explored (Veiga et al., 2005).

Microarray technology such as gene expression analysis has been proven as important tool for rapid and broadband analysis of the functional effects of venomous substances on host cells and tissues (Gallagher et al., 2005; Gallagher et al., 2003). The use of toxins in low concentrations such that they do not produce phenotypic changes on cells in tissue culture, but can produce effects in the gene expression profiles of these cells have provide significant insight in the novel functionalities of venom components, thereby providing a more complete and in some case relevant understanding of the biological activities associated to the venom.

The hypothesis of our study is that *L. obliqua* venom produces effects in the gene expression profile of cells in tissue culture indicative of an indirect response from the host which contributes to the observed pathophysiology of envenomation. Together, the direct action of *L. obliqua* venomous proteins and the change in the expression pattern of cells would be in concert and perhaps synergistically be responsible for the profound symptoms observed in during the envenomation. In this study we demonstrate that in fact venom alteration of host gene expression profiles can contribute to the observed effects of *Lonomia* envenomation.

Material and Methods

Lonomia obliqua bristle extract

L. obliqua caterpillars were kindly provided by Centro de Informações Toxicológicas (CIT), Porto Alegre, Rio Grande do Sul, Brazil. The insects were collected by local inhabitants directly from trees. *Lonomia obliqua* bristle extract (LOBE) was obtained as described elsewhere (Pinto et al., 2006). Briefly, bristles were cut at the caterpillars' tegument insertion, homogeneized in buffer (20 mM Tris.HCl, pH 7.5) and centrifuged at 9,600xg for 20 min. The supernatant was stored at -20^{o}C until use.

Cell cultures

Human fibroblasts cell strain HS68 (ATCC CRL-1635, from newborn foreskin) was maintained in DMEM (Invitrogen, Carlsbad, CA), containing 10% fetal calf serum and supplemented with 4 mM L-glutamine, 1.5 g/L sodium pyruvate, 4.5 g/L glucose, essential and non-essential amino acids. Cells were grown at 37^{o}C with 5% CO_2 and

passaged using trypsin (0.05%)-EDTA (0.02%) solution (Invitrogen, Carlsbad, CA). The effects of LOBE on the fibroblast cells viability (Cell Titer-Blue Cell Viability Assay, Promega, USA) and apoptotic state (Apo-One Homogeneous Caspase-3/7 Assay, Promega, USA) were tested prior main experiments.

Target preparation, GeneChip hybridization and data analysis

Fibroblasts were grown to 90-95% confluence in tissue culture flasks. Culture medium was aspired and replaced with fresh serum-free medium containing 25 μg/mL LOBE or only serum free medium as control. Cells were incubated for 1 h at 37^{o}C/5% CO_2. The media were aspired and saved for further experiments. Total RNA was isolated using Qiagen RNEasy kit and labeled cRNA was synthesized according to standard Affymetrix protocols. Samples of biotin-labeled cRNA (10 μg) were hybridized to Affymetrix HuGeneFL probe arrays, containing probe sets representing approximately 7000 genes, for 16 h, and scanned with the Affymetrix GeneArray Scanner.

Scanned gene array images were first examined for visible defects and then checked for grid alignment. When passed, the image file was analyzed to generate composite data files ("cell files"). From this point on, a coordination of two paths of analysis was carried out using the Affymetrix Microarray Analysis Suite version 5.0 (MAS 5.0, Affymetrix, Santa Clara, CA) and the Dchip software (Li and Wong, 2001; Schadt et al., 2001). The detection of a particular gene, called "present", "absent", or "marginal", was made using MAS 5.0 and these detections calls were later imported into and used by the Dchip program. Quantification of gene expression was obtained using Dchip, which applied a model-based approach to derive the probe sensitivity index and expression index. The two indices were used in a linear regression to quantify a particular gene. When certain probes or transcripts deviated from the model to a set extent, they were excluded from the quantification process. Normalization of the arrays was done using the invariant set approach. Comparative analysis of the samples was done based on Dchip-generated fold changes and unpaired sample t test. Typically, we considered a p of less than 0.05, a fold change greater than 1.5 or less than -1.5, and a signal intensity difference of greater than 100 or less than -100 as indications of significant change in gene expression.

Quantitative RT-PCR

Total RNA samples used were prepared as described for the Affymetrix GeneChip experiments. Reverse transcription was performed with MultiScribe reverse transcriptase (Applied Biosystems, Forster City, CA) and random hexamers as per the manufacturer's instruction. The resulting cDNA was then subjected to quantitative RT-PCR. Specific primers were designed for each transcript of interest using the Primer Express 2.0 software (Applied Biosystems). The target sequences were retrieved from the Affymetrix Probe Sequence Database (Liu et al., 2001). Three PCR reactions were carried out for each transcript using cDNA sample equivalent to 50ng of starting total RNA, 6 μL of each respective forward and reverse primer (5μM), and the fluorescent indicator SYBR® Green I Dye. Amplification PCR and monitoring of the fluorescent emission in real time were performed in an ABI Prism 7900HT Sequence Detection System (Applied Biosystems) as recommended by the manufacturer (ABI SYBR Green Protocol). To verify that only a single PCR product was amplified per transcript, dissociation curve data was analyzed utilizing the 7900HT Sequence Detection Software (SDS). Quantitative PCR was also performed for each cDNA sample using primers for human glyceraldehydes-3-phosphate dehydrogenase (GAPDH) as a housekeeping gene. Threshold cycles (Ct) of detection were defined for the target and the housekeeping gene in each cDNA sample. In order to convert the Ct value into a relative abundance of target and housekeeping gene per sample, a standard curve was generated for the housekeeping gene, using serial dilutions of cDNA sample: an arbitrary value of template was first assigned to the highest standard, then corresponding values were assigned to the subsequent dilutions, and these relative values were plotted against the Ct value determined for each dilution, resulting in the generation of the standard curve. The relative amount of target and housekeeping gene in each sample was then determined using the comparative Ct method (Applied Biosystems, 2001). The relative quantity (RQ) of target, normalized to a housekeeping gene and relative to a calibrator (the Rox reference dye), is given by: $RQ = 2^{-\Delta\Delta Ct}$, where $\Delta\Delta Ct$ represents the difference in Ct between the transcript and the housekeeping gene for the same RNA sample. The ratio of the RQs for the treated sample and the experiment sample was used to derive the fold change.

APTT assay

In order to determine whether treatment of fibroblasts by LOBE could indirectly affect the host, tissue culture media from treated fibroblasts was assayed for its ability to alter coagulation time. Activated partial thromboplastin time (APTT) assay was performed using the APTTest (WienerLab, Argentina). Human plasma (50μL) was incubated at 37^{o}C with media of fibroblasts treated with LOBE (Fb-LOBE) or non-treated (Fb-control). After 3 minutes, cephallin with ellagic acid (50μL) was added and incubated for more 3 minutes. The coagulation was initiated by addition of 50 mM $CaCl_2$ (50μL) and the kinetic of the coagulation reaction followed at 650 nm in the SpectraMax equipment (Molecular Devices, USA).

Results

Incubation of fibroblasts with LOBE

The fibroblast cells were chosen for these experiments based on the fact that the stroma is one of the first tissues that come in contact with the caterpillar's secretions during the envenomation. Following 2 h incubation at venom concentration up to 50 μg/mL, fibroblasts had normal adherent morphology and normal cell viability assessed by Cell Titer-Blue cell viability assay. Apoptosis was not detected with the tested concentrations with the caspase-3/7 assay (data not shown).

Gene expression analysis of LOBE fibroblasts

The results of the significantly up-regulated genes in fibroblasts treated with LOBE are shown in Table I. Fifty nine genes were determined to be up-regulated at levels of 1.5 or greater (p<0.05) in the *L. obliqua* treated fibroblasts compared to the untreated cells. The gene identified with the greater transcription increment in treated cells was interleukin 8 (IL-8), with 4.07 fold (Table I). IL-8 is a member of the CXC chemokine family and is one of the major mediators of the inflammatory response. Another member of this family, CXCL1, was up-regulated 3.93 fold. Also related with inflammatory response, the gene of interleukin 6 (IL-6) and CCL2 were up-regulated 2.25 and 1.66 fold, respectively.

Table I. Up and down regulated genes of *Loomia obliqua* bristle extract-treated fibroblasts.

Up Regulated Genes	Affymetrix ID	Fold Change	p value
interleukin 8	NM_000584	4.07	0.012323
natural cytotoxicity triggering receptor 2	NM_004828	3.94	0.04011
chemokine (C-X-C motif) ligand 1	NM_001511	3.93	0.002767
dimethylarginine dimethylaminohydrolase 1	NM_012137	2.46	0.00771
dual specificity phosphatase 6	BC005047	2.39	0.039138
regulator of G-protein signalling 4	BC000737	2.36	0.006177
interleukin 6	NM_000600	2.25	0.041571
centromere protein H	AL572471	2.18	0.049505
glycine receptor a1	NM_000171	2.17	0.046747
RGC32 protein	NM_014059	2.16	0.014495
sclerostin domain containing 1	AI927000	2.14	0.024795
prostaglandin-endoperoxide synthase 2	NM_000963	2.01	0.005891
core promoter element binding protein	BE675435	1.94	0.032063
ectodermal-neural cortex (with BTB-like domain)	NM_003633	1.9	0.009534
Urokinase-Plasminogen Activator Receptor	AY029180	1.9	0.029381
lectin, mannose-binding 2	NM_006816	1.82	0.037009
keratin, hair, acidic, 9A	NM_004100	1.70	0.029209
ADP-ribosylation factor guanine nucleotide factor 6	NM_015310	1.76	0.032621
fibroblast growth factor 5	NM_004464	1.76	0.018866
thymosin, beta 4, Y-linked	NM_004202	1.75	0.011449
MAX protein	M64240	1.74	0.028584
RAB-8b protein	AB038995	1.74	0.014602
DnaJ (Hsp40) homolog, subfamily B, member 6	AF080569	1.73	0.043053
regulator of G-protein signalling 4	AL514445	1.72	0.004728
endothelial cell-specific molecule 1	NM_007036	1.72	0.04702
phosphoprotein regulated by mitogenic pathways	NM_025195	1.71	0.022946
Homo sapiens hypothetical gene supported by NM_033266	AB047079	1.71	0.047183
AD-003 protein	BC001396	1.7	0.032724
early growth response 2 (Krox-20 homolog, Drosophila)	NM_000399	1.68	0.02285
Polypeptide N-acetylgalactosaminyltransferase 13 (GalNAc-T13)	BF346193	1.67	0.017088
chemokine (C-C motif) ligand 2	S69738	1.66	0.046156
eukaryotic translation initiation factor 4E	AW268640	1.64	0.033049
vascular endothelial growth factor	H95344	1.63	0.015695
hypothetical protein MGC5309	BC003353	1.62	0.034577
replication factor C (activator 1) 2, 40kDa	M87338	1.61	0.037797
intercellular adhesion molecule 3	NM_002162	1.6	0.014891
keratin associated protein 1-5	AJ406928	1.6	0.028029
tumor necrosis factor, alpha-induced protein 6	AW188198	1.59	0.023336
putative membrane protein	AF277194	1.58	0.028772
Human lipocortin (LIP) 2 pseudogene mRNA	M62895	1.57	0.034938
hypothetical protein FLJ90406	AL117590	1.57	0.012777
fumarate hydratase	AI333836	1.56	0.034346
menage a trois 1 (CAK assembly factor)	NM_002431	1.56	0.013867
TRAP/Mediator complex component	AI026938	1.56	0.048396
Tissue Factor, Coagulation Factor III	NM_001993	1.55	0.029502
Tetratricopeptide repeat, ankyrin repeat and coiled-coil containing 1	AI330378	1.55	0.010753
APG12 autophagy 12 like (S. cerevisiae)	NM_004707	1.54	0.045332
ribosomal protein S6 kinase, 90kDa, polypeptide 2	AW025216	1.54	0.029596
hypothetical protein HSPC111	NM_016391	1.53	0.032369
interleukin 8 receptor, alpha	NM_000634	1.53	0.029813
Glycosyltransferase 28 domain containing 1	NM_018466	1.53	0.026577
peptidylprolyl isomerase B (cyclophilin B)	NM_000942	1.52	0.028399
polymerase (RNA) I polypeptide C, 30kDa	AF008442	1.52	0.023345
Homo sapiens transcribed sequences	AI806370	1.52	0.024257
hypothetical protein LOC253827	BC040053	1.51	0.041349
chromosome 6 open reading frame 108	NM_006443	1.51	0.032881
general transcription factor IIF, polypeptide 2, 30kDa	BC001771	1.51	0.033328
chromosome 20 open reading frame 166	AL449263	1.51	0.04743

Down Regulated Genes	Affymetrix ID	Fold Change	p value
sal-like 1 (Drosophila)	AU152837	-1.5	0.015256
glycogen synthase kinase 3β	BC000251	-1.51	0.040516
chromosome 19 open reading frame 7	AB028987	-1.51	0.019572
bromodomain containing 2	S78771	-1.51	0.036851
brother of CDO	AY027658	-1.51	0.024793
cisplatin resistance associated	AK097000	-1.52	0.037556
cytoskeleton-associated protein 4	AW029619	-1.52	0.034026
fibulin 1	Z95331	-1.52	0.014029
laminin, alpha 2 (merosin, congenital muscular dystrophy)	AK026829	-1.52	0.01039
MAX interacting protein 1	NM_005962	-1.53	0.006061
multiple endocrine neoplasia I	NM_000244	-1.53	0.024739
proline arginine-rich end leucine-rich repeat protein	AA573140	-1.53	0.026464
xylosyltransferase II	NM_022167	-1.54	0.047916
RAN binding protein 2	AI681120	-1.55	0.049817
hypothetical protein MGC13024	AW517464	-1.56	0.033937
baculoviral IAP repeat-containing 6 (apollon)	AI017106	-1.56	0.049696
zinc finger protein	NM_010101	-1.57	0.037541
Hypothetical protein LOC644215	BC009463	-1.59	0.017794
collagen, type IV, a2	AA909035	-1.59	0.01726
similar to collagen, type I, a1 chain precursor	AB018345	-1.59	0.010536
cyclin-dependent kinase inhibitor 1C (p57, Kip2)	N33167	-1.61	0.03579
Neurogenic locus Notch protein precursor	BE732345	-1.61	0.028067
mannosidase, alpha, class 1C, member 1	NM_020379	-1.61	0.021307
Trophoblast-derived noncoding RNA	AV659198	-1.61	0.046431
UEX domain containing 1	BE467577	-1.62	0.015362
thymidine kinase 2, mitochondrial	AA524412	-1.63	0.022263
ankyrin repeat domain 9	AW194999	-1.64	0.043212
homeo box A13	BG289306	-1.64	0.005879
uroporphyrinogen III synthase	BC024936	-1.65	0.016524
collagen, type IV, a3 (Goodpasture antigen) binding protein	NM_005713	-1.65	0.044409
chromosome 5 open reading frame 4	NM_016348	-1.65	0.042697
protein phosphatase 1, regulatory (inhibitor) subunit 3C	N26005	-1.66	0.010614
zinc finger protein 503	AA603467	-1.66	0.043014
PC4 and SFRS1 interacting protein 2	AI252087	-1.67	0.044502
transducer of ERBB2, 1	BF240286	-1.68	0.014826
abhydrolase domain containing 2	BE671816	-1.71	0.043279
Rho GTPase activating protein 5	AK023014	-1.71	0.040149
myosin regulatory light chain interacting protein	AF212221	-1.72	0.038618
similarity to protein ubiquinol-cytochrome-c reductase core protein I - human	N54506	-1.84	0.04722
coagulation factor C homolog, cochlin (Limulus polyphemus)	BC007230	-1.86	0.010016
Janus kinase 1 (a protein tyrosine kinase)	AL555086	-1.87	0.024578
HIF-1 responsive RTP801	NM_019058	-1.87	0.007313
Ras-like without CAAX 1	AL037450	-1.88	0.02531
KIAA1199 protein	BC020256	-1.89	0.017463
insulin receptor	AI215106	-1.91	0.028524
cell division cycle 42 (GTP binding protein, 25kDa)	N92917	-1.94	0.008139
A kinase (PRKA) anchor protein (gravin) 12	BF114967	1.94	0.043532
hypothetical protein FLJ23119	AW792857	-1.96	0.019428
IQ motif containing GTPase activating protein 1	AI679073	-1.99	0.038549
MAX dimerization protein 4	BC002713	-2.01	0.024111
non-metastatic cells 7, protein expressed in (nucleoside-diphosphate kinase)	AI094580	-2.01	0.023886
chromosome 14 open reading frame 43	NM_018678	-2.03	0.026059
chromosome 21 open reading frame 6	AF212232	-2.08	0.041913
bromodomain containing 4	AA702437	-2.14	0.041624
Homo sapiens, clone IMAGE:4732650, mRNA	AV702787	-2.18	0.044274
EphB3	NM_004443	-2.26	0.033241
ubiquitin specific protease 7 (herpes virus-associated)	BF433061	-2.31	0.046582
solute carrier family 7, member 8	AL365343	-2.34	0.036443
ubiquitin-conjugating enzyme E2B (RAD6 homolog)	AI499236	-2.37	0.027477
Homo sapiens, clone IMAGE:4732650, mRNA	BC020911	-2.57	0.045002
HMBA-inducible	AW665096	-3.12	0.028051
hypothetical protein dJ462O23.2	W15435	-3.39	0.014501
emopamil binding protein (sterol isomerase)	N58493	-3.5	0.018701

Other five genes of interest were found up-regulated in the fibroblast cells treated with LOBE: dimethylarginine dimethylaminohydrolase 1 (DDAH, 2.46 fold), prostaglandin-endoperoxide synthase 2 (PTGS2, 2.01 fold), urokinase-type plasminogen activator receptor (uPAR, 1.9 fold), ICAM-3 (1.6 fold) and tissue factor (1.55 fold).

Sixty four genes were significantly decreased (1.5 or greater) in LOBE treated cells compared with the non-treated cells (Table II). Proteins from the extracellular matrix and other related proteins were observed in the down-regulated genes, such as collagen type IV binding protein (-1.59 fold), laminin (-1.52 fold) and fibulin (-1.52 fold).

Validation of GeneChip data with quantitative RT-PCR

As an approach to validate the GeneChip data, five genes of interest were subjected to quantitative RT-PCR analysis (Figure 1). Quantitatively, the results of the RT-PCR were in general agreement with those of the GeneChip data. The fold changes from the RT-PCR data were lower but qualitatively consistent than that observed with Gene Chips.

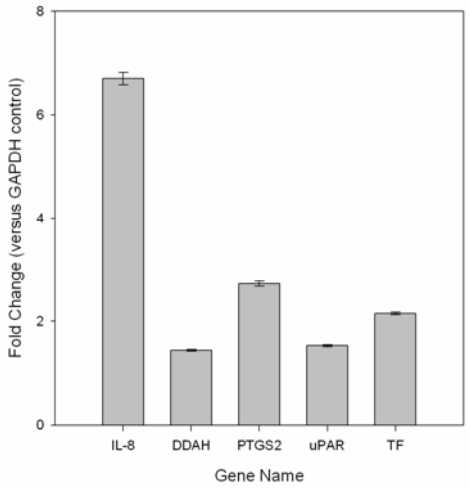

Figure 1. Changes of selected transcript levels. Bars represent LOBE treated cells. Responses were analysed at 1 hour after cell treatment. IL-8, Interleukin 8; DDAH, dimethylarginine dimethylaminohydrolase 1; PTGS2, prostaglandin-endoperoxide synthase 2; uPAR, urokinase-type plasminogen activator receptor; TF, tissue factor.

Outcome of gene expression alteration of LOBE treated fibroblast on coagulation

Coagulation assays using the APTT test were performed using Fb-LOBE conditioned media (25 μg/mL, 1 h incubation) and Fb-control media. In these experiments, Fb-LOBE medium was preincubated with human plasma prior to APTT test. Fb-LOBE presented a dose-dependent pro-coagulant activity, as shown in Figure 2. To test if this effect was a direct response to the presence of the *L. obliqua* bristle extract in the culture media, a dose-response curve of LOBE was made. Considering the amount of venom in the media (25 μg/mL), the curve used a range of protein content compatible with the treated media experiments. These amounts of venom were unable to reduce the coagulation time in the same proportion (data not shown).

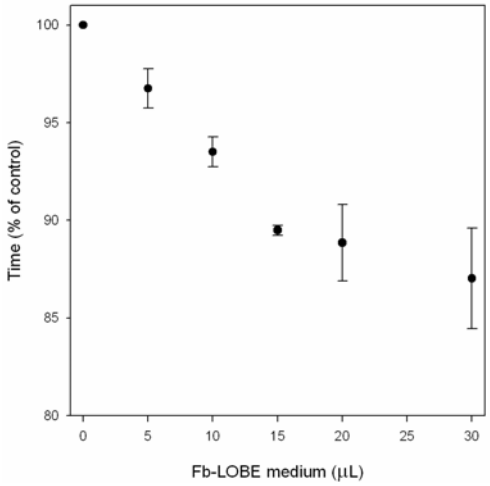

Figure 2. APTT coagulation assay. Dose dependent pro-coagulant activity of the Fb-LOBE medium compared to Fb-control. Experiments were performed in triplicate.

To rule out the participation of *L. obliqua* procoagulant proteins in this assay, anti-lonomic serum was previously incubated with both LOBE treated and non-treated control media. The incubation with anti-lonomic serum (sufficient to neutralize 1.75 μg of venom) did not change the procoagulant activity of the treated medium in the APTT assay (Figure 3).

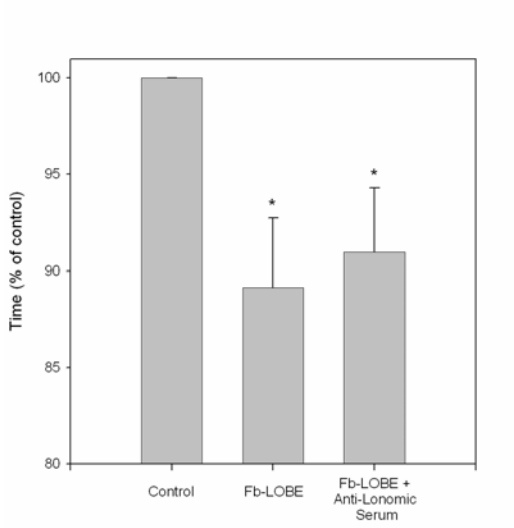

Figure 3. Effect of the anti-lonomic serum in the procoagulant activity of Fb-LOBE. Fb-LOBE (20 μL) was pre-incubated for 10 minutes with or without anti-lonomic serum (enough to inhibit 1.75 μg of venom). After incubation, coagulation assay (APTT) was performed. Experiments were performed in triplicate.

Discussion

Contact with *Lonomia obliqua* caterpillars can cause a severe hemorrhagic disorder called lonomism. Patients involved in this kind of accident frequently present a drastic depletion of coagulation factors and activation of fibrinolytic system. Initial studies with *L. obliqua* venom components were made using the extract from the caterpillar's bristles. The bristle extract is mainly procoagulant due to the presence of a prothrombin activator and a factor X activator (Donato et al., 1998). Later, other proteins potentially involved with the envenomation were described: a phospholipase A2-like enzyme called lonomiatoxin (Arocha-Pinango et al., 2000; Seibert et al., 2006) and fibrinolytic enzymes from the bristle extract and other caterpillar's secretions (Fritzen et al., 2003; Pinto et al., 2004; Pinto et al., 2006; Veiga et al., 2003). Other envenomation aspects were also investigated, leading to the characterization of edematogenic and nociceptive components (de Castro Bastos et al., 2004), inflammatory response (Alvarez Flores et al., 2006; Fritzen et al., 2005), hemolysis (Seibert et al., 2004; Seibert et al., 2003) and hyaluronidases named lonoglyases (Gouveia et al., 2005).

More recently, the transcriptome of *L. obliqua* showed the presence of several proteins in the caterpillar's secretions which are not acting directly upon coagulation and fibrinolytic systems such as defense proteins, lipocalins, lectincs and serpins. These proteins are inoculated in the envenomed victim, and probably constitute active principles involved direct or indirectly in the clinical profile manifestations (Veiga et al., 2005).

During venom extraction, after removal of all bristles structures, each caterpillar produces approximately 1 mg of crude bristle extract. This is an artificial method of extraction since it was proposed that venom inoculation occurs by dislodgement of the tips of the bristles when caterpillar's hairs brushes against the skin. This would release only a small amount of venom per caterpillar.

In this study we utilized microarray technology to obtain an alternative perspective of the pathogenesis of caterpillar venom.. The aim was to determine whether treatment of fibroblasts, a common cell type in stroma, with caterpillar venom could alter the gene expression pattern of the cells. Further, we proposed that analysis of those changes could provide insight into an "indirect" mechanism by which the venom could cause some of the observed pathologies associated with caterpillar envenomation.

To do this, crude *L. obliqua* bristle extract was used to mimicry an envenomation condition. Several up-regulated genes are coherent with clinical manifestations and were involved in previously described *in vitro* and *in vivo* results.

L. obliqua in vivo experiments have already demonstrated the migration of neutrophils and monocytes to sites of envenomation (Reis et al., 2001), probably due to stimulation of IL-8 and ICAM-1 expression in endothelial cells (Fritzen et al., 2005). The GeneChip data of envenomed fibroblasts show the up-regulation of several pro-inflammatory mediators. IL-8, presenting a 4.07 fold change compared to non-treated control cell, is a chemoattractant for neutrophils, basophils and T-cells and is also involved in the process of neutrophil activation. IL-8 is released by several cell types in response to an inflammatory stimulus (Van Damme et al., 1988). IL-6, involved in cell mediated immune response, and CCL2, chemoattractant of monocytes and basophils, were also present in the up-regulated genes, as well as the adhesive molecule ICAM-3. The up-regulation of pro-inflammatory mediators in an envenomed tissue could be related with leukocyte recruitment at sites of envenomation.

On of the local symptoms of the envenomation is edema. Injection of *L. obliqua* venom in rat paws produced intense edematogenic response for more than 6 hours after injection (de Castro Bastos et al., 2004). In this experimental model, the edema response was not inhibited by a cyclooxygenase inhibitor (indomethacin), but an anti-histaminic compound (loratadine) produced significant inhibition, pharmacological characteristics compatible with a mild inflammatory condition. Based on this information, our data indicates that the edematogenic response could be partially due to inflammatory response being activated by up-regulation of pro-inflammatory mediators.

Increase in nitric oxide (NO) generation was already reported in endothelial cells treated with *L. obliqua* venomous proteins (Fritzen et al., 2005). Our data show an increase in the expression of the enzyme dimethylarginine dimethylaminohydrolase (DDAH), responsible for metabolization of two endogenous nitric oxide synthase (NOS) inhibitors (MacAllister et al., 1996). The up-regulation of DDAH would diminish the concentration of nitric oxide inhibitors, consequently increasing the synthesis of NO. The data here presented shows that NO generation is caused by interference in the nitric oxide synthesis pathway, through metabolization of two NOS inhibitors.

LOCBE produced a dose-dependet nociceptive effect in rats, characterized by a syndrome of shaking and lifting of the inject paw. This nociceptive effect appear to be mainly mediated by prostaglandin release, since it was strongly inhibited by a cyclooxygenase inhibitor (indomethacin) pretreatment (de Castro Bastos et al., 2004). The inhibition by indomethacin indicates a strong involvement of prostaglandin in this response. It was suggested a correlation with a phospholipase A2-like enzyme present in *L. obliqua* bristle extract (Arocha-Pinango et al., 2000; Seibert et al., 2003), which would produce large amounts of arachidonic acid promptly converted to prostaglandin by cyclooxygenase (de Castro Bastos et al., 2004). Alternatively, our data indicate that the venom itself also stimulates an up-regulation of the expression pattern of prostaglandin-endoperoxide synthase-2 (PTGS2). Prostaglandin-endoperoxide synthase or cyclooxygenase, is the key enzyme in prostaglandin biosynthesis. Differently from the constitutively expressed isoform PTGS1, PTGS2 is inducible and regulated by specific stimulatory events, suggesting that it is responsible for the prostanoid biosynthesis involved in inflammation (Miller, 2006).

In patients envenomed with *Lonomia obliqua*, only a mild alteration in plasmatic urokinase plasminogen activator (uPA) was reported; plasminogen (PLG) and α2-antiplasmin (α2-AP) levels were reduced in patients, though (Zannin et al., 2003). Low levels of PLG and α2-AP are coherent with fibrinolytic system activation. Until now, no direct plasminogen activator activity was reported in *L. obliqua* venomous secretions, even though in recent publication, Pinto and collaborators reported a high amidolytic activity upon a synthetic chromogenic substrate of urokinase (Pinto et al., 2006). *L. obliqua* secretions also possess direct fibrinogenolyic and fibrinolytic enzymes (Pinto et al., 2004; Pinto et al., 2006; Veiga et al., 2003). Gene expression profile of cells envenomed with LOBE shows up-regulation of urokinase plasminogen activator receptor (uPAR), a glycosylphosphatydilinositol-anchored protein which binds uPA with high affinity and interacts with extracellular matrix proteins such as vitronectin and integrin family members. uPAR-uPA complex formation focuses proteolytic activity of uPA to the cell surface and serves to inactivate the enzyme when complexed with soluble inhibitors, such as plasminogen activator inhibitor-1 (PAI-1) (Mondino and Blasi, 2004). Knockout experiments have shown that uPAR does not have a major role in direct fibrinolysis. However, uPAR might indirectly participate in local fibrinolysis by exerting its chemoattractant properties, participating in the recruitment and activation of pro-inflammatory cells and thereby amplifying tissue-remodeling events. Over-expression of uPAR increases cell-surface proteolysis through uPA activation. uPAR facilitates plasminogen activation, generating plasmin which, in turn, digests ECM components and activates pro-matrix metalloproteinases (Mondino and Blasi, 2004). This sequence of events generates a site of intense proteolytic activity, which can affect ECM proteins and soluble proteins. The plasmin generated is responsible not only for the fibrin degradation but also matrix metalloproteinase activation, facilitating cell migration and tissue repair. Besides its specificity to fibrin, plasmin is also capable of degrading other plamatic proteins, such as fibrinogen, factor V and factor VIII (Vaughan and Declerck, 1998). It is conceivable that the increased level of plasmin generated due to uPAR up-regulation, could be, to a certain extent, responsible for the activation of the fibrinolytic system, with degradation not only of fibrin but also decrease in factors V and VIII levels seen in patients (Zannin et al., 2003).

The most potent activity in the caterpillar bristle extract is the procoagulant activity. The identification of two coagulation activators has been considered the main cause of this aspect of the clinical profile. Our gene expression results indicate an up-regulation of the coagulation cascade factor III or tissue factor. Tissue factor (TF) is an enzyme activator that forms a catalytic complex with factor VIIa and initiates coagulation by activation of factors IX and X, which leads to thrombin formation. Active TF has been detected in endothelial cells and circulating in procoagulant microparticules. Additionally, an alternatively spliced form of tissue factor (asHTF) has recently been described to be a soluble isoform of TF present in blood (Bogdanov et al., 2003). Endothelial and epithelial cells as well as leukocytes were documented as possible sources for asHTF in extracellular fluids (Szotowski et al., 2005).

To validate a potentially important over-expression of TF in envenomed cells, cell culture media was tested in a classic coagulation test. As seen in Figure 2, Fb-LOBE medium shows a dose dependent pro-coagulant activity. To rule out the participation of LOBE in this procoagulant activity, *L. obliqua* anti-serum (enough to inhibit 1.75 μg of venom) was added in an experiment with 20 μL of Fb-LOBE (containing 0.5 μg of LOBE, theoretically). There was no statically difference between the two treatments, suggesting the presence of a procoagulant factor produced by the envenomed fibroblasts. We propose here the expression and liberation of either procoagulant microparticle containing TF or the soluble form of TF (asHTF).

In summary, we have presented evidence using gene expression profiling that demonstrate the direct effect on *Lonomia obliqua* venom in the gene expression of envenomed cells. Besides the direct effects of the venom in the victim's plasma, causing coagulation and fibrinolysis, there are several genes up-regulated that could be involved in the generation and amplification of the clinical manifestation in the envenomation. Here we suggest that the envenomation might occur in the different steps. Initially the venomous proteins act enzymatically on the victim's plasma components generating effects such as intense coagulation, fibrinolysis and some degree of inflammation. In a second moment, venom components would stimulate a cellular response through up-regulation of several genes, causing activation and migration of inflammatory cells, extracelular matrix and plasmatic proteins degradation and increase in the procoagulant

activity in patient's plasma. These up-regulated genes would be partially responsible for effects such as inflammation, edema and pain sensation and involved in the amplification of fibrinolytic system activation and disseminated intravascular coagulation.

References

Alvarez Flores, M.P., Fritzen, M., Reis, C.V. and Chudzinski-Tavassi, A.M. (2006) Losac, a factor X activator from Lonomia obliqua bristle extract: its role in the pathophysiological mechanisms and cell survival. *Biochem Biophys Res Commun*, **343**, 1216-1223.

Arocha-Pinango, C.L. and Guerrero, B. (2001) Lonomia genus caterpillar envenomation: clinical and biological aspects. *Haemostasis*, **31**, 288-293.

Arocha-Pinango, C.L. and Layrisse, M. (1969) Fibrinolysis produced by contact with a caterpillar. *Lancet*, **1**, 810-812.

Arocha-Pinango, C.L., Marval, E. and Guerrero, B. (2000) Lonomia genus caterpillar toxins: biochemical aspects. *Biochimie*, **82**, 937-942.

Arocha-Pinango, C.L. and Pepper, D.S. (1981) Studies of a fibrinolytic enzyme from the larvae of Lonomia achelous (Cramer) using chromogenic peptide substrates. *Thromb Haemost*, **46**, 710-713.

Bogdanov, V.Y., Balasubramanian, V., Hathcock, J., Vele, O., Lieb, M. and Nemerson, Y. (2003) Alternatively spliced human tissue factor: a circulating, soluble, thrombogenic protein. *Nat Med*, **9**, 458-462.

Coll-Sangrona, E. and Arocha-Pinango, C.L. (1998) Fibrinolytic action on fresh human clots of whole body extracts and two semipurified fractions from Lonomia achelous caterpillar. *Braz J Med Biol Res*, **31**, 779-784.

de Castro Bastos, L., Veiga, A.B., Guimaraes, J.A. and Tonussi, C.R. (2004) Nociceptive and edematogenic responses elicited by a crude bristle extract of Lonomia obliqua caterpillars. *Toxicon*, **43**, 273-278.

Donato, J.L., Moreno, R.A., Hyslop, S., Duarte, A., Antunes, E., Le Bonniec, B.F., Rendu, F. and de Nucci, G. (1998) Lonomia obliqua caterpillar spicules trigger

human blood coagulation via activation of factor X and prothrombin. *Thromb Haemost*, **79**, 539-542.

Duarte, A.C., Crusius, P.S., Pires, C.A., Schilling, M.A. and Fan, H.W. (1996) Intracerebral haemorrhage after contact with Lonomia caterpillars. *Lancet*, **348**, 1033.

Fritzen, M., Flores, M.P., Reis, C.V. and Chudzinski-Tavassi, A.M. (2005) A prothrombin activator (Lopap) modulating inflammation, coagulation and cell survival mechanisms. *Biochem Biophys Res Commun*, **333**, 517-523.

Fritzen, M., Schattner, M., Ribeiro, A.L., Batista, I.F., Ventura, J., Prezoto, B.C. and Chudzinski-Tavassi, A.M. (2003) Lonomia obliqua venom action on fibrinolytic system. *Thromb Res*, **112**, 105-110.

Gallagher, P., Bao, Y., Serrano, S.M., Laing, G.D., Theakston, R.D., Gutierrez, J.M., Escalante, T., Zigrino, P., Moura-da-Silva, A.M., Nischt, R., Mauch, C., Moskaluk, C. and Fox, J.W. (2005) Role of the snake venom toxin jararhagin in proinflammatory pathogenesis: in vitro and in vivo gene expression analysis of the effects of the toxin. *Arch Biochem Biophys*, **441**, 1-15.

Gallagher, P.G., Bao, Y., Serrano, S.M., Kamiguti, A.S., Theakston, R.D. and Fox, J.W. (2003) Use of microarrays for investigating the subtoxic effects of snake venoms: insights into venom-induced apoptosis in human umbilical vein endothelial cells. *Toxicon*, **41**, 429-440.

Gouveia, A.I.D., da Silveira, R.B., Nader, H.B., Dietrich, C.P., Gremski, W. and Veiga, S.S. (2005) Identification and partial characterisation of hyaluronidases in Lonomia obliqua venom. *Toxicon*, **45**, 403-410.

Li, C. and Wong, W.H. (2001) Model-based analysis of oligonucleotide arrays: expression index computation and outlier detection. *Proc Natl Acad Sci U S A*, **98**, 31-36.

Liu, G., Loraine, A.E., Shigets, R.C., M., Cheng, J., Chervitz, S.A., Kulp, D. and Siani-Rose, M.A. (2001) Affymetrix White Paper.

MacAllister, R.J., Parry, H., Kimoto, M., Ogawa, T., Russell, R.J., Hodson, H., Whitley, G.S. and Vallance, P. (1996) Regulation of nitric oxide synthesis by dimethylarginine dimethylaminohydrolase. *Br J Pharmacol*, **119**, 1533-1540.

Miller, S.B. (2006) Prostaglandins in health and disease: an overview. *Semin Arthritis Rheum*, **36**, 37-49.

Mondino, A. and Blasi, F. (2004) uPA and uPAR in fibrinolysis, immunity and pathology. *Trends Immunol*, **25**, 450-455.

Pinto, A.F., Dobrovolski, R., Veiga, A.B. and Guimaraes, J.A. (2004) Lonofibrase, a novel alpha-fibrinogenase from Lonomia obliqua caterpillars. *Thromb Res*, **113**, 147-154.

Pinto, A.F., Silva, K.R. and Guimaraes, J.A. (2006) Proteases from Lonomia obliqua venomous secretions: comparison of procoagulant, fibrin(ogen)olytic and amidolytic activities. *Toxicon*, **47**, 113-121.

Reis, C.V., Farsky, S.H., Fernandes, B.L., Santoro, M.L., Oliva, M.L., Mariano, M. and Chudzinski-Tavassi, A.M. (2001) In vivo characterization of Lopap, a prothrombin activator serine protease from the Lonomia obliqua caterpillar venom. *Thromb Res*, **102**, 437-443.

Schadt, E.E., Li, C., Ellis, B. and Wong, W.H. (2001) Feature extraction and normalization algorithms for high-density oligonucleotide gene expression array data. *J Cell Biochem Suppl*, **Suppl 37**, 120-125.

Scoble, M.J. (1992) *The Lepidoptera - Form, Function and Diversity*. Oxford Univ. Press, New York.

Seibert, C.S., Oliveira, M.R., Goncalves, L.R., Santoro, M.L. and Sano-Martins, I.S. (2004) Intravascular hemolysis induced by Lonomia obliqua caterpillar bristle extract: an experimental model of envenomation in rats. *Toxicon*, **44**, 793-799.

Seibert, C.S., Shinohara, E.M. and Sano-Martins, I.S. (2003) In vitro hemolytic activity of Lonomia obliqua caterpillar bristle extract on human and Wistar rat erythrocytes. *Toxicon*, **41**, 831-839.

Seibert, C.S., Tanaka-Azevedo, A.M., Santoro, M.L., Mackessy, S.P., Torquato, R.J.S., Lebrun, I., Tanaka, A.S. and Sano-Martins, I.S. (2006) Purification of a phospholipase A(2) from Lonomia obliqua caterpillar bristle extract. *Biochemical and Biophysical Research Communications*, **342**, 1027-1033.

Szotowski, B., Antoniak, S., Poller, W., Schultheiss, H.P. and Rauch, U. (2005) Procoagulant soluble tissue factor is released from endothelial cells in response to inflammatory cytokines. *Circ Res*, **96**, 1233-1239.

Van Damme, J., Van Beeumen, J., Opdenakker, G. and Billiau, A. (1988) A novel, NH2-terminal sequence-characterized human monokine possessing neutrophil chemotactic, skin-reactive, and granulocytosis-promoting activity. *J Exp Med*, **167**, 1364-1376.

Vaughan, D.E. and Declerck, P.J. (1998) Fibrinolysis and its regulation. In Loscalso, J. and Schafer, A.I. (eds.), *Thrombosis and Hemorrhage*. Williams & Wilkins, Baltimore, pp. 155-170.

Veiga, A.B., Pinto, A.F. and Guimaraes, J.A. (2003) Fibrinogenolytic and procoagulant activities in the hemorrhagic syndrome caused by Lonomia obliqua caterpillars. *Thromb Res*, **111**, 95-101.

Veiga, A.B., Ribeiro, J.M., Guimaraes, J.A. and Francischetti, I.M. (2005) A catalog for the transcripts from the venomous structures of the caterpillar Lonomia obliqua: identification of the proteins potentially involved in the coagulation disorder and hemorrhagic syndrome. *Gene*, **355**, 11-27.

Zannin, M., Lourenco, D.M., Motta, G., Dalla Costa, L.R., Grando, M., Gamborgi, G.P., Noguti, M.A. and Chudzinski-Tavassi, A.M. (2003) Blood coagulation and fibrinolytic factors in 105 patients with hemorrhagic syndrome caused by accidental contact with Lonomia obliqua caterpillar in Santa Catarina, southern Brazil. *Thromb Haemost*, **89**, 355-364.

4. Conclusões

Os resultados aqui apresentados demonstram a complexidade da composição dos venenos animais e suas interações com o sistema hemostático das vítimas de envenenamento.

No primeiro capítulo desta tese, exploramos um pouco o universo das metaloproteinases de venenos de serpentes (SVMPs). As SVMPs são alvos de inúmeros estudos de caracterização estrutural e funcional por seu papel primário na lesão do tecido vascular e na hemorragia. Além do importante papel no envenenamento, SVMPs também são usadas como modelos para o estudo de metaloproteinases endógenas de mamíferos, as MMPs e as ADAMs, pela sua similaridade de seqüência e estrutura.

Dentre a família dos inibidores de metaloproteinases (TIMPs), mostramos que N-TIMP-3, um inibidor de amplo espetro, é o único membro dessa família capaz de interferir na atividade de metaloproteinases de veneno de serpentes. Alguns dos requerimentos estruturais para a função da TIMP-3 e N-TIMP-3 já foram elucidados. Utilizando técnicas de modelagem e dinâmica molecular, mostramos que alguns desses requerimentos estão também envolvidos com a inibição de SVMPs. A exploração das bases moleculares da interação pode auxiliar no desenho de novos inibidores mais efetivos tanto para SVMPs quanto para ADAMs e MMPs

Uma das características intrigantes da ação das SVMPs é a potência das enzimas da classe PIII. Essa maior atividade hemorrágica está relacionada com a presença de domínios não-catalíticos em sua estrutura. O domínio rico-em-cisteínas de SVMPs foi relacionado com a inibição de agregação plaquetária e interação com proteínas de matriz

extracelular. Em um estudo utilizando peptídeos sintéticos do domínio rico-em-cisteínas da SVMPs da classe PIII jararragina, identificamos dois peptídeos desse domínio capazes de interagir com o fator de von Willebrand. Porém, esses peptídeos não foram capazes de bloquear agregação plaquetária induzida por colágeno. Estudos de modelagem molecular da jararragina mostraram que apenas um dos peptídeos encontra-se na superfície da proteína, sendo capaz de interagir com outras proteínas. Finalmente, utilizando modelagem e dinâmica molecular, um modelo de interação entre o domínio rico-em-cisteínas e o domínio A de von Willebrand (vWA) foi proposto. Considerando que muitas proteínas de matriz possuem domínios vWA, especulamos que a interação do domínio rico-em-cisteínas com domínios vWA seja uma característica chave no direcionamento da toxina para substratos relevantes e na geração do efeito hemorrágico.

Os dados da literatura até então disponíveis mostraram que SVMPs são capazes de degradar diversos componentes isolados da matriz extracelular em ensaios *in vitro*. O desenvolvimento de técnicas de proteômica quantitativa possibilitou estudos de degradação proteolítica de substratos complexos através da análise por espectrometria de massas. Fazendo uso de uma dessas tecnologias, mostramos pela primeira vez que SVMPs são capazes de degradar componentes específicos da matriz extracelular de células em cultura. A identificação dessas proteínas mostrou ação na desestabilização da matriz extracelular e interferência em mecanismos de agregação plaquetária, coagulação e inflamação.

No segundo capítulo da tese o estudo de secreções tóxicas de *Lonomia obliqua* foi abordado. O acidente pelo contato com esses animais em fase larval provoca reações

graves que levam a um quadro clínico caracterizado por efeitos pró-coagulantes e hemorrágicos.

Os estudos com as proteínas tóxicas de *L. obliqua* têm sido focados nos componentes do extrato produzido a partir das espículas que revestem o corpo do animal. Através de um estudo comparativo, mostramos diferenças quali-quantitativas na composição de diferentes secreções venenosas. Duas das secreções testadas (criosecreção e hemolinfa) apresentaram alta atividade amidolítica sobre substratos sintéticos, atividade pró-coagulante moderada e alta capacidade de degradação de fibrinogênio. Por outro lado, as outras duas secreções venenosas (extrato de espículas e de tegumento) mostraram baixa atividade amidolítica e fibrinogenolítica. Dentre todas as secreções, o extrato de espículas apresentou a maior atividade pró-coagulante. A diferente participação de cada uma dessas secreções durante o contato com as lagartas pode levar a grande variabilidade de sintomas e gravidade do acidente com *Lonomia obliqua*.

Muitos dos sintomas causados pelo lonomismo parecem incoerentes com as pequenas quantidades de venenos que são injetadas na vítima durante o envenenamento. Utilizando análise de padrões de expressão gênica de células em cultura, mostramos efeitos do veneno na expressão de genes que estariam relacionados ao quadro clínico do envenenamento. Estes estudos de microarranjos de DNA mostraram, por exemplo, um aumento de expressão de fator tecidual em fibroblastos envenenados com extrato de espículas de *L. obliqua*. Segundo a teoria de cascata de coagulação baseada em superfícies celulares, a presença de fator tecidual e outros fatores da coagulação em regiões extravasculares seriam responsáveis por baixos níveis de ativação de fator X e protrombina (coagulação basal). Neste trabalho sugerimos que o aumento na expressão

de fator tecidual após o envenenamento pela taturana provocaria um aumento significativo na coagulação basal dos pacientes. Assim, danos vasculares, mesmo pequenos, desencadeariam uma resposta aumentada da coagulação, contribuindo com os efeitos já descritos dos ativadores da coagulação presentes no veneno da taturana.

O avanço tecnológico e criação de novas técnicas permitiram o desenvolvimento de novas abordagens no estudo de venenos animais. Análise de padrões de expressão gênica e proteômica quantitativa permitem hoje a avaliação dos efeitos de proteínas tóxicas em sistemas complexos, como células e tecidos. Esses novos enfoques permitem aprimoramento do conhecimento e desenvolvimento de novas teorias sobre a ação de venenos e toxinas animais, bem como de tratamentos mais eficientes para envenenamentos e doenças molecularmente relacionadas.

5. Referências Bibliográficas

Abella, H.B., Torres, J.B., Marques, M.G.B., Duarte, A.C. e Barros, E. (1998) *Manual de Diagnóstico e Acidentes por Lonomia*. CIT (Centro de Informações Toxicológica), Porto Alegre.

Andrews, R.K. e Berndt, M.C. (2004) Platelet physiology and thrombosis. *Thromb Res*, **114**, 447-453.

Arocha-Pinango, C.L., de Bosch, N.B., Torres, A., Goldstein, C., Nouel, A., Arguello, A., Carvajal, Z., Guerrero, B., Ojeda, A., Rodriguez, A. e et al. (1992) Six new cases of a caterpillar-induced bleeding syndrome. *Thromb Haemost*, **67**, 402-407.

Arocha-Pinango, C.L. e Guerrero, B. (2001) Lonomia genus caterpillar envenomation: clinical and biological aspects. *Haemostasis*, **31**, 288-293.

Arocha-Piñango, C.L. e Layrisse, M. (1969) Fibrinolysis produced by contact with a caterpillar. *Tha Lancet*, **1**, 810-812.

Arocha-Pinango, C.L., Marval, E. e Guerrero, B. (2000) Lonomia genus caterpillar toxins: biochemical aspects. *Biochimie*, **82**, 937-942.

Baramova, E.N., Shannon, J.D., Bjarnason, J.B. e Fox, J.W. (1989) Degradation of extracellular matrix proteins by hemorrhagic metalloproteinases. *Arch Biochem Biophys*, **275**, 63-71.

Bjarnason, J.B. e Fox, J.W. (1994) Hemorrhagic metalloproteinases from snake venoms. *Pharmacol Ther*, **62**, 325-372.

Bjarnason, J.B. e Fox, J.W. (1995) Snake venom metalloendopeptidases: reprolysins. *Methods Enzymol*, **248**, 345-368.

Blobel, C.P. (2005) ADAMs: key components in EGFR signalling and development. *Nat Rev Mol Cell Biol*, **6**, 32-43.

Braud, S., Bon, C. e Wisner, A. (2000) Snake venom proteins acting on hemostasis. *Biochimie*, **82**, 851-859.

Champagne, D.E. (2005) Antihemostatic molecules from saliva of blood-feeding arthropods. *Pathophysiol Haemost Thromb*, **34**, 221-227.

Collen, D. (1999) The plasminogen (fibrinolytic) system. *Thromb Haemost*, **82**, 259-270.

Costa, R.M. (1994) Acidentes por Lagartas Venenosas. In Barraviera, B. (ed.), *Venenos animais: uma visão integrada*. Ed. de Publicação Científicas, Rio de Janeiro, pp. 327-228.

Couppie, P., Marty, C., Sainte-Marie, D. e Pradinaud, R. (1998) [Poisonous caterpillars in French Guyana. 5 cases]. *Ann Dermatol Venereol*, **125**, 489-491.

Da Silva, W.D., Campos, C.M., Goncalves, L.R., Sousa-e-Silva, M.C., Higashi, H.G., Yamagushi, I.K. e Kelen, E.M. (1996) Development of an antivenom against toxins of Lonomia obliqua caterpillars. *Toxicon*, **34**, 1045-1049.

Dahlback, B. (2000) Blood coagulation. *Lancet*, **355**, 1627-1632.

Daltry, J.C., Ponnudurai, G., Shin, C.K., Tan, N.H., Thorpe, R.S. e Wuster, W. (1996) Electrophoretic profiles and biological activities: intraspecific variation in the venom of the Malayan pit viper (Calloselasma rhodostoma). *Toxicon*, **34**, 67-79.

Davie, E.W. e Ratnoff, O.D. (1964) Waterfall Sequence for Intrinsic Blood Clotting. *Science*, **145**, 1310-1312.

de Castro Bastos, L., Veiga, A.B., Guimaraes, J.A. e Tonussi, C.R. (2004) Nociceptive and edematogenic responses elicited by a crude bristle extract of Lonomia obliqua caterpillars. *Toxicon*, **43**, 273-278.

Diaz, J.H. (2005) The evolving global epidemiology, syndromic classification, management, and prevention of caterpillar envenoming. *Am J Trop Med Hyg*, **72**, 347-357.

Donato, J.L., Moreno, R.A., Hyslop, S., Duarte, A., Antunes, E., Le Bonniec, B.F., Rendu, F. e de Nucci, G. (1998) Lonomia obliqua caterpillar spicules trigger human blood coagulation via activation of factor X and prothrombin. *Thromb Haemost*, **79**, 539-542.

Duarte, A.C., Caovilla, J., Lorini, I., Lorini, D., Mantovani, G., Sumida, J., Manfre, P.C., Silveira, R.C. e de Moura, S.P. (1990) Insuficiência Renal aguda por acidentes com lagartas. *Jornal Brasileiro de Nefrologia*, **12**, 184-186.

Escalante, T., Shannon, J.D., Moura-da-Silva, A.M., Gutiérrez, J.M. e Fox, J.W. (2006) Novel insights into capillary vessel basement membrane damage by snake venom hemorrhagic metalloproteinases: A biochemical and immunohistochemical study. *Arch Biochem Biophys*, **in press**.

Fox, J.W. e Serrano, S.M. (2005) Structural considerations of the snake venom metalloproteinases, key members of the M12 reprolysin family of metalloproteinases. *Toxicon*, **45**, 969-985.

Fraiha Neto, H., Amaral, I.M. e Ballarini, A.J. (1985) Lonomia achelous (Cramer) (Lepidoptera, Saturniidae), o "tapuru da seringueira", agente do acidente hemorrágico por contato com larvas de mariposa no território Federal do Amapá. *XX Congresso da Sociedade Brasileira de Medicina Tropical*, São Paulo, p. 24.

Francischetti, I.M., Castro, H.C., Zingali, R.B., Carlini, C.R. e Guimaraes, J.A. (1998) Bothrops sp. snake venoms: comparison of some biochemical and physicochemical properties and interference in platelet functions. *Comp Biochem Physiol C Pharmacol Toxicol Endocrinol*, **119**, 21-29.

Fritzen, M., Flores, M.P., Reis, C.V. e Chudzinski-Tavassi, A.M. (2005) A prothrombin activator (Lopap) modulating inflammation, coagulation and cell survival mechanisms. *Biochem Biophys Res Commun*, **333**, 517-523.

Fritzen, M., Schattner, M., Ribeiro, A.L., Batista, I.F., Ventura, J., Prezoto, B.C. e Chudzinski-Tavassi, A.M. (2003) Lonomia obliqua venom action on fibrinolytic system. *Thromb Res*, **112**, 105-110.

Furtado, M.F., Maruyama, M., Kamiguti, A.S. e Antonio, L.C. (1991) Comparative study of nine Bothrops snake venoms from adult female snakes and their offspring. *Toxicon*, **29**, 219-226.

Gamborgi, G.P., Metcalf, E.B. e Barros, E.J. (2006) Acute renal failure provoked by toxin from caterpillars of the species Lonomia obliqua. *Toxicon*, **47**, 68-74.

Guerrero, B., Perales, J., Gil, A. e Arocha-Pinango, C.L. (1999) Effect on platelet FXIII and partial characterization of Lonomin V, a proteolytic enzyme from Lonomia achelous caterpillars. *Thromb Res*, **93**, 243-252.

Guerrero, B.A., Arocha-Pinango, C.L. e Gil San Juan, A. (1997a) Degradation of human factor XIII by lonomin V, a purified fraction of Lonomia achelous caterpillar venom. *Thromb Res*, **87**, 171-181.

Guerrero, B.A., Arocha-Pinango, C.L. e Gil San Juan, A. (1997b) Lonomia achelous caterpillar venom (LACV) selectively inactivates blood clotting factor XIII. *Thromb Res*, **87**, 83-93.

Hettasch, J.M. e Greenberg, C.S. (1998) Fibrin Formation and Stabilization. In Loscalso, J. e Schafer, A.I. (eds.), *Thrombosis and Hemorrhage*. Williams & Wilkins, Baltimore, pp. 129-154.

Hite, L.A., Jia, L.G., Bjarnason, J.B. e Fox, J.W. (1994) cDNA sequences for four snake venom metalloproteinases: structure, classification, and their relationship to mammalian reproductive proteins. *Arch Biochem Biophys*, **308**, 182-191.

Hoffman, M. (2003a) A cell-based model of coagulation and the role of factor VIIa. *Blood Rev*, **17 Suppl 1**, S1-5.

Hoffman, M. (2003b) Remodeling the blood coagulation cascade. *J Thromb Thrombolysis*, **16**, 17-20.

Hoffman, M. e Monroe, D.M., 3rd. (2001) A cell-based model of hemostasis. *Thromb Haemost*, **85**, 958-965.

Jenny, N.S. e Mann, K.G. (1998) Coagulation Cascade: An Overview. In Loscalso, J. e Schafer, A.I. (eds.), *Thrombosis and Hemorrhage*. Williams & Wilkins, Baltimore, pp. 3-27.

Jia, L.G., Wang, X.M., Shannon, J.D., Bjarnason, J.B. e Fox, J.W. (1997) Function of disintegrin-like/cysteine-rich domains of atrolysin A. Inhibition of platelet aggregation by recombinant protein and peptide antagonists. *J Biol Chem*, **272**, 13094-13102.

Jia, L.G., Wang, X.M., Shannon, J.D., Bjarnason, J.B. e Fox, J.W. (2000) Inhibition of platelet aggregation by the recombinant cysteine-rich domain of the hemorrhagic snake venom metalloproteinase, atrolysin A. *Arch Biochem Biophys*, **373**, 281-286.

Kelen, E.M.A., Duarte, A.C., Tomy, S.C., Sano-Martins, I.S., Castro, S.C.B., Guerreeo, B. e Arocha-Piñango, C.L. (1996) Acquired haemorrhagic syndrome from caontct with a caterpillar (Lonomia obliqua Walker 1855, Saturniidae). *Toxicon*, **34**, 146.

Lorini, L.M. (1997) Aspectos Biológicos e Morfológicos de Lonomia obliqua Walker, 1855 (Lepidoptera, Saturniidae), em Laboratório. Pontifícia Universidade Católica do Rio Grande do Sul, Porto Alegre, Vol. Mestrado, p. 72.

Lorini, L.M. (1999) *A Taturana - Aspectos biológicos e morfológicos da Lonomia obliqua*. EDIUPF, Passo Fundo.

Lu, Q., Clemetson, J.M. e Clemetson, K.J. (2005) Snake venoms and hemostasis. *J Thromb Haemost*, **3**, 1791-1799.

Luccas, S. (1991) Perigo: esta lagarta pode matar. *Guia Rural*, Vol. Março, pp. 29-33.

Macfarlane, R.G. (1964) An Enzyme Cascade in the Blood Clotting Mechanism, and Its Function as a Biochemical Amplifier. *Nature*, **202**, 498-499.

Marcus, A.J. e Safier, L.B. (1993) Thromboregulation: multicellular modulation of platelet reactivity in hemostasis and thrombosis. *Faseb J*, **7**, 516-522.

Markland, F.S. (1998) Snake venoms and the hemostatic system. *Toxicon*, **36**, 1749-1800.

Marsh, N.A. (1994) Snake venoms affecting the haemostatic mechanism--a consideration of their mechanisms, practical applications and biological significance. *Blood Coagul Fibrinolysis*, **5**, 399-410.

Monteiro, R.Q., Yamanouye, N., Carlini, C.R., Guimaraes, J.A., Bon, C. e Zingali, R.B. (1998) Variability of bothrojaracin isoforms and other venom principles in individual jararaca (Bothrops jararaca) snakes maintained under seasonally invariant conditions. *Toxicon*, **36**, 153-163.

Pinto, A.F., Dobrovolski, R., Veiga, A.B. e Guimaraes, J.A. (2004) Lonofibrase, a novel alpha-fibrinogenase from Lonomia obliqua caterpillars. *Thromb Res*, **113**, 147-154.

Pinto, A.F., Silva, K.R. e Guimaraes, J.A. (2006) Proteases from Lonomia obliqua venomous secretions: comparison of procoagulant, fibrin(ogen)olytic and amidolytic activities. *Toxicon*, **47**, 113-121.

Porter, S., Clark, I.M., Kevorkian, L. e Edwards, D.R. (2005) The ADAMTS metalloproteinases. *Biochem J*, **386**, 15-27.

Reis, C.V., Kelen, E.M., Farsky, S.H., Portaro, F.C., Sampaio, C.A., Fernandes, B.L., Camargo, A.C. e Chudzinski-Tavassi, A.M. (1999) A Ca++ activated serine protease (LOPAP) could be responsible for the haemorrhagic syndrome caused by the caterpillar Lonomia obliqua. L obliqua Prothrombin Activator Protease. *Lancet*, **353**, 1942.

Ribeiro, J.M. e Francischetti, I.M. (2003) Role of arthropod saliva in blood feeding: sialome and post-sialome perspectives. *Annu Rev Entomol*, **48**, 73-88.

Roberts, H.R., Hoffman, M. e Monroe, D.M. (2006) A cell-based model of thrombin generation. *Semin Thromb Hemost*, **32 Suppl 1**, 32-38.

Seibert, C.S., Oliveira, M.R., Goncalves, L.R., Santoro, M.L. e Sano-Martins, I.S. (2004) Intravascular hemolysis induced by Lonomia obliqua caterpillar bristle extract: an experimental model of envenomation in rats. *Toxicon*, **44**, 793-799.

Serrano, S.M., Jia, L.G., Wang, D., Shannon, J.D. e Fox, J.W. (2005a) Function of the cysteine-rich domain of the haemorrhagic metalloproteinase atrolysin A: targeting adhesion proteins collagen I and von Willebrand factor. *Biochem J*, **391**, 69-76.

Serrano, S.M., Shannon, J.D., Wang, D., Camargo, A.C. e Fox, J.W. (2005b) A multifaceted analysis of viperid snake venoms by two-dimensional gel electrophoresis: an approach to understanding venom proteomics. *Proteomics*, **5**, 501-510.

Takeda, S., Igarashi, T., Mori, H. e Araki, S. (2006) Crystal structures of VAP1 reveal ADAMs' MDC domain architecture and its unique C-shaped scaffold. *Embo J*, **25**, 2388-2396.

Usami, Y., Fujimura, Y., Miura, S., Shima, H., Yoshida, E., Yoshioka, A., Hirano, K., Suzuki, M. e Titani, K. (1994) A 28 kDa-protein with disintegrin-like structure (jararhagin-C) purified from Bothrops jararaca venom inhibits collagen- and ADP-induced platelet aggregation. *Biochem Biophys Res Commun*, **201**, 331-339.

Vaughan, D.E. e Declerck, P.J. (1998) Fibrinolysis and its Regulation. In Loscalso, J. e Schafer, A.I. (eds.), *Thrombosis and Hemorrhage*. Williams & Wilkins, Baltimore, pp. 155-170.

Veiga, A.B., Pinto, A.F. e Guimaraes, J.A. (2003) Fibrinogenolytic and procoagulant activities in the hemorrhagic syndrome caused by Lonomia obliqua caterpillars. *Thromb Res*, **111**, 95-101.

Veiga, A.B., Ribeiro, J.M., Guimaraes, J.A. e Francischetti, I.M. (2005) A catalog for the transcripts from the venomous structures of the caterpillar Lonomia obliqua: identification of the proteins potentially involved in the coagulation disorder and hemorrhagic syndrome. *Gene*, **355**, 11-27.

Veiga, A.B.G., Blochtein, B. e Guimaraes, J.A. (2001) Structures involved in production, secretion and injection of the venom produced by the caterpillar Lonomia obliqua (Lepidoptera, Saturniidae). *Toxicon*, **39**, 1343-1351.

von Ihering, R. (1914) Estudo biologico das lagartas urticantes ou tatoranas. *Annaes Paulistas de Medicina e Cirurgia*, **3**, 129-139.

Zannin, M., Lourenco, D.M., Motta, G., Dalla Costa, L.R., Grando, M., Gamborgi, G.P., Noguti, M.A. e Chudzinski-Tavassi, A.M. (2003) Blood coagulation and fibrinolytic factors in 105 patients with hemorrhagic syndrome caused by accidental contact with Lonomia obliqua caterpillar in Santa Catarina, southern Brazil. *Thromb Haemost*, **89**, 355-364.

Anexo 1 – Curriculum vitae

CURRICULUM VITAE

RESUMIDO

Outubro, 2006

DADOS PESSOAIS

Nome Antônio Frederico Michel Pinto
Filiação Jorge Antonio Pinto e Maria Luiza Michel Pinto
Nascimento 01/01/1980 - Porto Alegre/RS - Brasil

Endereço profissional: Universidade Federal do Rio Grande do Sul, Centro de Biotecnologia, Laboratório de Bioquímica Farmacológica.
Av. Bento Gonçalves, 9500 - Prédio 43431- Laboratório 214 - Campos do Vale
Agronomia
91501970 Porto Alegre, RS – Brasil
Telefone: (51) 33166062
E-mail: pinto@cbiot.ufrgs.br

Endereço residencial: Avenida Protásio Alves, 7157 apto 401 bl 4
Alto Petrópolis
91310003 Porto Alegre, RS - Brasil
Telefone: (51) 33813710
E-mail: antmananthill@gmail.com

FORMAÇÃO ACADÊMICA/TITULAÇÃO

2002 Doutorado em Biologia Celular e Molecular.
Universidade Federal do Rio Grande do Sul, UFRGS, Porto Alegre, Brasil
Título: Novos enfoques no estudo dos mecanismos de ação de metaloproteinases e outras proteínas tóxicas envolvidas no envenenamento ofídico e lonômico
Orientador: Jorge Almeida Guimarães
Bolsista do(a): Coordenação de Aperfeiçoamento de Pessoal de Nível Superior, CAPES

2001 - 2002 Mestrado em Biologia Celular e Molecular.
Universidade Federal do Rio Grande do Sul, UFRGS, Porto Alegre, Brasil
Título: Purificação e Caracterização de uma Enzima Fibrino(geno)lítica de *Lonomia obliqua*
Orientador: Jorge Almeida Guimarães
Bolsista do(a): Conselho Nacional de Desenvolvimento Científico e Tecnológico

1997 - 2000 Graduação em Biologia.
Universidade Federal do Rio Grande do Sul, UFRGS, Porto Alegre, Brasil
Título: Identificação e Caracterização de Atividades Anti-Hemostáticas de Secreções Venenosas da Taturana Lonomia obliqua
Orientador: Jorge Almeida Guimarães
Bolsista do(a): Conselho Nacional de Desenvolvimento Científico e Tecnológico

ATIVIDADES CIENTÍFICAS E TÉCNICAS

Publicações em Periódicos

1. PINTO, A. F. M., TERRA, R. M. S., GUIMARÃES, J. A., FOX, J. W. Mapping von Willebrand Factor A Domain Binding Sites on a Snake Venom Metalloproteinase Cysteine-Rich Domain. Archives of Biochemistry and Biophysics. , v.457,p.41 - 46, 2007.

2. PINTO, A. F. M., SILVA, K. R. L. M., GUIMARÃES, J. A. Proteases from Lonomia obliqua venomous secretions: Comparison of procoagulant, fibrin(oen)olytic and amidolytic activities. Toxicon. , v.47, p.113 - 121, 2006.

3. PINTO, A. F. M., TERRA, R. M. S., GUIMARÃES, J. A., KASHIWAGI, M., NAGASE, H., SERRANO, S. M. T., FOX, J. W. Structural features of the reprolysin Atrolysin C and tissue inhibitors of metalloproteinases (TIMPs) interactions. Biochemical and Biophysical Research Communications. , v.347, p.641 - 648, 2006.

4. PINTO, A. F. M., DOBROVOLSKI, R., VEIGA, A. B. G., GUIMARÃES, J. A. Lonofibrase, a Novel a-Fibrinogenase from Lonomia obliqua Caterpillars. Thrombosis Research. , v.113, p.147 - 154, 2004.

5. VEIGA, A. B. G., PINTO, A. F. M., GUIMARÃES, J. A. Fibrinogenolytic and procoagulant activities in the hemorrhagic syndrome caused by Lonomia obliqua caterpillars.. Thrombosis Research. , v.111, p.95 - 101, 2003.

Trabalhos apresentados em Congressos e Simpósios

1. SILVA, W. O. B., BERGER, M. O., SANTI, L., PINTO, A. F. M., GUIMARÃES, J. A., SCHRANK, A., VAINSTEIN, M.H. Partial purification of a spore surface lipase from the entomopathogenic and acaricide fungus Metarhizium anisopliae In: XXXV Reunião Anual da SBBq, 2006, Águas de Lindóia. **Livro de Resumos**, 2006. p.L94.

2. BERGER, M. O., PINTO, A. F. M., AMORIM, H. L. N., GUIMARÃES, J. A. Bothrojaractivase, a prothrombin activating enzyme isolated from Bothrops jararaca venom In: XXXV Reunião Anual da SBBq, 2006, Água de Lindóia. **Livro de Resumos**, 2006. p.L95.

3. PINTO, A. F. M., TERRA, R. M. S., NAGASE, H., SERRANO, S. M. T., GUIMARÃES, J. A., FOX, J. W. Insights into the molecular interaction of snake venom metalloproteinase, atrolysin C, and tissue inhibitors of metalloproteinases In: XXXV Reunião Anual da SBBq, 2006, Águas de Lindóia. **Livro de Resumos**, 2006. p.N1.

4. RICCI, C. G., PINTO, A. F. M., BERGER, M. O., TERMIGNONI, C. Purification of a thrombin exosite inhibitor from the cattle tick Boophilus microplus In: XXXV Reunião Anual da SBBq, 2006, Águas de Lindóia. **Livro de Resumos**, 2006. p.L75.

5. PINTO, A. F. M., WANG, D., SERRANO, S. M. T., GUIMARÃES, J. A., FOX, J. W. Mapping von Willebrand Factor A Domain Binding Sites on Snake Venom Metalloproteinase Cysteine-Rich Domain In: Gordon Conference - Small Integrin-Binding Proteins, 2005, Big Sky, Montana, EUA. **Abstract Book**, 2005.

6. BERGER, M. O., PINTO, A. F. M., de AMORIM, H. L. N., GUIMARÃES, J. A. Purification and characterization of a prothrombin activator from Bothrops jararaca venom In: XXXIV Reunião Anual da SBBq, 2005, Águas de Lindóia. **Livro de Resumos**, 2005. p.L-68.

7. RICCI, C. G., PINTO, A. F. M., TERMIGNONI, C. Purification and characterization of a thrombin inhibitor from Boophilus microplus gut extract In: XXXIV Reunião Anual da SBBq, 2005, Águas de Lindóia. **Livro de Resumos**, 2005. p.S-21.

8. RICCI, C. G., PINTO, A. F. M., VEIGA, Ana Beatriz Gorini da, GUIMARÃES, J. A. Isolation and Characterization of a Fibrin(ogen)olytic Activity from Lonomia obliqua Bristle Extract In: XXXIII Reunião Anual da Sociedade Brasileira de Bioquímica e Biologia Molecular - SBBq, 2004, Caxambu - MG. **Livro de Resumos**, 2004.

9. DOBROVOLSKI, Ricardo, PINTO, A. F. M., VEIGA, Ana Beatriz Gorini da, GUIMARÃES, J. A. Anti-hemostatic activities of Lonomia obliqua: Procoagulant and phospholipase A2 activities In: XXXII Reunião Anual da Sociedade Brasileira de Bioquímica e Biologia Molecular, 2003, Caxambu, MG. **Livro de Resumos**, 2003.

10. SILVA, Kátia Rosana Lima de Moura da, VEIGA, Ana Beatriz Gorini da, PINTO, A. F. M., GUIMARÃES, J. A. Caracterização diferencial de proteínas do veneno de Lonomia obliqua In: XVIII Reunião Anual da Federação de Sociedades de Biologia Experimental, 2003, Curitiba, PR. **Livro de Resumos**, 2003.

11. PINTO, A. F. M., DOBROVOLSKI, Ricardo, VEIGA, Ana Beatriz Gorini da, GUIMARÃES, J. A. Lonofibrase, a new a-fibrinogenase isolated from Lonomia obliqua In: XVIII Reunião Anual da Federação de Sociedades de Biologia Experimental, 2003, Curitiba, MG. **Livro de Resumos**, 2003.

12. PINTO, A. F. M., VEIGA, Ana Beatriz Gorini da, DOBROVOLSKI, Ricardo, GUIMARÃES, J. A. Lonofibrase, a new a-fibrinogenase isolated from Lonomia obliqua In: XXXII Reunião Anual da Sociedade Brasileira de Bioquímica e Biologia Molecular, 2003, Caxambu, MG. **Livro de Resumos**, 2003.

13. KOBE, Simone, DOBROVOLSKI, Ricardo, PINTO, A. F. M., GUIMARÃES, J. A. Princípios ativos do veneno da abelha Apis mellifera com ação na hemostasia In: XVIII Reunião Anual da Federação de Sociedades de Biologia Experimental, 2003, Curitiba, PR. **Livro de Resumos**, 2003.

14. BORHER, C. B., PINTO, A. F. M., BASTIANI, Michele, TERMIGNONI, C., GUIMARÃES, J. A. Purification of a kininase from Lonomia obliqua caterpillar In: XXXII Reunião Anual da Sociedade Brasileira de Bioquímica e Biologia Molecular, 2003, Caxambu, MG. **Livro de Resumos**, 2003.

15. ASSAFIM, Mariane, FRATANE, Flávia, DOBROVOLSKI, Ricardo, PINTO, A. F. M., VEIGA, Ana Beatriz Gorini da, GUIMARÃES, J. A., ZINGALI, Russolina Benedeta. The use of thrombosis experimental model for the study of crude venom, caterpillar secretions and synthetic drugs In: XXXII Reunião Anual da Sociedade Brasileira de Bioquímica e Biologia Molecular, 2003, Caxambu, MG. **Livro de Resumos**, 2003.

16. PINTO, A. F. M., DOBROVOLSKI, Ricardo, VEIGA, Ana Beatriz Gorini da, GUIMARÃES, J. A. CHARACTERIZATION OF FIBRIN(OGEN)OLYTIC ACTIVITIES PRESENT IN A LONOMIA OBLIQUA SECRETION In: XVII Reunião Anual da Federação de Sociedades de Biologia Experimental FeSBE, 2002, Salvador. **Livro de Resumos**, 2002.

17. DOBROVOLSKI, Ricardo, PINTO, A. F. M., VEIGA, Ana Beatriz Gorini da, GUIMARÃES, J. A. Comparative study of anti-hemostatic activities from different materials of Lonomia obliqua In: XXXI Reunião Anual da SBBq, 2002, Caxambú, MG. **Livro de Resumos**, 2002. p.121 - 121

18. RUSSO, C., PINTO, A. F. M., JULIANO, M., de AMORIM, H. L. N., GUIMARÃES, J. A. Docking studies of an anticoagulant peptide fragment derived from Nitrophorin-2 in the active site of factor Xa: perspectives to drug design In: XXXI Reunião Anual da SBBq, 2002, Caxambú, MG. **Livro de Resumos**, 2002. p.170 - 170

19. VEIGA, Ana Beatriz Gorini da, PINTO, A. F. M., GUIMARÃES, J. A. EFFECTS OF LONOMIA OBLIQUA VENOMOUS SECRETIONS UPON BLOOD COAGULATION AND FIBRINOLYSIS In: XVII Reunião Anual da Federação de Sociedades de Biologia Experimental FeSBE, 2002, Salvador. **Livro de Resumos**, 2002.

20. VEIGA, Ana Beatriz Gorini da, PINTO, A. F. M., DOBROVOLSKI, Ricardo, GUIMARÃES, J. A. Fibrin(ogen)olytic activity of four materials from Lonomia obliqua In: XXXI Reunião Anual da SBBq, 2002, Caxambú, MG. **Livro de Resumos**, 2002. p.122 - 122

21. VEIGA, Ana Beatriz Gorini da, PINTO, A. F. M., DOBROVOLSKI, Ricardo, GUIMARÃES, J. A. Phospholipase A2, Procoagulant and Fibrinolytic Activities From Lonomia obliqua Venom In: VII Simpósio da Sociedade Brasileira de Toxinologia (SBTx), 2002, Pirenópolis, GO. **Livro de Resumos**, 2002. p.311 -

22. PINTO, A. F. M., DOBROVOLSKI, Ricardo, VEIGA, Ana Beatriz Gorini da, GUIMARÃES, J. A. Purification and characterization of a fibrin(ogen)olytic activity from Lonomia obliqua caterpillars In: XXXI Reunião Anual da SBBq, 2002, Caxambú, MG. **Livro de Resumos**, 2002. p.122 - 122

23. VEIGA, Ana Beatriz Gorini da, PINTO, A. F. M., BLOCHTEIN, B., SCHRANK, A., GUIMARÃES, J. A. Biochemical and Molecular Characterization of the secretory epithelium Involved in Venom Production in Lonomia obliqua caterpillar In: XXX Reunião Anual da Sociedade Brasileira de Bioquímica e Biologia Molecular - SBBq, 2001, Caxambú. **Livro de Resumos**, 2001. p.30 -

24. PINTO, A. F. M., VEIGA, Ana Beatriz Gorini da, GUIMARÃES, J. A. Fibrinogenolytic activity from Lonomia obliqua caterpillars secretions In: XXX Reunião Anual da Sociedade Brasileira de Bioquímica e Biologia Molecular - SBBq, 2001, Caxambú. **Livro de Resumos**, 2001. p.129 -

25. PINTO, A. F. M., GUIMARÃES, J. A. Characterization and Inhibition of a Ca++-Dependent Serine-Protease from Lonomia obliqua Caterpillars In: VI Simpósio da Sociedade Brasileira de Toxinologia SBTx, 2000, São Pedro, SP. **Livro de Resumos**, 2000.

26. PINTO, A. F. M., GAMBORGI, G., GUIMARÃES, J. A. Fibrinolytic Activity From Lonomia obliqua Secretions In: XV Reunião Anual da Federação de Sociedades de Biologia Experimental FeSBE, 2000, Caxambú, MG. **Livro de Resumos**, 2000.

27. PINTO, A. F. M., VEIGA, Ana Beatriz Gorini da, BLOCHTEIN, B., GUIMARÃES, J. A. Proteases from Different Secretions Are Involved on the Paradoxal (Pro-Coagulant and Hemorrhagic) Envenomation Caused by Lonomia obliqua Caterpillars In: XII World Congress of the International Society on Toxinology (IST), 2000, Paris. **Abstract Book**. , 2000. p.P 178 -

Participação em Congressos e Reuniões

1 Reunião Anual da Sociedade Brasileira de Bioquímica e Biologia Molecular (SBBq). 2006. (Participação em eventos/Congresso).

2 Gordon Conference – Small Integrin-Binding Proteins - 2005. (Participação em eventos/Conferência).

3 Reunião Anual da Sociedade Brasileira de Bioquímica e Biologia Molecular (SBBq). 2004. (Participação em eventos/Congresso).

4 Reunião Anual da Sociedade Brasileira de Bioquímica e Biologia Molecular (SBBq). 2003. (Participação em eventos/Congresso).

5 Reunião Anual da Federação de Sociedades de Biologia Experimental (FeSBE). 2003. (Participação em eventos/Congresso).

6 Reunião Anual da Sociedade Brasileira de Bioquímica e Biologia Molecular (SBBq). 2002. (Participação em eventos/Congresso).

7 Reunião Anual da Federação de Sociedades de Biologia Experimental (FeSBE). 2002. (Participação em eventos/Congresso).

8 Reunião Anual da Sociedade Brasileira de Bioquímica e Biologia Molecular (SBBq). 2001. (Participação em eventos/Congresso).

9 Simpósio de Toxinologia (SBTx) 2000. (Participação em eventos/Simpósio).

10 Reunião Anual da Federação de Sociedades de Biologia Experimental (FeSBE). 2000. (Participação em eventos/Congresso).

ORIENTAÇÕES E SUPERVISÕES

Supervisões concluídas

Iniciação científica

1. Clarisse Gravina Ricci. **Purificação e caracterizaçã de um inibidor de trombina presente no intestino do carrapato Boophilus microplus**. 2006. Iniciação científica (Farmácia) - Universidade Federal do Rio Grande do Sul

2. Ricardo Dobrovolski. **A Taturana Lonomia obliqua e a Hemostasia**. 2003. Iniciação científica (Biologia) - Universidade Federal do Rio Grande do Sul

Supervisões em andamento

Iniciação científica

1. Markus Berger de Oliveira. **Ativação de Protrombina pelo veneno das serpentes Bothrops jararaca e Oxyuranus scutelatus**. 2004. Iniciação científica (Farmácia) - Universidade Federal do Rio Grande do Sul